

CLOCK-BASED SEGMENTATION IN THE RED FLOUR BEETLE *TRIBOLIUM
CASTANEUM*

by

EZZAT EL-SHERIF

MSc, Cairo University, 2008

AN ABSTRACT OF A DISSERTATION

submitted in partial fulfillment of the requirements for the degree

DOCTOR OF PHILOSOPHY

Genetics Program
College of Arts and Sciences

KANSAS STATE UNIVERSITY
Manhattan, Kansas

2013

Abstract

In *Drosophila*, all segments form in the blastoderm where morphogen gradients spanning the entire anterior-posterior axis of the embryo provide positional information. However, in the beetle *Tribolium castaneum* and most other insects, a number of anterior segments form in the blastoderm, and the remaining segments form sequentially from a posterior growth zone during germband elongation. In this work, I show that segmentation at both blastoderm and germband stages of *Tribolium* is based on a segmentation clock. Specifically, I show that the *Tribolium* primary pair-rule gene, *Tc-even-skipped* (*Tc-eve*), is expressed in waves propagating from the posterior pole and progressively slowing until they freeze into stripes; such dynamics are a hallmark of clock-based segmentation. Phase shifts between *Tc-eve* transcripts and protein confirm that these waves are due to expression dynamics. Such waves, like their counterparts in vertebrates, are assumed to arise due to the modulation of a molecular clock by a posterior-to-anterior frequency gradient. I provide evidence that the posterior gradient of *Tc-caudal* (*Tc-cad*) expression regulates the oscillation frequency of pair-rule gene expression in *Tribolium*. I show this by correlating the gradient of *Tc-cad* expression to the spatiotemporal dynamics of *Tc-even-skipped* expression in wild type as well as in different knockdowns of *Tc-cad* regulators. Specifically, the spatial extent, frequency, and width of *Tc-eve* waves correlate with the spatial extent, expression level, and slope of *Tc-cad* gradient, respectively, as predicted by computer modeling. These results pose intriguing evolutionary questions, since *Drosophila* and *Tribolium* segment their blastoderms using the same genes but different mechanisms, and highlight the role of frequency gradients in pattern formation.

CLOCK-BASED SEGMENTATION IN THE RED FLOUR BEETLE TRIBOLIUM
CASTANEUM

by

EZZAT EL-SHERIF

MSc, Cairo University, 2008

A DISSERTATION

submitted in partial fulfillment of the requirements for the degree

DOCTOR OF PHILOSOPHY

Genetics Program
College of Arts and Sciences

KANSAS STATE UNIVERSITY
Manhattan, Kansas

2013

Approved by:

Major Professor
Susan J. Brown

Copyright

EZZAT EL-SHERIF

2013

Abstract

In *Drosophila*, all segments form in the blastoderm where morphogen gradients spanning the entire anterior-posterior axis of the embryo provide positional information. However, in the beetle *Tribolium castaneum* and most other insects, a number of anterior segments form in the blastoderm, and the remaining segments form sequentially from a posterior growth zone during germband elongation. In this work, I show that segmentation at both blastoderm and germband stages of *Tribolium* is based on a segmentation clock. Specifically, I show that the *Tribolium* primary pair-rule gene, *Tc-even-skipped* (*Tc-eve*), is expressed in waves propagating from the posterior pole and progressively slowing until they freeze into stripes; such dynamics are a hallmark of clock-based segmentation. Phase shifts between *Tc-eve* transcripts and protein confirm that these waves are due to expression dynamics. Such waves, like their counterparts in vertebrates, are assumed to arise due to the modulation of a molecular clock by a posterior-to-anterior frequency gradient. I provide evidence that the posterior gradient of *Tc-caudal* (*Tc-cad*) expression regulates the oscillation frequency of pair-rule gene expression in *Tribolium*. I show this by correlating the gradient of *Tc-cad* expression to the spatiotemporal dynamics of *Tc-even-skipped* expression in WT as well as in different knockdowns of *Tc-cad* regulators. Specifically, the spatial extent, frequency, and width of *Tc-eve* waves correlate with the spatial extent, expression level, and slope of *Tc-cad* gradient, respectively, as predicted by computer modeling. These results pose intriguing evolutionary questions, since *Drosophila* and *Tribolium* segment their blastoderms using the same genes but different mechanisms, and highlight the role of frequency gradients in pattern formation.

Table of Contents

List of Figures	ix
List of Tables	x
List of Supplementary Figures.....	xi
List of Supplementary Tables	xii
List of Movies.....	xiii
List of Equations.....	xiv
Acknowledgements.....	xv
Chapter 1 - Comparisons of the embryonic development of <i>Drosophila</i> , <i>Nasonia</i> , and <i>Tribolium</i> 1	
Introduction.....	1
A tale of two models: <i>Nasonia</i> and <i>Tribolium</i>	2
AP polarity and patterning.....	5
Maternal inputs into AP patterning.....	6
The Anterior system.....	6
The Posterior System	9
caudal function and regulation.....	9
nanos regulation and function.....	10
The terminal system.....	12
Gap genes.....	13
The identity of segments that are formed is described in the gray boxes at the top of each panel. Diluted color in an expression domain indicates reduced expression. A question mark means the expression domain is not reported in literature. A, abdominal segments; G, gnathal segments; T, thoracic segments.....	17
Pair-rule genes	19
Segment polarity genes	22
Homeotic genes.....	22
DV patterning	23
The source of nuclear Dorsal gradient	27
Head development	29

Germline specification	31
Morphogenesis	34
Gastrulation.....	34
Extraembryonic membranes	36
Conclusions and Perspectives.....	38
References.....	41
Chapter 2 - A segmentation clock operating in blastoderm and germband stages of insect	
development.....	52
Summary.....	52
Introduction.....	53
Waves of <i>Tc-eve</i> gene expression are observed in both blastoderm and germband stages of <i>Tribolium</i> development.....	54
<i>Tc-eve</i> waves are due to transcription dynamics, rather than cell movement or oriented cell division.....	59
Determining the frequency of <i>Tc-eve</i> oscillations	61
Probable molecular basis and implications for segmentation mechanisms	63
Materials and Methods.....	64
In situ hybridization and immunocytochemistry	64
Wildtype strains and transgenic lines.....	64
Live imaging and cell tracking.....	64
Egg collections for developmental time windows	64
Correlation of time-lapse movie and blastoderm stainings.....	65
Supplementary materials.....	65
Acknowledgements.....	70
References.....	70
Chapter 3 - Caudal regulates the spatiotemporal dynamics of pair-rule waves in <i>Tribolium</i>	
Summary.....	74
Introduction.....	74
Results.....	76
Characterizing Tc-cad expression in <i>Tribolium</i>	76
Regulation of the Tc-cad gradient.....	78

Tc-cad gradient regulates Tc-eve waves in <i>Tribolium</i>	81
Graded frequency profile as a buffer against noise	87
Conclusion	88
Materials and Methods.....	89
In situ hybridization, immunocytochemistry, and RNAi.....	89
Egg collections for developmental time windows	89
Comparing Tc-cad gradients in two egg collections.....	89
Calculating class durations from class distribution graphs.....	90
Supplementary materials.....	90
References.....	92
Chapter 4 - Conclusions.....	96
Clock-based segmentation in <i>Tribolium</i>	96
The role of Caudal in segmentation.....	96
The patterning capacity of frequency gradients and the robustness of the clock-and-wavefront model	97
The molecular basis of clock modulation by a frequency gradient	98
Supplementary materials.....	100
References.....	101

List of Figures

Figure 1.1 Phylogenetic relationships of selected insect models, and schematic representations of their early embryonic fate maps.....	5
Figure 1.2 Maternal provision of anterior-posterior (AP) patterning information in <i>Drosophila</i> , <i>Tribolium</i> , and <i>Nasonia</i>	6
Figure 1.3 Comparison of gap gene expression patterns and their regulatory relationships in <i>Drosophila</i> and <i>Tribolium</i>	15
Figure 1.4 Comparison of gap genes phenotypes in <i>Drosophila</i> and <i>Tribolium</i>	16
Figure 1.5 Hox gene expression in wild type (wt) and gap gene RNAi and mutant embryos.	17
Figure 1.6 Initial and resolving expressions of primary pair-rule genes in <i>Tribolium</i>	20
Figure 1.7 Dorsal-ventral (DV) fate map and expression domains of genes involved in DV patterning in <i>Drosophila</i>	24
Figure 1.8 Comparison between <i>Toll</i> phenotype in <i>Drosophila</i> and <i>Tribolium</i>	26
Figure 1.9 Regulatory relationships between major components in dorsal-ventral (DV) axis patterning.	28
Figure 1.10 Germ cell formation in <i>Drosophila</i> , <i>Nasonia</i> , and <i>Tribolium</i>	32
Figure 1.11 Mechanisms of gastrulation in <i>Drosophila</i> , <i>Tribolium</i> , and <i>Nasonia</i>	35
Figure 2.1 Waves of <i>Tc-eve</i> expression propagate from posterior to anterior in both blastoderm and germband stages of <i>Tribolium</i> development.	55
Figure 2.2 <i>Tc-eve</i> waves are due to transcription dynamics, rather than cell movements.	60
Figure 2.3 Periodicity of <i>Tc-eve</i> oscillation in the blastoderm and germband.	62
Figure 3.1 <i>Tc-cad</i> expression in <i>Tribolium</i>	76
Figure 3.2 Characterization of <i>Tc-cad</i> gradient in WT and RNAi knockdowns of <i>Tc-cad</i> regulators.	79
Figure 3.3 <i>Tc-eve</i> expression in WT, mild <i>Tc-cad</i> RNAi, and <i>Tc-cad</i> regulators RNAi.	82
Figure 3.4 Temporal dynamics of <i>Tc-eve</i> expression at the posterior end of the embryo in knockdown of <i>Tc-cad</i> and its regulators in comparison with that of WT.	84
Figure 3.5 Frequency profile and robustness of the clock-and-wavefront model.	88
Figure 4.1 Probable molecular basis for frequency regulation.	100

List of Tables

Table 1.1 - Techniques and Tools Available in <i>Drosophila</i> , <i>Tribolium</i> , and <i>Nasonia</i>	3
Table 2.1 Mapping the temporal order of <i>Tc-eye</i> patterns.....	57

List of Supplementary Figures

Supp. Figure 2.1 <i>Tc-eve</i> expression dynamics in the germband.....	65
Supp. Figure 2.2 No significant localized or oriented cell division in the segmented part of class B7 blastoderms.....	67
Supp. Figure 3.1 Detailed temporal dynamics of <i>T-cad</i> expression gradient in the blastoderm. .	90
Supp. Figure 3.2 <i>Tc-eve</i> is abolished in severe <i>Tc-cad</i> knockdown.	91

List of Supplementary Tables

Supp. Table 2.1 Primary <i>Tc-eve</i> stripes are generated approximately every 3 hours in the germband.....	68
---	----

List of Movies

Movie 2.1 Computer simulation of <i>Tc-eve</i> dynamics in the blastoderm.....	69
Movie 2.2 Time-lapse recording of nuclear GFP in <i>Tribolium</i> blastoderm and early germband.	70
Movie 2.3 Computer simulation of phase shifts between <i>Tc-eve</i> transcript and Tc-EVE protein distributions in the blastoderm.....	70
Movies 3.1 Modeling <i>Tc-eve</i> waves in WT and knockdowns.....	91
Movies 3.2 Utilizing a graded frequency profile renders the clock-and-wavefront more robust to noise in axis elongation.....	92
Movies 4.1 Simulation of the proposed pair-rule GRN in WT and knockdowns.....	101

List of Equations

Equation 4.1 Differential equation representation of the proposed pair-rule GRN.....	101
--	-----

Acknowledgements

I would like to express my deepest gratitude to Dr. Sue Brown for her support and encouragement of my transition from Engineering to Biology. Had it not been for her patience and guidance, I would not have discovered my love to Science, and this work would not have been possible.

I am thankful to my committee members for their guidance and assistance. I would like also to thank Xin Zhu, Jinping Fu, Jeremy Lynch, and Michalis Averof for their contribution to this work, and Cassandra M. Coleman and Barb VanSlyk for technical support.

This work is supported by the National Institutes of Health [grant 5R01HD29594]; and the Kansas IDeA Network of Biomedical Research Excellence (K-INBRE) [grant P20RR016475].

Chapter 1 - Comparisons of the embryonic development of *Drosophila*, *Nasonia*, and *Tribolium*

Jeremy A. Lynch^{†1}, Ezzat El-Sherif^{†2}, Susan J. Brown³

Introduction

For the past three decades, the fruit fly *Drosophila melanogaster* has served as the premiere model for understanding the molecular basis of developmental patterning mechanisms. In particular, the array of powerful genetic tools available in this organism has allowed the thorough dissection of the events leading to the establishment of cell fates in the *Drosophila* embryo, and the regulatory networks underlying this process stand as the mostly thoroughly characterized among multi-cellular organisms. For those interested in the evolution of developmental mechanisms, the highly detailed description of *Drosophila* embryonic patterning is an appealing starting point for understanding the origin of complex gene regulatory networks, and how these networks can change in the course of evolution.

One of the appealing features of the *Drosophila* embryo as a developmental model system is that, until gastrulation, it can be thought of as a two dimensional Cartesian coordinate system, with the two orthogonal axes (anterior-posterior (AP) and dorsal-ventral (DV)) being patterned independently, but more or less simultaneously. The ability to rapidly establish cell fates representing the entire future organism at this early stage is enabled by maternally localized mRNAs which provide high levels of positional information that can be interpreted and refined by downstream target genes.

The mode of embryogenesis employed by *Drosophila* is termed long germ embryogenesis, which for the purposes of this review is defined by the establishment of all segmental fates at the blastoderm stage prior to gastrulation (Tautz, Friedrich et al. 1994; Davis

[†] These authors contributed equally.

¹ Institute for Developmental Biology, University of Cologne, Cologne, Germany.

² Genetics Program, Kansas State University, Manhattan, KS 66506, USA.

³ Division of Biology, Kansas State University, Manhattan, KS 66506, USA.

and Patel 2002). This is a derived mode of embryogenesis that is only found in scattered species among the Holometabola. Insects of more basally branching lineages use a conceptually different mode of embryogenesis, where only the most anterior segments are specified before gastrulation, while the more posterior segments are generated and patterned progressively from a posterior region called the growth zone. This is termed short, or intermediate germ embryogenesis, depending on the number of segments established at the blastoderm stage (Davis and Patel 2002).

Different approaches have been combined to understand how major transitions in embryonic patterning strategies have occurred in the course of insect evolution. One approach has generated a highly detailed understanding of embryogenesis in an insect employing the ancestral, short/intermediate germ mode of embryogenesis. By comparing this to the derived mode found in *Drosophila*, many insights into how regulatory networks were rewired to pattern a long germ embryo have been revealed. In a complementary strategy, the embryo of an insect that independently derived a long germ mode of embryogenesis has been examined and then compared to *Drosophila* as well as the short/intermediate germ species. This approach has uncovered common strategies underlying the transition from short to long germ embryogenesis.

Two holometabolous insects, the intermediate germ beetle *Tribolium castaneum* and the long germ wasp *Nasonia vitripennis*, have emerged as powerful comparative model organisms with which these topics can be addressed. In this review, we will describe the contributions of these “non-model” models to understanding the evolution of development, and provide perspectives on the bright future such lines of research hold.

A tale of two models: *Nasonia* and *Tribolium*

To enable the characterization of developmental regulatory networks at high enough resolution to make evolutionary comparisons meaningful, tools for identifying, cloning and manipulating genes and their regulatory elements must be available and robust in each comparative model system. The availability of such tools is summarized in Table 1.1 and described in detail below. Access to the fully sequenced genomes of both *Nasonia* and *Tribolium* (Richards, Gibbs et al. 2008; Werren, Richards et al. 2010) facilitates the identification of *Drosophila* gene orthologs, including descriptions of complete gene families, and identification of potential regulatory elements. The main method used to manipulate gene

function in both of these organisms is parental RNA interference (pRNAi) (Bucher, Scholten et al. 2002; Lynch and Desplan 2006). In this technique, *in vitro* synthesized dsRNA of the gene of interest is injected into the abdominal hemocoel of female pupae or adults, where it is taken up by the cells, and leads to the degradation of the target mRNA of interest. If developing oocytes take up the dsRNA the effect perdures in the fertilized eggs (unless the gene knock-down causes adult lethality or sterility), and thus the developmental consequences of reducing the expression of any gene of interest can be examined in embryos or early larvae. This technique is so efficient in *Tribolium* that there is currently an effort underway to knock down and characterize every gene in the genome (Gregor Bucher, personal communication, see <http://ibeetle.uni-goettingen.de/>).

Table 1.1 - Techniques and Tools Available in *Drosophila*, *Tribolium*, and *Nasonia*

	<i>Drosophila</i>	<i>Tribolium</i>	<i>Nasonia</i>
in situ hybridization, immunohistochemistry	Y	Y	Y
Parental RNAi	N	Y	Y
Embryonic RNAi	Y	Y	Y
Germline Transformation	Y	Y	y
Enhancer Trapping	Y	Y	n
Misexpression constructs	Y	Y	n
Amenable to Forward genetics	Y	Y	Y
Ability to screen in F1 generation	N	N	Y
Sequenced Genome	Y	Y	Y
Detailed Transcriptome Data	Y	Y	Y
Availability of Custom Transcriptome Microarray	Y	y	Y

Another critical technique for characterizing developmental networks is the ability to engineer the genome to alter endogenous sequences or express exogenous ones through the use of germ-line transformation. These techniques are well established in *Tribolium* (Berghammer, Klingler et al. 1999), and have been used to perform a genome-wide insertional mutagenesis and enhancer-trapping screen that has yielded many interesting and useful transgenic lines (Trauner, Schinko et al. 2009). Furthermore, techniques for tissue and time specific misexpression have been developed by implementing the GAL4-UAS system in *Tribolium* (Schinko, Weber et al. 2010). The methodology in *Nasonia* is not as advanced, but some promising success has been gained in establishing germ-line transformation in *Nasonia* (Claude Desplan, personal communication).

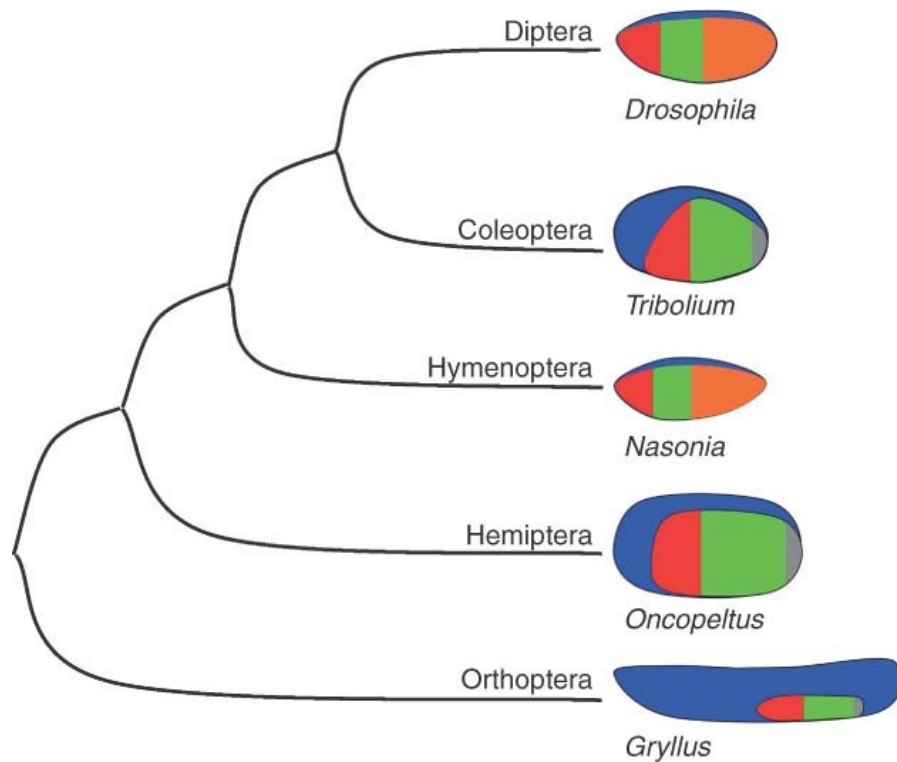
Nasonia has an additional attractive feature, which is its haplo-diploid mode of sex determination. Unfertilized eggs develop as haploid males, allowing mutations affecting embryonic patterning to be rapidly identified by screening the progeny of the F1 generation (Pultz, Zimmerman et al. 2000). A screen employing this method has already provided valuable insight into the mechanisms patterning the *Nasonia* embryo (Pultz, Pitt et al. 1999).

Nasonia and *Tribolium* represent the two most speciose orders of insects (the Hymenoptera and Coleoptera, respectively). Together with *Drosophila*, these three comparative models represent most of the diversity of holometabolous insects. Recent molecular phylogenies place the Hymenoptera at the base of the holometabolous radiation (Figure 1.1), with the Coleoptera and Diptera diverging a relatively short time later. These phylogenetic relationships allow hypotheses concerning the direction of evolutionary change in embryonic patterning as well as trends associated with the different modes of embryogenesis to be tested. For example, characters shared by *Tribolium* and *Drosophila*, but not *Nasonia*, may represent novelties that arose after the divergence of the Hymenoptera from the rest of the Holometabola (alternatively, the character could be ancestral but lost in *Nasonia*), while characters shared by *Nasonia* and *Drosophila*, but not *Tribolium*, might represent common strategies for dealing with the long germ mode of embryogenesis. Any such hypothesis can then be tested by sampling other insect lineages, including more basally branching hemimetabolous species, for the character of interest. The highly detailed understanding of embryonic patterning now obtainable in *Nasonia*, *Tribolium* and *Drosophila* can be used to generate hypotheses that will both broaden and deepen our understanding of how developmental strategies can evolve. Indeed, such studies have

already contributed much to understanding how establishment and patterning of the AP and DV axes of the embryo, as well as the establishment of the germline, have evolved within holometabolous insects.

Figure 1.1 Phylogenetic relationships of selected insect models, and schematic representations of their early embryonic fate maps.

Blue, extraembryonic tissue; red, segments of the head; green, thoracic segments; orange, abdominal segments; and gray, growth zone primordium.



AP polarity and patterning

The AP axis of *Drosophila* is patterned by a hierarchy of regulatory gene functions that progressively increases the resolution and precision of positional information. This process starts with maternal coordinate genes that provide broad, graded information emanating from both ends of the embryo. These gradients are interpreted by the gap genes (the first zygotically activated segmentation genes). The expression domains of these genes subdivide the embryo in large, partially overlapping yet precisely defined blocks, and also provide short-range graded

information. The pair-rule genes interpret these short-range gradients and are expressed in a double segment periodicity to give the first hints of the metameric body plan of the fly. Pair-rule gene expression patterns are then interpreted by the segment polarity genes, which function to establish the borders between, and fates within each segment. Contributions to understanding the evolution of patterning mechanisms at each level of this hierarchy have been made by studying *Tribolium* and *Nasonia*.

Maternal inputs into AP patterning

In *Drosophila*, three maternally derived patterning systems provide spatial information that progressively subdivides the embryo along the anterior-posterior axis: the anterior, posterior, and terminal systems. Two of these systems, the anterior and posterior, rely on localized mRNAs responding to the internal polarity of the oocyte (*bicoid* and *nanos*, respectively), while the terminal system relies on modifications to the eggshell during oogenesis to provide its patterning function (see Figure 1.2). Work in *Nasonia* and *Tribolium* has provided insights into how strategies for providing patterning information may be correlated with the mode of embryogenesis employed.

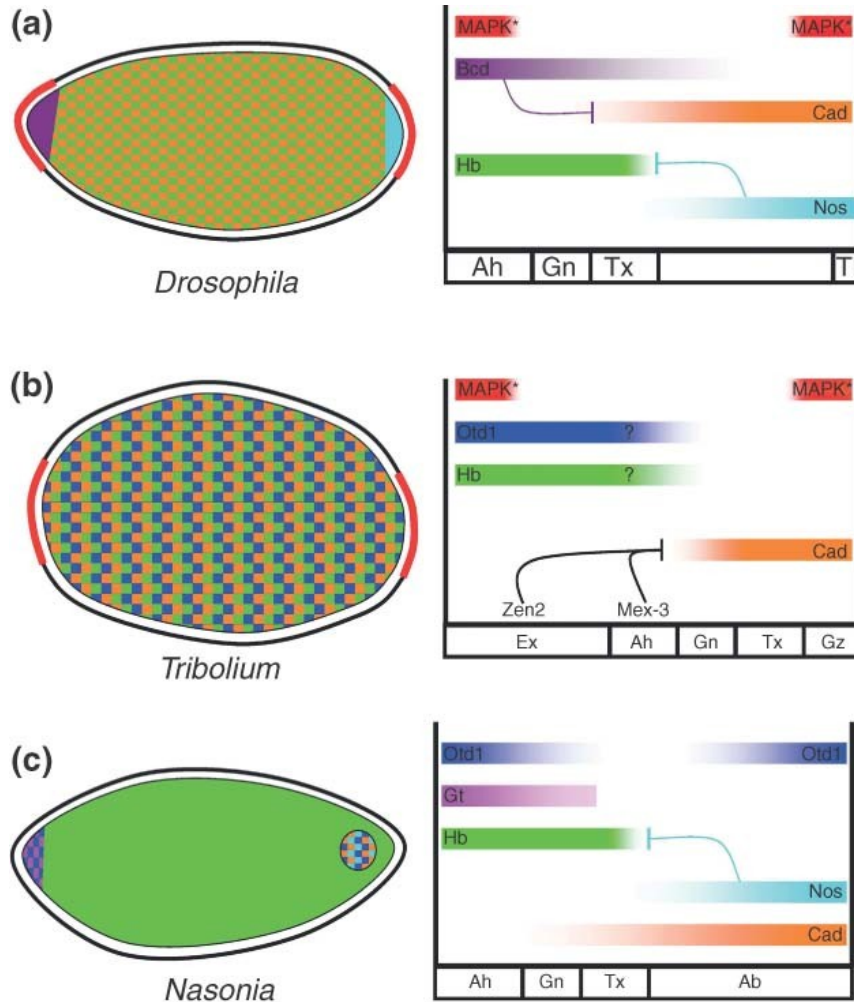
The Anterior system

Establishment of cell fates along AP axis of the *Drosophila* embryo requires a symmetry-breaking event leading to AP polarity and subsequent patterning along the AP axis. In *Drosophila* both steps are provided by *bcd*: anterior localization of *bcd* mRNA provides a symmetry breaking event and its translation into a protein gradient along the AP axis provides positional information to the gap genes for patterning.

Figure 1.2 Maternal provision of anterior-posterior (AP) patterning information in *Drosophila*, *Tribolium*, and *Nasonia*.

Left: schematic representation of *Drosophila* (a), *Tribolium* (b), and *Nasonia* (C) embryos showing distribution of maternally provided mRNAs. Right: representation of resulting protein gradients. Red curves in left panel on (a) and (b) represent the distribution of *tsl* expression, and correspond with the red bars at right representing the resulting activation of MAP kinase in the embryo. Question marks for Otd and Hb in panel (b) indicate their now doubted role in providing

positional information to the early embryo. Ab, abdomen; Ah, anterior head; Gn, gnathal; Gz, growth zone; Tl, telson; Tx, thorax.



The Bcd gradient of *Drosophila* acts as a morphogen with both permissive and instructive functions that provides positional information along most of the length of the embryo. The permissive function of the Bcd gradient arises from the ability of this protein to bind and repress translation of *caudal* mRNA into protein where it would interfere with anterior development (Dubnau and Struhl 1996; RiveraPomar, Niessing et al. 1996). The instructive function arises from the differential sensitivity of AP target genes to Bcd concentration, such that the expression of genes that respond to low levels of Bcd extends further towards the posterior, while the expression of those that are less sensitive is restricted to the anterior (Driever and

Nusslein-Volhard 1988; Driever, Thoma et al. 1989). Although essential to AP patterning in *Drosophila*, *bcd* is an evolutionary novelty of higher Diptera (Stauber, Jackle et al. 1999). It is derived from the Hox cluster, but unlike most Hox proteins, possesses a Lysine (K) at position 50 of its homeodomain, giving it a distinct DNA binding affinity in comparison to typical Hox homeodomains which possess a glutamine (Q) at this position (Treisman, Gonczy et al. 1989).

Localized mRNAs, in combination with permissive and instructive protein functions, are also critical in patterning the anterior half of the *Nasonia* embryo (da Fonseca, Lynch et al. 2009). *Nv-orthodenticle1* (*Nv-otd1*) mRNA is tightly localized to the anterior (and posterior, see below) pole of the embryo (Lynch, Brent et al. 2006), where a gradient of translated protein performs the instructive function (Figure 1.2). pRNAi against *Nv-otd1* significantly shifts the anterior fatemap, resulting in the loss of all head segments, including some thoracic segments in the most extreme cases. *Nv-otd1* does not act alone, but rather cooperates with *Nv-hunchback* (*Nv-hb*) in activating target genes. This is similar to the cooperation of Bcd with Hb in activating anterior target genes in *Drosophila*, and indicates that cooperation between K50 homeodomain proteins and Hb is an ancient strategy for anterior patterning in holometabolous insects (Lynch, Brent et al. 2006) (Figure 1.2).

No clear analog of the permissive function of Bcd has been identified for Nv-Otd1, which is not surprising, given the posterior localization of *Nv-cad* mRNA (see below). However, an anteriorly localized, permissive patterning factor with novel function has been found in the wasp. *Nv-giant* (*gt*) mRNA is localized to the anterior pole of the oocyte (Figure 1.2). After egg activation it disperses, forming a cap of *Nv-gt* mRNA at the anterior pole at the early blastoderm stage. Once translated into protein, this early source of Nv-Gt is critical to prevent the expansion of *Nv-Kr* and concomitant loss of *Nv-hb* expression in the anterior half of the embryo (Brent, Yucel et al. 2007). When *Nv-gt* and *Nv-Kr* are knocked down simultaneously, most of the anterior patterning defects seen in *Nv-gt* single pRNAi, are rescued, demonstrating that the primary function of maternal *Nv-gt* is to prevent the expression of *Nv-Kr* in the anterior half of the embryo, either by repressing it directly or indirectly through activation of *Nv-hb*.

The situation in *Tribolium* appears to differ significantly from what has been observed in *Nasonia* and *Drosophila*. This is likely due, at least in part, to differences in the blastodermal fate map of short/intermediate type embryos. Instead of many head segments that require high levels of patterning information to set their borders, most of the anterior end of the *Tribolium*

embryo is devoted to extraembryonic cell fates, fates that are restricted to the dorsal side of the embryo in *Drosophila* and *Nasonia*. Thus, it is not clear whether *Tribolium* needs the high levels of patterning information provided by localized mRNAs as in *Nasonia* and *Drosophila*.

However, positional information is needed in *Tribolium* at least to specify the border between embryonic and extraembryonic tissues. It was proposed that *Tribolium orthodenticle1* (*Tc-otd1*), which is provided maternally and appeared to result in an anterior to posterior protein gradient due to translational repression (Schröder 2003) (Figure 1.2), along with hunchback act as bicoid-like morphogens in *Tribolium*. Recently, doubt has been cast on the putative role of *Tc-otd1* in providing positional information along the AP axis (Marques-Souza, Aranda et al. 2008; Kotkamp, Klingler et al. 2010). However, anteriorly localized mRNAs have been found in *Tribolium* (Bucher, Farzana et al. 2005), and seem to have effects on early fatemap (S. J. Brown, manuscript under preparation).

The Posterior System

In *Drosophila*, posterior patterning relies on two major maternal factors: *caudal* (*cad*) and *nanos* (*nos*) (Figure 1.2). Together these two genes, acting in distinct ways, ensure proper specification of abdominal fates: *cad* encodes a transcription factor that activates posterior target genes, while *nos* encodes a translational factor that acts permissively for abdominal specification. Both of these genes are conserved in *Tribolium* and *Nasonia*, and analyses of their functions have revealed both conserved and divergent strategies for patterning the posterior segments in insects.

caudal function and regulation

In the early *Drosophila* embryo, ubiquitous maternal *cad* mRNA, translationally repressed by the Bicoid gradient, produces a reciprocal Cad gradient (Dubnau and Struhl 1996; RiveraPomar, Niessing et al. 1996). The posterior patterning function of Cad provides activating input to pair-rule genes to form posterior stripes but only weakly activates posterior gap genes. It does not appear to act as a morphogen, and it seems that the repressive function of Bcd on *cad* mRNA is mainly to prevent ectopic Cad from disrupting head patterning (Mlodzik, Gibson et al. 1990).

Nv-cad mRNA is localized to the posterior pole of the oocyte, and upon egg laying it diffuses, forming a posterior to anterior gradient. This posterior localization of maternal *Nv-cad*

obviates the need for translational repression at the anterior. *Nv-cad* has a more fundamental role in patterning the wasp embryo, as the strongest mutant and pRNAi phenotypes delete all abdominal and thoracic segments, while the strongest *Drosophila cad* mutants have variable defects restricted to the abdomen. (Olesnicky, Brent et al. 2006) In addition, *Nv-cad* functions higher in the patterning hierarchy than does its fly counterpart, as it is absolutely required for the proper expression of posterior gap genes (Olesnicky, Brent et al. 2006).

caudal also plays a critical role in patterning most of the segmented embryo in *Tribolium*. At the embryonic stage just prior to the onset of gastrulation (termed differentiated blastoderm stage), there are three developmentally distinct regions: the extraembryonic membrane primordia, the anterior head (pregnathal), and segmented germband (that part of the embryo patterned by pair-rule genes, including gnathal and trunk segments). *Tc-cad* is responsible for specifying this last region (Figure 1.2); its knock down leads to the complete loss of posterior head and all trunk segments. The phenotype, even more severe than that of *Nv-cad* RNAi, is also observed in most non-*Drosophila* insects (Wilson, Havler et al.; Shinmyo, Mito et al. 2005), indicating a larger ancestral role for Caudal in general body patterning. An important downstream target of Tc-Cad is likely to be *Tc-even-skipped* (*Tc-eve*), a gene which is critical for the maintenance of the progressive segmentation process of *Tribolium* (see below the section on pair-rule genes).

As is the case for its *Drosophila* and *Nasonia* orthologs, Tc-Cad function must be repressed in the anterior regions of the embryo. However, *Tribolium* does not contain a *bcd* ortholog and *Tc-cad* mRNA is not posteriorly localized as it is in *Nasonia*. The beetle uses another strategy: two zygotically activated genes, *Tc-mex3*, expressed in the anterior head primordia, and *Tc-zen2*, expressed in the serosal anlage (the anteriormost extraembryonic region), are required to repress Tc-Cad protein production in these regions of the differentiated blastoderm embryo. Interestingly, the *C. elegans* ortholog of *Tc-mex3* is also involved in translational regulation of the worm *cad* ortholog, indicating that this mechanism for regulating *cad* expression along the AP axis was in place in at least the common ancestor of the Ecdysozoa (van der Zee, Berns et al. 2005; Schoppmeier, Fischer et al. 2009).

nanos regulation and function

In the fly, localization of *nanos* (*nos*) mRNA to the posterior pole of the embryo is critical for proper patterning of the abdominal segments. Only localized *nos* mRNA (which

represents just 4% of total *nos* mRNA present in the embryo) is translated (Bergsten and Gavis 1999), giving rise to a gradient of Nos protein in the posterior half of the embryo that represses translation of maternal *hb* mRNA, which would, if translated, interfere with posterior gap gene regulation, and result in the disruption of posterior abdominal segments (Lehmann and Nusslein-Volhard 1991). Localization of *nos* mRNA occurs late in oogenesis and depends on properly assembled germ plasm (Ephrussi, Dickinson et al. 1991). Thus, *osk*, *vas*, and *tudor* mutants have abdominal defects identical to that of *nos*.

So far no expression or functional data have been presented for *nos* in *Tribolium*, so it is not clear what, if any, role this factor plays in patterning the beetle embryo. Intriguingly, Nanos Response Elements (NREs), the sequence motifs through which Nanos exerts its repressive influence, have been detected in the 3' UTRs of both *Tc-otd1* and *Tc-hb*, and both of these genes show evidence of translational repression at the posterior pole (Wolff, Sommer et al. 1995; Schröder 2003). However, the functional significance of these NREs requires further validation.

In *Nasonia*, *Nv-otd1* and *Nv-hb* mRNAs both also possess NREs in their 3' UTRs, and both also show posterior translational repression (Pultz, Westendorf et al. 2005; Lynch, Brent et al. 2006). *Nasonia nanos* (*Nv-nos*) mRNA is localized to the posterior pole, in the oosome, a structure that is the wasp equivalent of polar granules in the fruitfly. When *Nv-nos* is knocked down via pRNAi, the domain of maternal Nv-Hb protein expression expands to the posterior pole, revealing that the role of *Nv-nos* in repressing *Nv-hb* translation is conserved with its *Drosophila* ortholog. *Nv-nos* pRNAi also leads to the misregulation of posterior gap genes, and the eventual loss of posterior segments in the larva (Lynch and Desplan 2010).

Regulation of the localization and function of *Nv-nos* shows some conservation with, as well as significant divergence from, the strategies employed in *Drosophila*. Like their *Drosophila* counterparts, *Nv-vas* and *Nv-osk* are required for the proper translation of *Nv-nos* mRNA at the posterior. Also as in the fly, this function of germ plasm genes seems to be in opposition to the activity of *smaug*, which represses translation of unlocalized *nos* mRNA (Smibert, Wilson et al. 1996). A major difference between the wasp and fly is that while *nos* localization in *Drosophila* is completely abolished in germ plasm deficient mutants, *Nv-nos* shows significant posterior localization after *Nv-vasa* or *Nv-osk* pRNAi, despite the absence of the oosome. Another major difference in the function of *Nv-nos* is that its action is delayed due to maternal provision of Nv-Hb protein, which is absent in *Drosophila*, but which is also found

in the holometabolous locust *Schistocerca* (Patel, Hayward et al. 2001). The lack of maternal Hb protein may have been important to the evolution of the rapid early syncytial cleavage divisions prior to blastoderm formation in *Drosophila*, which are considerably more rapid than in *Nasonia*.

The terminal system

In addition to the Bcd gradient, the terminal system is involved in patterning the termini of *Drosophila* embryo (Sprenger 1993). *torso*, encoding a receptor tyrosine kinase (Sprenger, Trosclair et al. 1993), and its ligand *trunk* are provided maternally and ubiquitously to the embryo (Casanova, Furriols et al. 1995). Spatial specificity for the system is first provided by the expression of *torso-like* (*tsl*) in the anterior and posterior follicle cells during oogenesis (Stevens, Frohnhofner et al. 1990), and later by incorporation of Tsl protein into the vitelline membrane (Stevens, Beuchle et al. 2003). *tsl* is required for production of the active form of *trunk*, by a still unknown mechanism, which defines the regions of terminal system activity at both embryonic poles (Furriols and Casanova 2003; Li 2005). Targets of Torso signaling include the terminal gap genes *tailless* (*tll*) and *huckebein* (*hkb*) (Weigel, Jurgens et al. 1990), which are initially expressed in caps covering both anterior and posterior poles. Both *tll* and *hkb* are important in patterning the unsegmented posterior region, the posterior abdominal segments, and the head (Jurgens 1993) (however, it was shown that in case of increased *bcd* expression, the terminal system is dispensable for head development (Schaeffer, Killian et al. 2000)).

In *Tribolium*, *Tc-tsl* is activated in the follicle cells located at both ends of the oocyte. Both *Tc-torso* and *Tc-tsl* knockdown result in the same defects at both embryo poles (no serosa is formed anteriorly, and no post-blastodermal segments emanate from posterior), indicating that Torso signaling plays similar roles in beetles and flies (Schoppmeier and Schröder 2005). However, *Tc-tll* is activated only at the posterior terminus in the early blastoderm. Only later, in the germ rudiment, is it activated in the head (Schröder, Eckert et al. 2000) (note that the *Tribolium* head anlage is located mid-embryo and not at the anterior pole, as in *Drosophila*). This indicates that the terminal system must signal through a gene other than *Tc-tll*. Torso signaling at the posterior pole of the *Tribolium* embryo is required for both Wnt signaling and zygotic activation of *Tc-cad* (with the possibility that Torso signaling is regulating zygotic *Tc-cad* through Wnt signaling), and thereby affecting post-blastodermal segmentation (Schoppmeier and Schröder 2005). However, it is not known whether this posterior action of Torso signaling is

carried out through *Tc-tll*. Anterior Torso signaling is required for *Tc-zen1* activation, and hence its importance in serosa formation.

An ortholog of *tailless* is expressed at the posterior pole and in the head anlage at the anterior during the blastoderm stages of *Nasonia* (Lynch, Olesnický et al. 2006). However, these expression domains are not regulated by the *torso* signaling cascade, as no ortholog of *trunk* could be found in the *Nasonia* genome, and activated MAP kinase is not observed at the poles of the embryo (JAL, personal observation). Rather, both the anterior and posterior domains of *Nv-tll* depend on *Nv-otd1* for their activation (Lynch, Olesnický et al. 2006). The terminal system is also lacking in the honey bee *Apis mellifera* (Wilson and Dearden 2009), indicating that either the terminal system originated after the divergence of Coleoptera and Diptera from the Hymenoptera, or that the terminal system was lost specifically in the Hymenoptera. Sampling from more basally branching hemimetabolous lineages will be required to resolve this question.

Gap genes

In the fly, the gap genes function at the second level of the embryonic AP patterning hierarchy, and are generally the first zygotic genes to interpret the maternal gradients. The transcription factors encoded by the gap genes form short-range gradients that are generally mutually repressive, leading to precise overlap of opposed gradients. Loss of gap gene function leads to the misregulation of downstream pair-rule genes and the loss of one or more contiguous blocks of segment primordia. In addition to their role in regulating pair-rule genes, gap genes also regulate the domains of Hox gene expression (Akam 1987; RiveraPomar and Jackle 1996).

Although limited, the data on the function of gap genes in *Nasonia* indicate that their functions and interactions are generally similar to their fly counterparts. In the first functional study of *Nasonia* embryogenesis, a number of potential gap gene mutations were identified by their phenotypic similarity to fly mutants, (Pultz, Zimmerman et al. 2000). One of these has been identified as a mutation in the *Nasonia hunchback* (*Nv-hb*) ortholog (Pultz, Westendorf et al. 2005). This mutation is of particular interest, since it affects only zygotic expression of the protein, yet results in a loss of segments (all of the head and most thorax) that is greater than the combined loss of maternal and zygotic contributions of *hb* in the fly. pRNAi against *Nv-Kr* and *Nv-gt* also showed that these genes possess canonical gap gene functions, and act at similar

positions along the AP axis as their fly homologs (Brent, Yucel et al. 2007; Lynch and Desplan 2010).

The mutually repressive interactions between gap genes also appear to be conserved in *Nasonia*, at least those between *Nv-Kr* and *Nv-hb*. In cases where the domain of either of these genes is altered by pRNAi or mutant backgrounds, the other expands or contracts to maintain a sharp border between the posterior edge of the *Nv-hb* domain and the anterior edge of the *Nv-Kr* domain (Brent, Yucel et al. 2007).

Tribolium orthologs of *hunchback*, *giant* and *Krüppel* are required for proper segmentation in the beetle (Bucher and Klingler 2004; Cerny, Bucher et al. 2005; Marques-Souza, Aranda et al. 2008). Surprisingly, *Tc-knirps* is important for head development but has only a minor effect on trunk segmentation (Cerny, Grossmann et al. 2008). In addition, a newly identified gap gene, *milles-pattes (mlpt)* (Savard, Marques-Souza et al. 2006) is unusual in that it encodes a series of small peptides, rather than a transcription factor.

In wildtype beetle embryos, the expression of *Tc-hb*, *Tc-gt*, *Tc-Kr* and *Tc-mlpt* changes dynamically between their initiation in the blastoderm stage and their resolution into domains covering one or more segments in the head and germband. *Tc-hb*, provided maternally, is found ubiquitously then clears from the posterior end. This early expression domain resolves to the serosa, while a new posterior blastoderm domain arises and resolves to the anterior head through first thoracic segment. Finally, a domain arises in abdominal segments A7 through the posterior end of the germband as those segments are added (Wolff, Sommer et al. 1995). *Tc-gt* is also expressed in a broad blastoderm domain that resolves to cover the anterior head as well as the mandibular and maxillary segments. An additional *Tc-gt* domain arises at the posterior pole of the embryo in the growth zone, the region from which the abdominal segments arise. As the germband elongates this domain broadens and splits into two stripes, one in third thoracic segment (T3) the other in the second abdominal segment (A2) (Bucher and Klingler 2004). *Tc-Kr* expression initiates in the posterior blastoderm, eventually resolving to cover the thorax (Cerny, Bucher et al. 2005). *Tc-mlpt* expression initiates in the blastoderm and resolves into domains covering the anterior head and mandibular segment, T2 – A4, and a small domain in A7 (Savard, Marques-Souza et al. 2006).

Although on the surface, gap gene functions in *Tribolium* appear similar to those of their *Drosophila* and *Nasonia* counterparts, in the end they are quite different. As in *Nasonia* and

Drosophila, *Tribolium* gap genes are expressed in domains that overlap several segment primordia, show some evidence of cross-regulation (see Figure 1.3 for a comparison between expression domains and regulatory relationships between gap genes in both *Drosophila* and *Tribolium*), and regulate pair-rule and homeotic genes to some extent. Their loss of function through RNAi or mutation leads to large patterning gaps in the resulting cuticles. However, careful analysis of the segmentation process during embryogenesis revealed that these apparent deletion phenotypes are actually combinations of germband truncation (halted elongation) and homeotic transformations (Cerny, Bucher et al. 2005; Marques-Souza 2007; Marques-Souza, Aranda et al. 2008; Kotkamp, Klingler et al. 2010) (see Figure 1.4 for a comparison between gap genes phenotypes of *Drosophila* and *Tribolium* and Figure 1.5 for Hox genes expression patterns for *Tribolium* in wildtype as well as gap genes mutants or RNAi embryos). Moreover, only very few pair-rule stripes appear to be specifically regulated by particular gap genes (S. J. Brown and M. Klingler, unpublished data), and most pair-rule pattern changes can be explained by halted elongation.

Figure 1.3 Comparison of gap gene expression patterns and their regulatory relationships in *Drosophila* and *Tribolium*.

Top panel: late blastodermal expression patterns of gap genes (nonterminal, nonhead) in *Drosophila* and their regulatory relationships. Bottom panel: postblastodermal expression patterns of gap genes (nonterminal, nonhead) in *Tribolium* after they emanate from the growth zone and before they fade, and a parsimonious interpretation of their regulatory relationships. An arrow represents positive regulation and a blunt line represents negative regulation. A, abdominal segment; G, gnathal segment; T, thoracic segment.

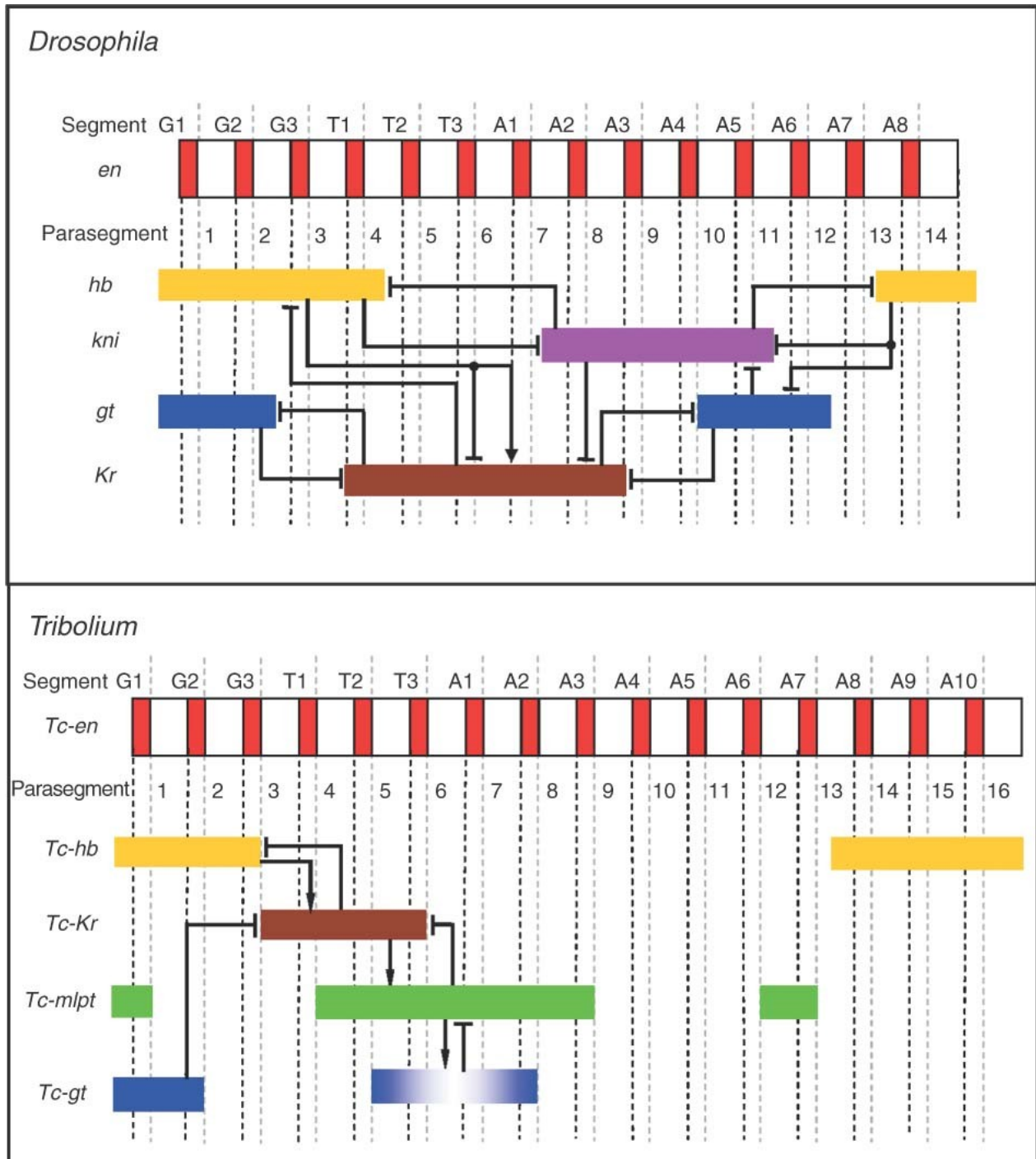


Figure 1.4 Comparison of gap genes phenotypes in *Drosophila* and *Tribolium*.

Expression of *Krüppel* (in blue) and *engrailed* (in red) and the resulting larval cuticles (bottom of each panel) in wild-type (WT; left of each panel) and *Krüppel* mutants (right of each panel). Left

panel (*Drosophila*): The strongest *Krüppel* phenotype in *Drosophila* results in loss of seven segments (marked by stars) within the expression domain of the gene *Krüppel*, which is a typical ‘gap’ phenotype. Right panel (*Tribolium*): In the *Krüppel* mutant (*jaws*), the segments within the *Tc-Krüppel* expression domain (marked by stars) form properly, and only a few more posterior segments develop, which are disorganized at first but later regulate to form intact segments. In addition to this ‘truncation’ phenotype, a homeotic transformation is observed in the larval cuticle, in which the three thoracic segments and the first abdominal segment are transformed to gnathal identity (maxillary-labial-maxillary-labial). This phenotype is best described as ‘truncation plus homeosis’, rather than ‘gap’. The yet unexplained ‘truncation after expression domain’ of *Tribolium* gap genes in contrast to ‘gap within expression domain’ of *Drosophila* is proved valuable here to show clearly the homeotic effect of gap genes phenotypes in *Tribolium*, whereas it is precluded by the loss of segments in *Drosophila* (except for some hypomorphic mutants).

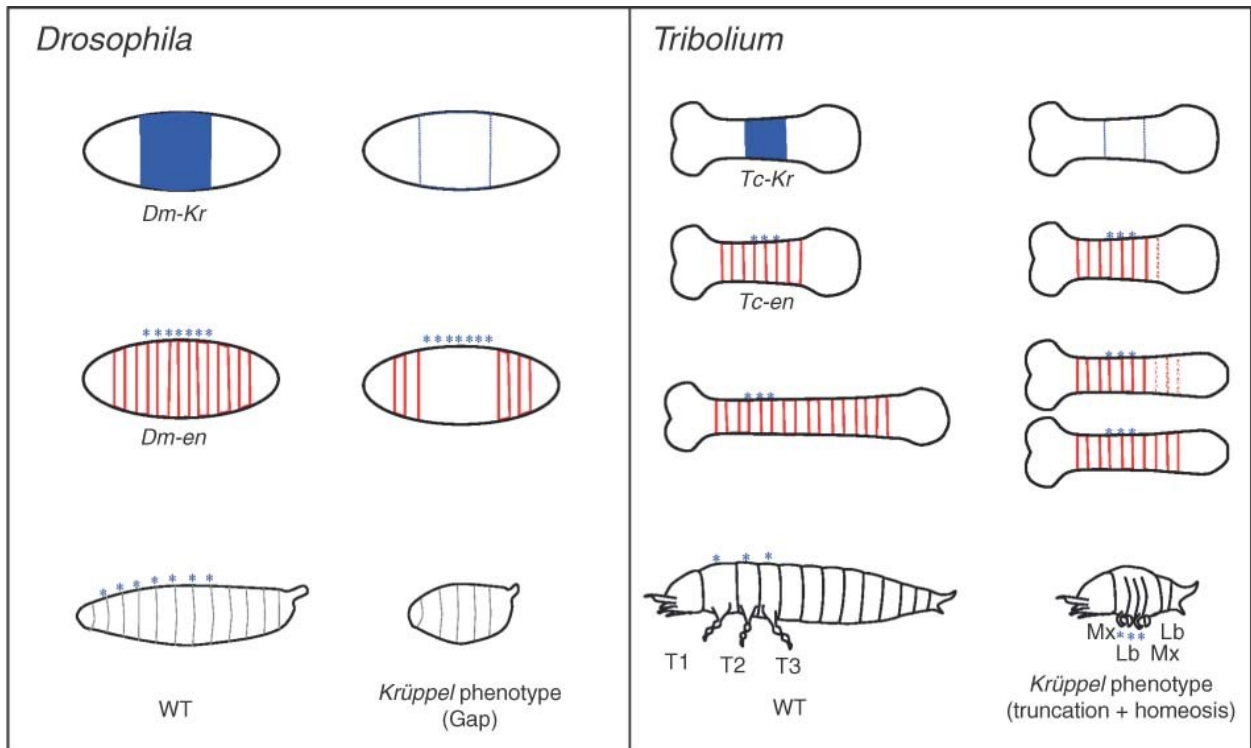
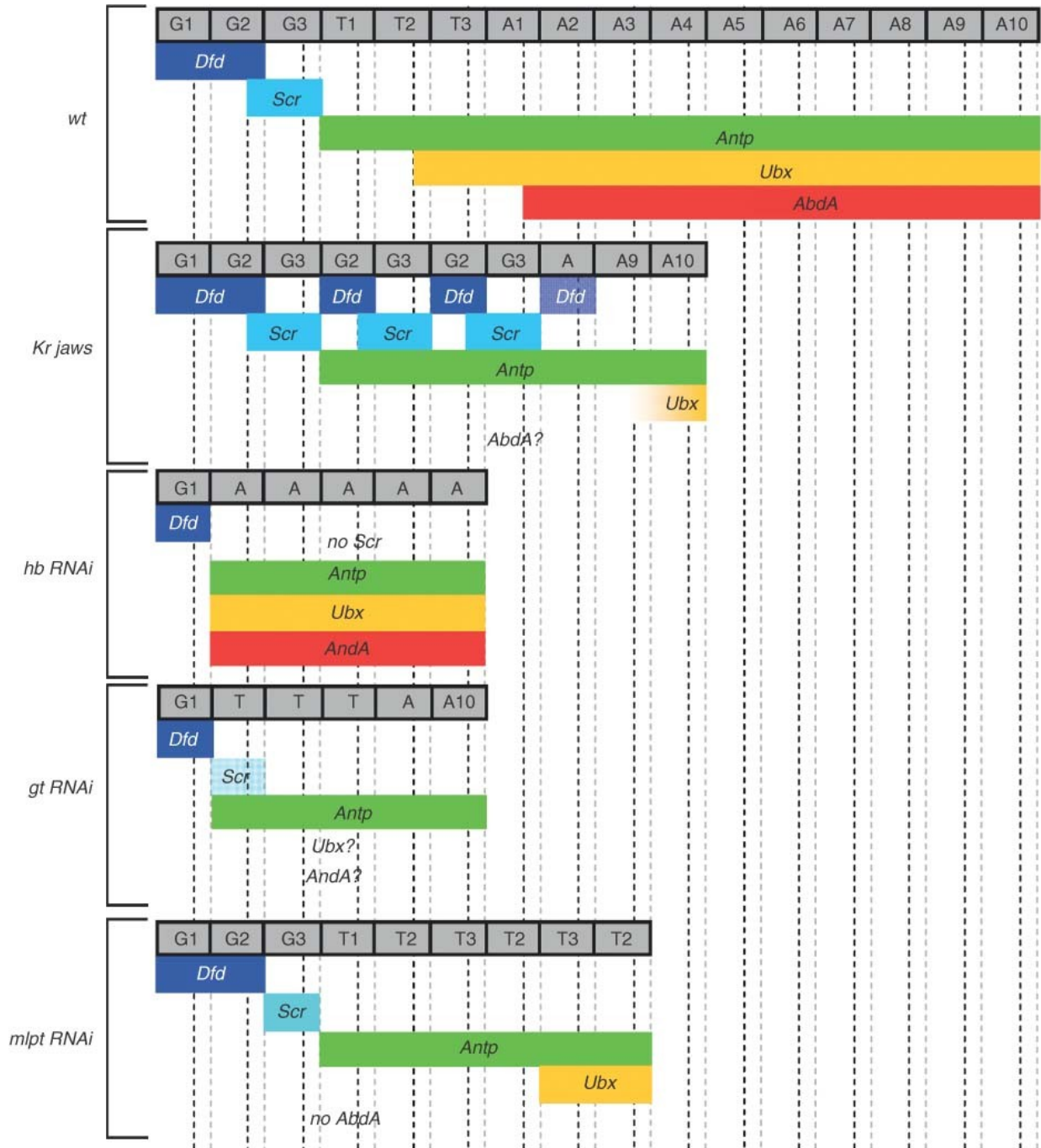


Figure 1.5 Hox gene expression in wild type (wt) and gap gene RNAi and mutant embryos.

The identity of segments that are formed is described in the gray boxes at the top of each panel. Diluted color in an expression domain indicates reduced expression. A question mark means the

expression domain is not reported in literature. A, abdominal segments; G, gnathal segments; T, thoracic segments.



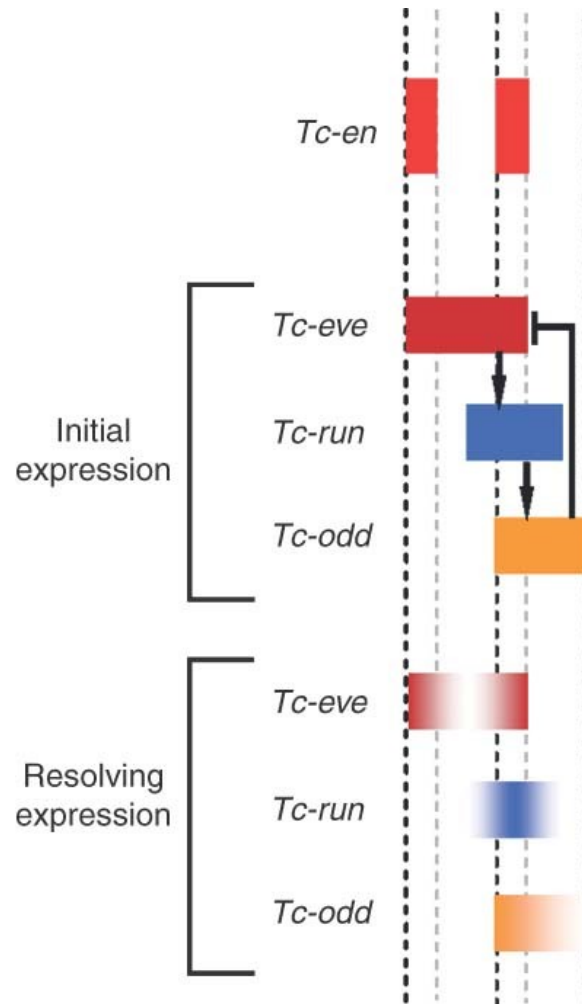
Pair-rule genes

Seven stripes of primary pair-rule gene expression (*even-skipped*, *runt* and *hairy*) are positioned in the *Drosophila* blastoderm by input from specific combinations of maternal and gap genes (Small, Kraut et al. 1991). These primary pair-rule genes interact to regulate one another and the secondary pair-rule genes (*ftz*, *odd*, *odd-paired*, *paired* and *slp*) (Ingham and Gergen 1988; Gutjahr, Vanario-Alonso et al. 1994; Fujioka, Jaynes et al. 1995). A complex network of interactions between primary and secondary pair-rule genes has been described (Sanchez, Chaouiya et al. 2008) that positions stripes of the segment polarity genes *wingless* (*wg*) and *engrailed* (*en*) to define the borders between segments. Although the use of *wg* and *en* to define segmental boundaries is highly conserved, the expression patterns and functions of pair-rule gene orthologs differ greatly among insects and arthropods (Damen 2007).

Similar to their *Drosophila* counterparts, *Tribolium* pair-rule genes are expressed in patterns of double segment periodicity (Sommer and Tautz 1993; Patel, Condrón et al. 1994; Choe, Miller et al. 2006; Choe and Brown 2007). However, in contrast to the simultaneous formation of pair-rule gene stripes in the *Drosophila* blastoderm, the *Tribolium* orthologs of *Drosophila* pair-rule genes are expressed in stripes sequentially from anterior to posterior, starting in the blastoderm and continuing during germband elongation. RNAi studies revealed that certain genes, *Tc-ftz*, *Tc-hairy* and *Tc-odd-paired*, are not required for proper segmentation, despite their striped expression patterns (Choe, Miller et al. 2006; Aranda, Marques-Souza et al. 2008). Classical pair-rule phenotypes are observed in *Tc-prd* and *Tc-slp* RNAi or mutant embryos (Maderspacher, Bucher et al. 1998; Choe and Brown 2007), but depletion of *Tc-even-skipped* (*Tc-eve*), *Tc-runt* (*Tc-run*) or *Tc-odd-skipped* (*Tc-odd*) leads to loss of all (in the case of *Tc-eve*) or almost all (in the case of *Tc-run* and *Tc-odd*) gnathal and trunk segments (Choe, Miller et al. 2006). Epistasis analysis revealed a negative feedback loop in which *Tc-eve* activates *Tc-run*, which activates *Tc-odd*, which in turn represses *Tc-eve* (Choe, Miller et al. 2006) (Figure 1.6) (however, this analysis was done using pupal injection; so while this verifies the circuit in the blastoderm phase, it is yet to be verified in the germband phase using embryonic injection). This negative feedback loop could serve as a self-regulatory segmentation mechanism, employing no or little cues from upstream maternal or gap genes. This is in contrast to the fly case, where pair-rule genes are under strict control of upstream maternal and gap genes.

Figure 1.6 Initial and resolving expressions of primary pair-rule genes in *Tribolium*.

A negative feedback loop between the three primary pair-rule genes *Tc-eve*, *Tc-run*, and *Tc-odd* are responsible for their initial double-segmental periodic expression. Later, they resolve into segmental periodic expression through a yet-to-be-identified genetic mechanism. This later segmental primary pair-rule expression regulates downstream genes to ultimately position segment polarity genes. An arrow represents positive regulation and a blunt line represents negative regulation. A, abdominal segment; G, gnathal segment; T, thoracic segment. It is worth noting that these regulatory relationships were verified for the anteriormost segments. Further experiments are needed to verify it for the following segments (using embryonic RNAi).



Components of this negative feedback loop in *Tribolium* are categorized as primary pair-rule genes, since the depletion of any one of the three affects the expression of the other two, as well as the expression of *Tc-prd* and *Tc-slp*, which, hence, are categorized as secondary pair-rule genes. Although the functions of *prd* and *slp* are conserved in that they regulate segment polarity genes in both beetles and flies, the evolutionary flexibility of these modules is reflected in the register of *slp* function; it is necessary for odd-numbered *en* stripes in flies, but for even-numbered stripes in beetles (Choe and Brown 2007). In *Drosophila*, stripes of *en* expression are precisely positioned by *eve* in odd-numbered segments and by *ftz* in even-numbered segments through complex interactions with several secondary pair-rule genes (Sanchez, Chaouiya et al. 2008). As noted above, the beetle orthologs of many of these genes are not required for proper segmentation. However, *Tc-eve* may regulate segment polarity genes in every segment since it can, in combination with *Tc-prd* or *Tc-runt*, activate *Tc-en* (Choe, Miller et al. 2006; Choe and Brown 2007). It is not known if other, as yet unidentified, genes function as secondary pair-rule genes in *Tribolium*. However, the different interactions between pair-rule genes that have evolved in beetles and flies still produce the same outcome; juxtaposed stripes of *wg* and *en* that define the segmental boundaries. This underscores the evolutionary modularity of the segmentation gene network in insects.

So far the only pair-rule ortholog described from *Nasonia* is *Nv-paired* (*prd*). Unlike its fly ortholog, *Nv-prd* expression initiates progressively from anterior to posterior, and shows no classical pair-rule expression, rather it appears in segmental stripes that alternate between strong and weak expression (Keller, Desplan et al. 2010). However, it is likely that genes with pair-rule functions exist in *Nasonia*, as several mutants with classic pair-rule phenotypes have been identified (Pultz, Zimmerman et al. 2000). Preliminary evidence also indicates that the pattern of pair-rule expression is similar to that of the honey bee, where pair-rule stripes are initiated progressively from anterior to posterior (Binner and Sander 1997). In addition, the most posterior abdominal segments may not be patterned by the pair-rule paradigm, as only six pair-rule stripes are observed at the blastoderm stage; the later segmental stripes appear to progressively split from the most posterior pair-rule stripe (Binner and Sander 1997) (Claude Desplan, personal communication). This may indicate that elements of the progressive growth and patterning that typify short germ embryogenesis are maintained in many “long-germ” embryos.

Segment polarity genes

Once segment polarity genes have been activated by pair-rule genes in *Drosophila*, their expression is maintained through a gene circuit including the transcription factor En, and two signaling pathways, Wnt and Hedgehog (DiNardo, Heemskerk et al. 1994). En and the components of the signaling pathways are highly conserved and have been identified in the both *Nasonia* and *Tribolium*. In *Tribolium*, RNAi analysis indicates both the Wnt and Hedgehog pathways play conserved roles in the segment polarity gene module (Oppenheimer, MacNicol et al. 1999; Farzana and Brown 2008; Choe and Brown 2009).

In *Tribolium*, loss of canonical Wnt signaling via depletion of *Tc-arrow* (which encodes a co-receptor for canonical Wnt pathway) or *Tc-procupine* (which encodes a Wnt ligand processing component), leads to germband truncation in the growth zone (Bolognesi, Fischer et al. 2009). Detailed RNAi analysis revealed that multiple Wnts, specifically Wnt1 and WntD/8, are involved in posterior growth and patterning (Bolognesi, Farzana et al. 2008). Additional studies will be required to determine the molecular mechanisms sensitive to Wnt signaling in the growth zone, but the need for a posterior source of Wnt signaling is conserved in other short germ insects (Miyawaki, Mito et al. 2004; Angelini and Kaufman 2005), other arthropods (McGregor, Pechmann et al. 2008) and indeed most other metazoans (Martin and Kimelman 2009). Interestingly, although *wg* is expressed at the posterior pole of *Drosophila* eggs, it is not required for germband elongation or posterior patterning; mutations in genes encoding Wnt pathway components lead to segment polarity defects (Nusse 2005).

Homeotic genes

Homeotic genes were the basis of the first “evo-devo” studies in many organisms (Angelini and Kaufman 2005), and like most insects examined to date, *Drosophila*, *Nasonia* and *Tribolium* contain a single complement of homeotic genes, including *labial*, *maxillopedia*, *Deformed*, *Sex combs reduced*, *Antennapedia*, *Ubx*, *abd-A* and *Abd-B*. As in other organisms, they direct regional development along the AP axis. Their expression domains are similar in beetles and flies, and loss of function phenotypes affect similar body regions. In homeotic mutants, one developmental fate is replaced by another; thus, legs may appear where mouth parts should be (Shippy, Brown et al. 2000), depending on the resulting combination of homeotic

genes expressed there (one exception to this is *Tc-labial* in *Tribolium*, which upon RNAi leads to deletion of the respective segment: intercalary (Posnien, Bashasab et al. 2009)). In addition to specifying a specific regional identity along the AP axis, homeotic genes also repress anterior development; complete loss of homeotic gene function in a particular segment or region results in antennae developing on that segment or the segments in that region (Brown, Shippy et al. 2002), and in the most extreme case, antennae develop on every segment (Stuart, Brown et al. 1991).

DV patterning

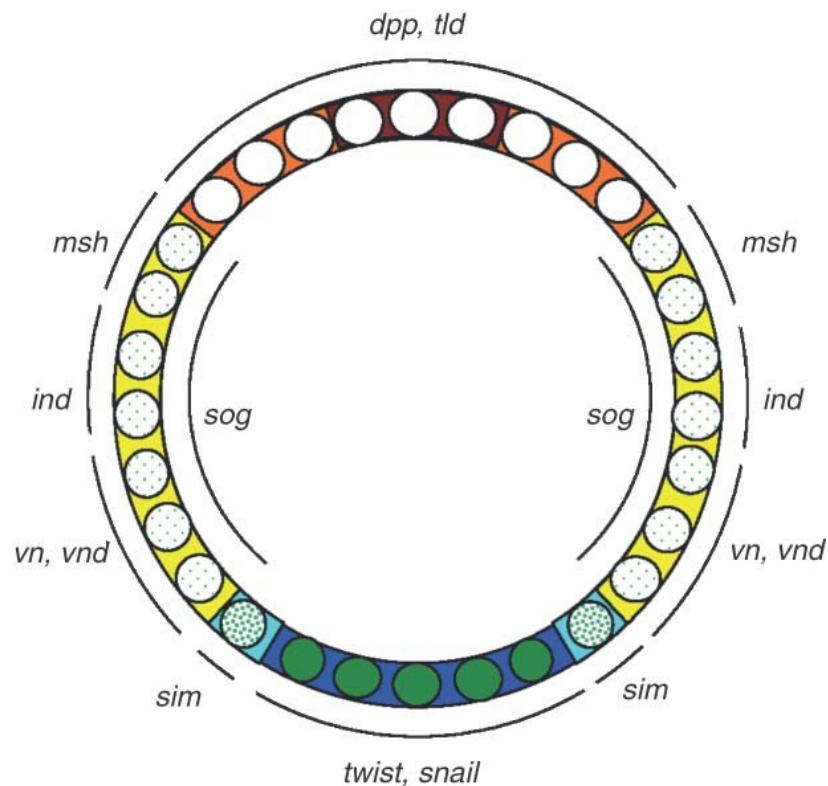
A key player in patterning the DV axis in *Drosophila* is the NFκB transcription factor Dorsal. Dorsal protein is expressed in all cells of the early *Drosophila* embryo. However, its nuclear uptake occurs in the form of a gradient with maximal levels on the ventral side of the embryo (Steward, Zusman et al. 1988). The differential expression of Dorsal target genes define various cell fates (broadly, the mesoderm, ectoderm and extraembryonic fates) along the DV axis (Figure 1.7) (Stathopoulos, Van Drenth et al. 2002; Reeves and Stathopoulos 2009). Cross-regulatory relationships between these target genes further refine DV gene expression domains, in a manner reminiscent of Bicoid and gap gene action in AP axis patterning. For example, while *twist* (*twi*) and *snail* (*sna*) respond to high levels of nuclear Dorsal ventrally to specify the mesoderm, they also repress expression of many genes that are activated by intermediate and low levels of nuclear Dorsal (e.g., *single-minded* (*sim*), *rhomboid* (*rho*) and *short gastrulation* (*sog*)) (Stathopoulos and Levine 2002; Hong, Hendrix et al. 2008).

Dorsal target genes of particular interest are those that encode components of other signaling pathways. For example, the BMP ligand *dpp* and the protease *tolloid* (*tld*) are both strongly repressed by Dorsal, and are thus restricted to the dorsal side of the embryo (Ray, Arora et al. 1991; Kirov, Childs et al. 1994), while *sog* (an extracellular BMP binding protein), activated by low Dorsal levels (Francois, Solloway et al. 1994)(and repressed by *snail*), is expressed in broad lateral stripes. The arrangement of these factors inhibits BMP signaling in the ectoderm, and produces peak levels of BMP signaling at the dorsal midline that are critical to specifying the amnioserosa. This latter phenomenon results from the binding of Sog to Dpp, which prevents signaling in ventral regions and enhances diffusion. The following cleavage of Sog by Tld on the dorsal side of the embryo releases transported Dpp from Sog mediated

inhibition (O'Connor, Umulis et al. 2006). In addition, a local gradient of the *rho* protease in mirror image ventrolateral stripes, regulated by intermediate levels of Dorsal activation and Snail repression, provides EFG signaling activity (Brown, Parrish et al. 1997; Gabay, Seger et al. 1997). The nuclear Dorsal gradient, in combination with BMP and EGF signaling further refines patterning of neuroectoderm into three domains defined by the columnar genes: *vnd*, *ind*, and *msh* (Von Ohlen and Doe 2000).

Figure 1.7 Dorsal-ventral (DV) fate map and expression domains of genes involved in DV patterning in *Drosophila*.

Different concentrations of nuclear Dorsal drive different sets of downstream genes and ultimately (with the help of BMP and EGF signaling) define DV fates. Blue, mesoderm; cyan, mesectoderm; yellow, neurogenic ectoderm; orange, dorsal ectoderm; red, amnioserosa; opaque green circles, high nuclear Dorsal concentration; heavily dotted green circles, intermediate nuclear Dorsal concentration; lightly dotted green circles, low nuclear Dorsal concentration; white nuclei, no nuclear Dorsal.



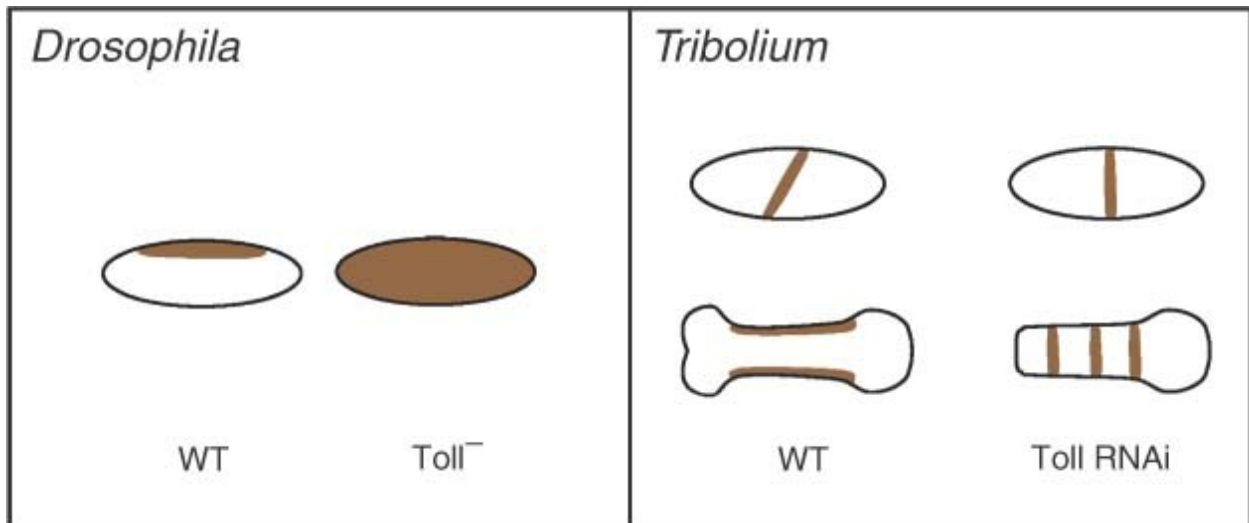
There are similarities as well as differences in DV patterning between *Tribolium* and *Drosophila*. As in *Drosophila*, the ventral-most expression of *Tc-twist* and *Tc-snail* defines the mesoderm, and adjacent stripes of *Tc-sim* demarcate the mesectoderm (Handel, Basal et al. 2005; Cande, Goltsev et al. 2009). As in *Drosophila*, a ventral domain of *Tc-sog* (somewhat wider than the ventrolateral domain of *sog* in *Drosophila*) is needed to transport Tc-Dpp to the dorsal side of the embryo where it is released from Tc-Sog by Tc-Tld (van der Zee, Stockhammer et al. 2006; da Fonseca, van der Zee et al. 2010). Active EGF signaling in the ventral neuroectoderm in *Tribolium* presumably regulates columnar gene expression (Wheeler, Carrico et al. 2005). Major blastoderm fate map differences between *Tribolium* and *Drosophila* are visible in the regulation of *dpp*. While *dpp* is restricted to the dorsal side of the embryo of *Drosophila*, *Tc-dpp* is initially expressed in a weak AP gradient, and then in an oblique stripe along the AP axis that defines the boundary between embryonic and extraembryonic cell fates. Despite these differences, the gradient of activated BMP signaling (as detected by phosphorylated-MAD) centered on the dorsal midline, is conceptually similar in the fly and beetle (van der Zee, Stockhammer et al. 2006).

While nuclearized Dorsal is essential to activate most DV patterning genes in *Drosophila*, it plays a less prominent role in *Tribolium*. The Tc-Dorsal gradient fades at the end of the blastoderm stage (see below), completely disappearing prior to gastrulation (Chen, Handel et al. 2000). This transient Tc-Dorsal expression initiates (but does not maintain) the most ventral fates. *Tc-twist* expression is activated at the ventral midline of the blastoderm and continues to be expressed at the posterior end of the germband after the Tc-Dorsal gradient disappears. As a result, abdominal segments emanating from the caudal end of the embryo continue to be correctly patterned with DV fates. *Tc-twist* expression is never initiated after *Tc-dorsal* depletion by RNAi, producing embryos that are symmetrical along the DV axis (da Fonseca, von Levetzow et al. 2008). However, additional sources of patterning capacity exist, as demonstrated by the self-regulatory features of BMP signaling. The initial AP-asymmetric, DV-symmetric expression of *Tc-dpp* during early blastoderm phase is transformed into both AP and DV asymmetric BMP signalling activity in the late blastoderm by Tc-Sog mediated uptransportation (van der Zee, Stockhammer et al. 2006). In *Tc-dorsal* RNAi, probably due to the depletion of *Tc-sog*, the late blastodermal BMP signalling loses its DV asymmetry and becomes purely AP asymmetric. As a result, during germband elongation, additional DV symmetric stripes of BMP

form along the AP axis in cells distant from the initial peak of BMP activity, indicating that a BMP-mediated self-regulatory mechanism is at work (da Fonseca, von Levetzow et al. 2008) (Figure 1.8). Interestingly, this same phenotype is not observed in *Tc-sog* RNAi embryos where DV fate specification is mostly normal, but with an additional peak of BMP activity replacing *Tc-sog* expression at the ventral midline (van der Zee, Stockhammer et al. 2006). This indicates that another factor downstream of Tc-Dorsal is capable of orienting BMP activity, and emphasizes the self-regulatory properties of BMP signaling in *Tribolium*.

Figure 1.8 Comparison between *Toll* phenotype in *Drosophila* and *Tribolium*.

Left panel (*Drosophila*): *dpp* (brown) is expressed dorsally in wild type (WT; left) and along the entire dorsal-ventral (DV) axis in a *Toll* mutant (right). Right panel (*Tribolium*): Early blastodermal *Tc-dpp* is expressed as an oblique stripe in WT (left upper embryo), and loses this obliqueness in *Toll* RNAi (right upper embryo). In *Tribolium*, the initial orientation of blastodermal *Tc-dpp* dictates the orientation of later reiterated germband expression of *Tc-dpp*. Consequently, *Tc-dpp* reiterates only twice in the DV direction in WT probably due to space constraints (left lower embryo), and many times in the anterior-posterior (AP) direction in *Toll* RNAi (right lower embryo).



The source of nuclear Dorsal gradient

In contrast to the Bcd protein gradient that forms by diffusion of newly translated protein from a localized mRNA source at the anterior pole, there is no localized point-like source from which to initiate a Dl nuclear uptake gradient (Roth 2003). Formation of the gradient can be traced back to the dorsal localization of *gurken* (*grk*) mRNA in the late oocyte, which results in dorsal activation of EGF signaling in the adjacent follicle epithelium. EGF signaling represses *pipe*, restricting its expression to the ventral side of the follicle epithelium (Peri, Technau et al. 2002). Pipe, a sulfotransferase, modifies vitelline membrane proteins (Zhang, Stevens et al. 2009) to define the region in which a protease cascade is initiated that ultimately activates the Toll ligand Spätzle (Spz). In the embryo, binding of the Spz to the Toll receptor leads to the phosphorylation and degradation of the Dorsal inhibitor Cactus (Cact), permitting translocation of Dorsal to the nucleus (Rushlow, Han et al. 1989). A still unanswered question is how the homogenous, sharp-bordered *pipe* domain is translated into the graded distribution of Toll activation through Spz. Some clues come from mutants in which Pipe expression is wider than in wildtype, leading to two ventrolateral peaks of Dorsal nuclear uptake instead of one ventral peak (Roth and Schupbach 1994). This suggests that behind the Spätzle gradient is a self-regulatory mechanism with a domain of action that is restricted ventrally by the maternal factor Pipe. Extending the Pipe domain makes it possible to adopt more than one peak of nuclear Dorsal (Moussian and Roth 2005).

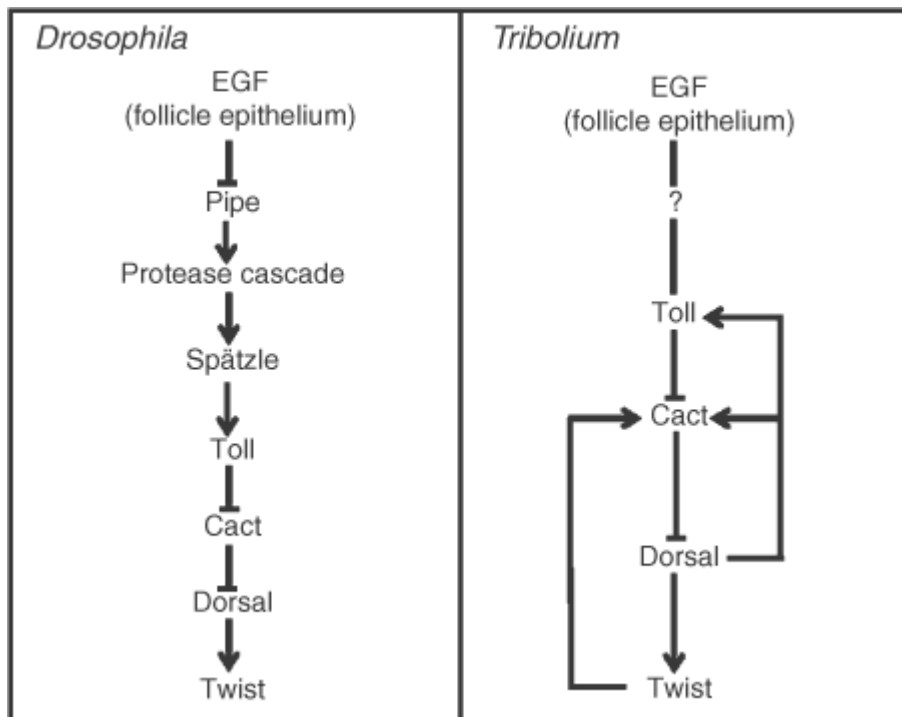
In contrast to the stable gradient of nuclear Dorsal in *Drosophila*, *Tribolium* nuclear Dorsal is highly dynamic. Starting as a very broad domain of nuclear localization along the DV axis, Tc-Dorsal clears from the dorsal side in a gradually shrinking gradient with its peak at the ventral side, and finally vanishes at the differentiated blastoderm stage (Chen, Handel et al. 2000). While the formation of the *Drosophila* Dorsal is to a great extent set by maternal factors, the dynamics of Tc-Dorsal gradient is generated mainly through its positive regulation of zygotic *Tc-Toll* as well as its own negative regulator, *Tc-cact* (da Fonseca, von Levetzow et al. 2008). The negative component of this self-regulatory system is stabilized by the inclusion of the autoactivation of Tc-Twist as a late positive regulator of *Tc-cact* transcription, which is required to keep Tc-Dorsal out of the nuclei during the germband extension stages.

The exact molecular interactions among Tc-Dorsal, Tc-Toll, and Tc-Cact that give rise to the dynamic nature of the Tc-Dorsal gradient are as yet unknown. The regulatory relationships

between these factors (Figure 1.9) indicate both negative and positive feedback loops, which in principle could generate self-regulated patterns by local activation and long-range inhibition in the mode proposed by Meinhard and Gierer (Meinhardt and Gierer 2000). The positive feedback loop between Tc-Toll and Tc-Dorsal satisfies the local activation requirement, while, in principle, Tc-Cact could satisfy the lateral inhibition requirement; however, it not yet know whether Tc-Cact has a long range effect, which is an important requirement of the model (da Fonseca, von Levetzow et al. 2008).

Figure 1.9 Regulatory relationships between major components in dorsal-ventral (DV) axis patterning.

Left panel (*Drosophila*): The DV axis patterning network in *Drosophila* is mostly a linear cascade with the exception of multiple positive and negative feedback loops within the protease cascade components. Right panel (*Tribolium*): Nothing is known about the involvement of a protease cascade in *Tribolium* similar to that involved in *Drosophila*. However, *Tribolium* possess multiple feedback loops at levels more downstream.



Self-regulatory mechanisms of the type found for Tc-Dorsal gradient formation are capable in principle of generating patterns by intensifying random early fluctuations without any maternal bias. However, in order to be useful in establishing axial polarity, such a system needs a mechanism to consistently orient itself perpendicular to the AP axis. This function is carried out by asymmetric activation of EGF signaling in the follicular epithelium overlying the oocyte nucleus during oogenesis. When EGF signaling is disrupted by pRNAi, the effects seen in the resulting embryos are highly variable, some show chaotically-positioned, duplicate peaks of nuclear Tc-Dorsal, while others produce Tc-Dorsal gradients oriented perpendicular to the DV axis (Lynch, Peel et al. 2010). Yet to be discovered is the sequence of events connecting EGF signaling in the follicle epithelium of the *Tribolium* oocyte to the point at which the symmetry of early nuclear Tc-Dorsal expression is lost.

Nasonia is an attractive model in which to further explore the evolution of DV patterning mechanisms, for much the same reasons it is attractive for studying the AP axis: at gastrulation, DV genes homologs are expressed in very similar patterns in *Nasonia* and *Drosophila* (Lynch, Peel et al. 2010). What is known so far is that, as in *Tribolium* and *Drosophila*, proper establishment of the DV axis depends on maternal EGF signaling (Lynch, Peel et al. 2010). In an interesting parallel, mRNA for the *Nasonia* EGF ligand is localized to the dorsal cortex, much like *grk* is localized in *Drosophila*, which is in sharp contrast to the lack of localized factors in *Tribolium*. Thus, heavier reliance on localized mRNAs also extends to patterning the DV axis in long germ insects.

Head development

The embryonic head anlage of *Drosophila* is partitioned by means of segment-polarity genes into six segments (listed in a posterior to anterior order): the labium, maxillary and mandible (composing the gnathocephalon), and intercalary, antenna, and ocular (composing the procephalon). Molecular arguments for the existence of a labral segment have been found in *Drosophila* (Schmidt-Ott and Technau 1992) but not in other insects (Scholtz and Edgecombe 2006; Posnien, Bashasab et al. 2009). Segmentation in the gnathocephalon is under the control of the segmentation hierarchy that defines the trunk segments, while procephalon segmentation is controlled by a different set of genes, the so-called “head gap-like genes” (*orthodenticle (otd)*, *buttonhead (btd)*, *empty-spiracles (ems)* and *sloppy-paired*) (Cohen and Jurgens 1990;

Grossniklaus, Pearson et al. 1992). These genes are expressed in overlapping domains, and mutations in them result in segmental deletions similar to the effects of gap gene mutations in the trunk (hence the name “gap-like”). Therefore, it was thought that they regulate the patterning of segment-polarity genes in the procephalon in a fashion similar to that of the trunk gap genes (directly or with the help of second order regulators instead of pair rule genes (Crozatier, Valle et al. 1996)). However, later studies indicate that head gap-like genes play only a permissive role for segment polarity genes expression, and do not regulate their metameric positions (Wimmer, Cohen et al. 1997), leaving the problem of head segmentation unresolved (Posnien, Schinko et al. 2010).

The situation is similar in *Tribolium*, where the head gap-like genes (*Tc-otd*, *Tc-btd*, and *Tc-ems*) are not even extensively overlapping (Schinko, Kreuzer et al. 2008). *Tc-otd* is the only one of these genes to have a gap-like phenotype (antennal and intercalary segments are missing in late embryonic knockdown). *Tc-ems* knockdown results in a partial deletion of the antennal segment, while *Tc-btd* knockdown has no effect at all, ruling out possible gap-like functions in *Tribolium* (Schinko, Kreuzer et al. 2008). However, RNAi analysis of the *knirps* homolog in *Tribolium* produces a gap in the head pattern (Cerny, Grossmann et al. 2008), which is in contrast to the normal early metameric patterning and late head defects of *knirps* mutants in *Drosophila* (Gonzalez-Gaitan, Rothe et al. 1994). Thus, *Tc-knirps* joins *Tc-otd* as a head gap-like gene in *Tribolium* (Posnien, Schinko et al. 2010).

In *Drosophila*, head gap-like genes receive input from three maternal systems: the anterior, terminal and DV systems (Jurgens 1993). In *Tribolium*, the terminal and DV systems are likely to be responsible for the high-level partitioning of the embryo into extraembryonic, head and trunk, mediated by the cross-regulation of *Tc-zen1*, *Tc-mex3*, and *Tc-cad* (see AP section). So far, *Tc-ems*, *Tc-knirps*, *Tc-collier* and *Tc-labial* have been shown to regulate segment polarity expression in the head (Schaeper, Pechmann et al.). Their exact mode of action and more genetic factors regulating their fine-tuning and ultimately positioning the metameric expression of segment-polarity genes are yet to be discovered.

Mapping embryonic head segments to their larval counterparts in *Drosophila* and insects in general was and still is subject to much debate (Scholtz and Edgecombe 2006). This is mainly because the larval head of the best-studied insect, *Drosophila*, undergoes a complex process of involution that introduces technical difficulties to mutant screens and expression assays. In

addition, the derived nature of the *Drosophila* is not representative of insect head development in general. In *Tribolium*, head segments are initially collinear with the AP axis during embryonic development (the later bend and zipper morphogenetic movements, however, changes the situation such that the eye becomes located posterior to the antenna – see below), making this beetle, with its available genetic tools, a good model system for studying typical insect head development (Posnien, Schinko et al. 2010). To support this line of inquiry, many larval morphological markers as well as many embryonic genetic markers have been characterized in the *Tribolium* head. Comparison of gene expression domains in *Tribolium* and *Drosophila* has helped reassess the assignment of morphological structures to individual segments (Economou and Telford 2009). These markers have also been used to compare embryonic and larval phenotypes in a variety of mutants, providing new insight into the fate map of the insect head (Posnien and Bucher 2010). Recently the “bend and zipper” model was formulated to describe the morphogenetic movements the insect head undergoes during development (Posnien and Bucher 2010). In addition, evidence supporting the hypothesis of the non-segmental, appendage-bearing nature of labrum was presented (Posnien, Bashasab et al. 2009). However, more technical advances in *Tribolium* are required to give unequivocal answers to the problem of *Tribolium* and insect head development in general.

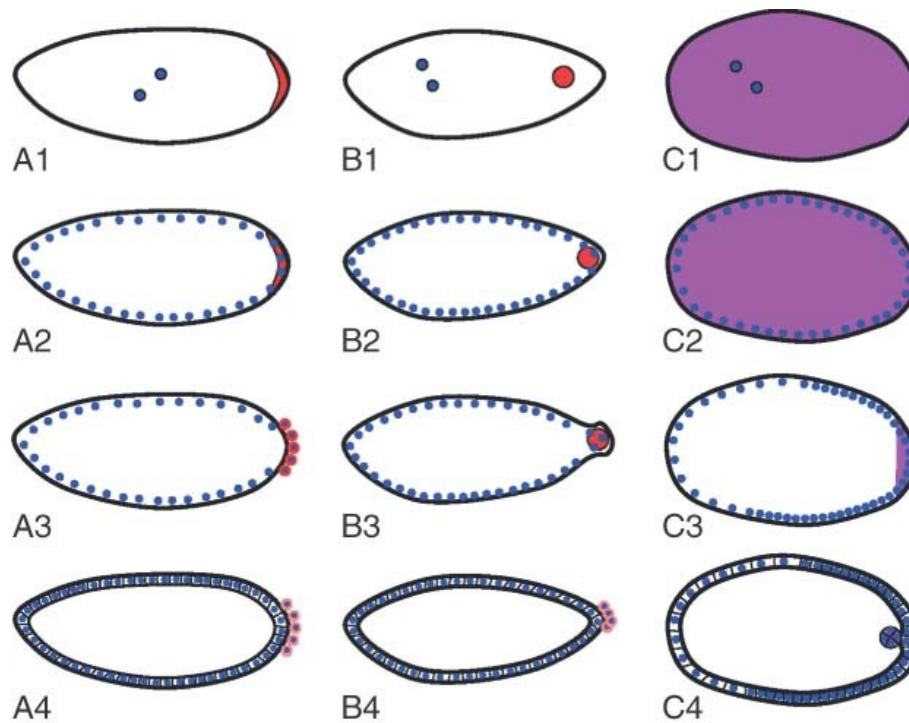
In contrast to the previously mentioned processes, head patterning is not well understood in *Drosophila*. Hence, it will be the task of future *Tribolium* research to establish the paradigm in this species while *Drosophila* and *Nasonia* provide interesting cases of parallel evolutionary adaptations to long germ embryogenesis. Additionally, in *Drosophila* the head involution is an intriguing evolutionary novelty the evolution of which remains to be understood.

Germline specification

In *Drosophila*, the germline is specified by cytoplasmic inclusions called polar granules, which are produced specifically at the posterior pole of the oocyte and the embryo (Figure 1.10, A1-A2). When the syncytial nuclei arriving at the plasma membrane during blastoderm formation become associated with these structures, they take on the germ line fate and become pole cells (Figure 1.10, A3-A4). The gene *oskar* (*osk*) is both necessary and sufficient to induce the polar granules (Ephrussi and Lehmann 1992), and thus the activity of this gene must be tightly regulated.

Figure 1.10 Germ cell formation in *Drosophila*, *Nasonia*, and *Tribolium*.

Red, *osk* mRNA; magenta, *Tc-vasa* mRNA; blue, nuclei. A1–C1: In the early cleavage stages of embryogenesis, *osk* mRNA is localized in the posterior pole plasm of *Drosophila* (A1) and oosome of *Nasonia* (B1), while *Tc-vasa* is ubiquitous in *Tribolium* (C1). A2–C2: As the syncytial blastoderm forms, posterior nuclei interact with the pole plasm (A2), or the oosome (B2) in fly and wasp, respectively, while nuclei enter an apparently homogenous environment in *Tribolium* (C2). A3–C3: Individual nuclei that enter the posterior pole plasm bud singly, forming the pole cells in *Drosophila* (A3). In contrast, the oosome along with multiple nuclei bud simultaneously from the posterior in *Nasonia* (B3). In the later blastoderm stages of *Tribolium*, *Tc-vasa* mRNA is cleared from the embryo, save for the most posterior pole. A4–C4: Production of pole cells is completed, and *osk* mRNA begins to be degraded in the cellular blastoderm stage in both *Drosophila* (A4) and *Nasonia* (B4). Posterior cells that retained *Tc-vasa* expression delaminate from the blastoderm into the interior of the embryo (C4) and will become the primordial germ cells of the beetle.



Neither maternally synthesized polar granules, nor early specification of the primordial germ cells in the form of pole cells, are ancestral features of insect development. These features are missing from all described hemimetabolous species, as well as from some holoemetabolous taxa, such as *Tribolium* and *Apis* (Weinstock, Robinson et al. 2006; Richards, Gibbs et al. 2008). These species use zygotic induction mechanisms to specify germline fate at varying times later in embryonic development (Dearden 2006). On the other hand, *Drosophila*-like, maternal inheritance modes of germline determination are found in most hymenopterans (including *Nasonia*) and dipterans, and in many beetles (Lynch, Ozuak et al. 2011). *osk* had, until recently, only been found in the genomes of Drosophilids and other Diptera, leading to the idea that *osk* was a novelty of the Diptera (Dearden, Wilson et al. 2006).

Recently, an *osk* ortholog was discovered in the genome of *Nasonia*. It is a component of the oosome (the functional equivalent of the posterior pole plasm in *Drosophila*), and is taken up into the pole cells as they form, until it is degraded during the cellular blastoderm stage in a pattern quite similar to *Drosophila osk* (Figure 1.10, B1-B4). pRNAi against *Nv-osk* leads to the loss of the oosome and pole cells, as well as posterior patterning defects (Lynch, Ozuak et al. 2011).

The discovery of an *oskar* ortholog performing a conserved function in generating maternal germ plasm in *Nasonia* has shed light on the evolutionary history of germline determination among insects. First, the latest time for the origin of the *oskar* gene is pushed back to the last common ancestor of the Holmetabola, indicating that it was lost independently multiple times (at least in the lineages leading *Apis*, *Tribolium* and *Bombyx*). Second, the general conservation of the regulatory networks both upstream and downstream of *Nv-osk* in the formation of germ plasm and pole cells, indicates that there was a single origin of the maternal inheritance mode of germline determination that coincided with *oskar*, and that the strong correlation of losses of *oskar* with losses of maternal inheritance are not coincidental.

The fact that the lack of pole cells is likely secondarily derived in *Tribolium* makes understanding how the germline is established in this species very interesting. So far little data exist. Tc-Vasa protein is not maternally localized, unlike the Vasa orthologs in *Drosophila* and *Nasonia*. However, its initially ubiquitous mRNA (Figure 1.10, C1-C2) appears to be selectively degraded, so that it is only found at the posterior pole at the onset of gastrulation (Figure 1.10 C3), after which it marks the primordial germ cells (Figure 1.10, C4) (Schröder 2006). It will be

interesting to see how this degradation is regulated and what factors are responsible for the induction of the rest of the germline program.

Morphogenesis

During the blastoderm stages when cell fates are being determined, the *Drosophila* embryo is a relatively simple two dimensional structure. Once cellularization has been completed and cell fates have been determined, numerous cell movements and rearrangements including gastrulation, dorsal closure, and germ band extension occur which transform the embryo into a dynamic, three-dimensional entity (Leptin 1999). Equivalent movements also occur in *Tribolium* and *Nasonia*, however the means by which they are carried out vary significantly due to the combination of the different embryonic architectures, and independent evolution of strategies to solve morphological problems in each species' respective lineage.

Gastrulation

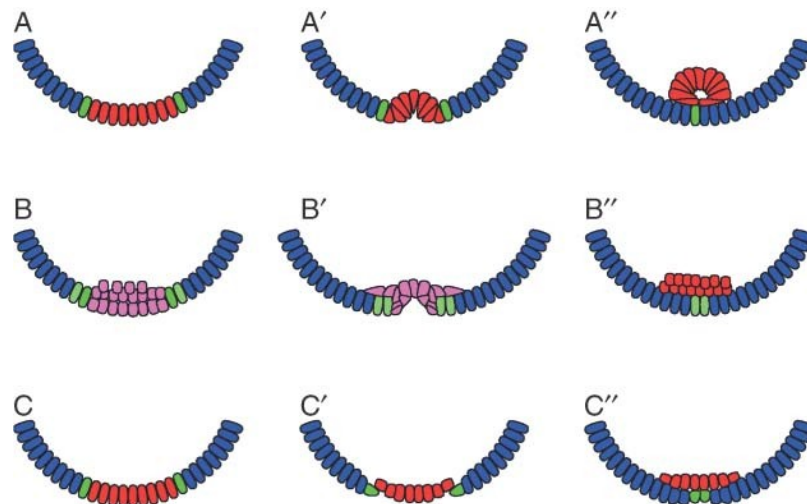
In *Drosophila* gastrulation begins with the formation of the ventral furrow, which forms more or less simultaneously along the entire AP axis of the embryo. In this process, cells on the ventral surface of the embryo expressing *twist* and *snail* contract at their apical sides, which leads to the internalization of the presumptive mesoderm, and formation of the ventral midline when the formerly lateral, *single-minded* (*sim*) expressing cells of the mesectoderm meet and fuse over the internalized mesoderm (Figure 1.11) (Leptin 1999).

The mesoderm is also ventrally located in *Tribolium*, it internalizes after cellularization of the blastoderm, which, during early stages, resembles invagination of the ventral furrow in *Drosophila* (Handel, Basal et al. 2005). In the fly, gastrulation is among the first morphogenetic movements, and is completed before the major movements of germ band extension and dorsal closure have been initiated. In contrast, gastrulation in *Tribolium* occurs first in the context of germ rudiment condensation, and continues during convergent extension of the germ band. In addition, extraembryonic membranes are enveloping the embryo (Handel, Grunfelder et al. 2000). Furthermore, both specification of new mesodermal cell populations and ventral closure leading to the formation of the ectodermal ventral midline occur progressively from anterior to posterior (Handel, Basal et al. 2005), contrasting sharply to the rapid, coordinated invagination along the AP axis in the fly. Finally, while a ventral furrow similar to that of *Drosophila* is observed at certain positions along the axis, the morphogenetic movements involved in

internalizing the mesoderm and closing the ventral ectoderm vary along the axis during *Tribolium* gastrulation. In segments derived from the growth zone, the presumptive mesodermal cells, which unlike *Drosophila* and more anterior *Tribolium* segments, do not express *twist*, lose their epithelial character to form a mass of multilayered tissue, and appear to be internalized chaotically as the ectoderm closes over them (Handel, Basal et al. 2005) (Figure 1.11 B-B''). Interestingly, after internalization at least a subset of the presumptive mesoderm cells reinitiate *Tc-twi* expression (Figure 1.11 B''). In addition, the mesoderm remains relatively flat in the head region, with ectodermal cells crawling over this substrate to meet at the midline (similar to what is seen in hymenopteran gastrulation, see below, Figure 1.11 C-C''). It will be interesting to see if these different morphogenetic movements are the result of different cell signaling interactions among the different cell types involved, or whether they result simply from different forces impinging on the mesoderm at different AP axis positions.

Figure 1.11 Mechanisms of gastrulation in *Drosophila*, *Tribolium*, and *Nasonia*.

A–A'': Gastrulation by furrow formation employed by *Drosophila*, and *Tribolium* in the anterior segments. B–B'': Gastrulation mode found in the segments deriving from the growth zone of *Tribolium*. A multilayered mass of cells loses its epithelial character and is internalized by the migration of the lateral ectodermal cells. C–C'': Hymenopteran mode of gastrulation, where the mesoderm forms a stiff plate, the ectoderm breaks contact with mesoderm and migrates ventrally until the free edges meet and fuse at the ventral midline. Blue, lateral ectoderm; green, mesectoderm; red, mesoderm precursors expressing *twist*; pink, mesoderm precursors not expressing *twist*. Other cell fates have been omitted for clarity.



The cellular and molecular underpinnings of gastrulation have been relatively unexplored in *Nasonia*. Observations on living embryos have shown, however, that the general features of *Nasonia* (Bull 1982) are similar to the unique strategies that are used in many other Hymenoptera (Fleig and Sander 1986). Here, no ventral furrow forms, rather the prospective mesoderm remains as a stiff sheet of cells while the ectodermal cells at the border of mesoderm break their lateral contact with their mesodermal neighbors (Figure 1.11 C-C'). The resulting free edges move across the rigid mesoderm cells until they meet and fuse, forming the ventral midline (Figure 1.11 C''). This process also occurs in an anterior to posterior progression, again in contrast to *Drosophila* (Fleig and Sander 1986)(JAL personal observation). These observations indicate that the molecular and cellular basis of *Nasonia* gastrulation also differ from that of the fly.

Extraembryonic membranes

In *Drosophila*, the vast majority of cells present at the end of the blastoderm stage will give rise to the future tissues of the embryo. However there is a small population of cells restricted to the dorsal midline fated to become the amnioserosa. This single extraembryonic membrane in the fly is important for proper germband retraction (Yip, Lamka et al. 1997) and dorsal closure of the embryo (Kiehart, Galbraith et al. 2000), and disappears in the course of the latter process. While the amnioserosa is critical for successful completion of embryogenesis, it is extremely reduced in comparison to the extraembryonic membranes found in most other insects (Rafiqi, Lemke et al. 2008).

Tribolium possesses a more typical insect complement of and investment in extraembryonic membranes (Panfilio 2008). There are distinct serosal and amnion tissues, the former occupying a large anterior-dorsal cap, while the latter is a relatively restricted domain located at the anterior and dorsal margins of the embryonic anlage (van der Zee, Berns et al. 2005). At the onset of gastrulation, these membranes undergo radical rearrangements. The serosal cells flatten and expand, and eventually move to envelope the embryo proper, causing the latter to sink slightly into the yolk. The amnion remains closely associated with the embryo during these movements. After the completion of germband extension and retraction, it is thought that the amnion and serosa fuse by cell intercalation of the two tissues into one, which eventually weakens and ruptures, thus uncovering the embryo. This membrane contracts to the

dorsal side of the embryo, and eventually disappears as the embryonic flanks expand and meet at the dorsal midline (van der Zee, Berns et al. 2005).

As in *Drosophila*, specification of extraembryonic membranes in *Tribolium* depends on transcription factors encoded by *zerknuellt* (*zen*) genes (van der Zee, Berns et al. 2005). There are two *zen* paralogs in *Tribolium* (*Tc-zen1* and *Tc-zen2*). Both of which are expressed in an anterior cap at the blastoderm stage corresponding to the presumptive serosa. *Tc-zen2* has an additional later domain in the amnion. Knockdown of *Tc-zen1* has dramatic effects on blastodermal patterning. The serosa is completely absent (and thus serosal *Tc-zen2* expression is also lacking), the amnion expands dorsally and anteriorly, and the anterior head anlage expands to the anterior pole of the egg. In addition, the embryo never sinks into the yolk, but remains on the surface of the egg throughout development. Despite these major early patterning defects, the majority of larvae look largely normal, indicating that there are mechanisms for compensating for the dramatic expansion of the head, and that the expanded amnion has some capacity to rescue the loss of the serosal fate or that the insect can develop in the absence of the serosa (van der Zee, Berns et al. 2005).

In contrast to *Tc-zen1*, the defects seen after *Tc-zen2* pRNAi are initially mild. No defects are seen at the blastoderm stage. However, after germband extension, the amnion fails to fuse with the serosa, and does not degenerate on the ventral side, thus preventing ventral eversion of the embryo. The persistent amnion contracts ventrally, dragging the dorsal flanks with it, leading to the inversion of the embryo trapped within the yolk (van der Zee, Berns et al. 2005).

The complicated movements of covering and uncovering the embryo in the course of extraembryonic development in *Tribolium* might seem superfluous, or at least unnecessarily baroque, given the ability of apparently wild type embryos to hatch in the absence of these movements and the entire serosal tissue after *Tc-zen1* pRNAi. However, the serosa likely has important roles beyond embryogenesis in, for example, providing protection to the embryo from a variety of environmental insults (Panfilio 2008). These insults are likely to be more extreme for embryos laid outside of laboratory conditions, thus the proper formation of the extraembryonic membranes is likely to be critical for the success of the organism in the wild. It is interesting to note that reduction in extrambyronic membranes is observed in many long germ species, which

may indicate that deposition of the egg in a less harsh environment may be an ecological factor that contributes to the evolution of this type of embryogenesis.

The extraembryonic membranes of the long germ embryo of *Nasonia* are again comparatively less well described, but the data that do exist indicate that they possess both *Drosophila* and *Tribolium*-like features. Observations of living embryos indicate that unlike *Drosophila*, both a distinct serosa and an amnion are present in the wasp (Bull 1982). However, like the fly these tissues are defined in a very narrow domain restricted to the dorsal midline of the embryo (Pultz, Westendorf et al. 2005) (JAL, personal observation). At the onset of gastrulation, the presumptive serosa expands from its dorsal domain, and crawls over the embryo proper until it completely envelops the embryo on the ventral side, while the amnion appears to expand from the dorsal flank of the embryo to cover the yolk until the completion of dorsal closure (Bull 1982; Pultz, Westendorf et al. 2005). Further experiments are required to determine whether the specification of these two fates bears any similarity to either *Drosophila* or *Tribolium* mechanisms.

Conclusions and Perspectives

The tripartite comparative system of *Drosophila*, *Nasonia*, and *Tribolium* has allowed a number of significant insights into how early embryogenesis has evolved among holometabolous insects, especially in relation to their changing embryonic patterning environments. One striking observation was that, although the specific molecules and some of the details differ, both of the long germ species use very similar strategies based on localized mRNAs to rapidly specify cell fates along the entire AP axis of the early embryo. This strategy includes an instructive anterior factor (*bcd* in *Drosophila*, *Nv-otd1* in *Nasonia*), factors permissive for anterior patterning (also *bcd* in *Drosophila*, maternal anteriorly localized *Nv-gt* and the posterior localization of *Nv-cad* in *Nasonia*), and a permissive posterior factor (*nanos* orthologs in both species). *Nasonia* employs an additional posterior instructive factor, the posterior aspect of *Nv-otd1* localization. The dependence of long germ species on localized mRNAs extends to the DV axis, as both *Nasonia* and *Drosophila* use localized mRNA encoding EGF ligands to establish a stable axis. The nature of the long germ patterning system is likely a major factor driving the acquisition of precisely localized sources of positional information, as embryos of this type must specify a large number of distinct cell fates in a short period of time, and thus require precise and robust patterning

information at a very early stage. Although localized factors have been found in *Tribolium* (Bucher, Farzana et al. 2005) that are functionally important (S. J. Brown, manuscript under preparation), it seems that they give guidance for self-regulatory mechanisms, other than giving extensive positional information as in the *Drosophila* case (E. El-Sherif, S. J. Brown, manuscript under preparation).

The reduced dependence of *Tribolium* on localized mRNAs is likely due in part to its mode of embryogenesis, where significantly fewer cell fates are established at a time accessible to maternally provided mRNAs. In place of maternally provisioned patterning information, *Tribolium* seems to rely on another powerful strategy for establishing pattern, namely emergent patterning based on self-regulatory systems. Examples of these include the zygotic self regulatory and feed-forward loops of the DV axis, the negative feedback pair-rule loop required for patterning and progressive growth of the germband, and perhaps the spatial and temporal cross regulation of the gap genes in the germband stage.

The ability to break with the *Drosophila* paradigm is another major development made possible by the establishment of *Nasonia* and *Tribolium* as comparative model systems. The discovery of the novel peptide encoding gene *mlpt* as a gap gene in *Tribolium*, the discovery that Wnt signaling is required for posterior growth zone and patterning, and the discovery of *mex-3* as an anciently conserved regulator of *cad* among the ecdysozoa are illustrative of this power. These types of discoveries should only increase as more genome wide and unbiased analyses of gene function in both species start bearing fruit.

Additional advances in understanding the developmental systems of *Tribolium* and *Nasonia* will come from taking advantage of the rapidly increasing set of transgenic and genomic tools and techniques available in these organisms. For example, germline transformation allows the assessment of putative enhancer regions that can be identified by genomic techniques (such as those discussed below). In addition, the development of techniques for conditionally inducible expression, introduction of fluorescent hybrid proteins, and live imaging will allow for a much more detailed description and genetic analysis of developmental events. This will be especially valuable for dynamic processes, such as the operation of the growth zone or the movements of the extraembryonic membranes, where static observations on fixed material are not sufficient for rigorous interpretation.

The availability of fully sequenced genomes allows for the application of powerful techniques for comprehensively unraveling the regulatory interactions underlying development. These include genome-wide analysis of expression level perturbation (e.g. microarrays) and genome-wide discovery of transcription factor binding sites (e.g. ChIP-seq). The combination of such techniques should provide robust descriptions of gene regulatory networks robust enough to compare meaningfully with those already described for *Drosophila*.

Finally, the evolutionary significance of the similarities and differences in embryonic patterning among *Nasonia*, *Tribolium*, and *Drosophila* will only be fully clarified by placing them in a more robust phylogenetic and ecological context. For example, sampling of other short germ species both within the beetles, and among hemimetabolous insects will allow the differentiation of characteristics that are typical for short germ embryos, and those which arose uniquely in *Tribolium*. Reciprocally, additional long germ species, particularly those among the beetles, will be particularly informative in identifying potential constraints or common strategies used in the transition from short germ embryogenesis. Such broad sampling of insect developmental data is increasingly feasible, given the wide applicability of pRNAi, and the increasing power of next generation sequencing techniques to rapidly generate candidate gene sequence data.

Understanding the evolutionary meaning of such expanded developmental data will require a more detailed understanding of the ecological contexts under which these embryos develop and hatch. These conditions could result in selection on the speed of embryogenesis, the relative need for protective extraembryonic membranes, or the relative complexity of the hatching larva. All of these potential selective pressures could have major impacts on the strategies used for early patterning and embryogenesis. For these experiments, the highly developed techniques and resources available in *Tribolium* and *Nasonia* will confer on them a status as rich sources of hypothesis generation in relation to the numerous emerging satellite models roughly equivalent to that which *Drosophila* held in the early days of the wasp and beetle systems. Hopefully the process of reciprocal illumination will continue whereby the results obtained in satellite systems spur further experiments in core model species and vice versa, leading to both a broad and deep understanding of the evolution of developmental mechanisms throughout the insects.

References

- Akam, M. (1987). "The Molecular-Basis for Metameric Pattern in the Drosophila Embryo." Development **101**(1): 1-&.
- Angelini, D. R. and T. C. Kaufman (2005). "Comparative developmental genetics and the evolution of arthropod body plans." Annu Rev Genet **39**: 95-119.
- Angelini, D. R. and T. C. Kaufman (2005). "Functional analyses in the milkweed bug *Oncopeltus fasciatus* (Hemiptera) support a role for Wnt signaling in body segmentation but not appendage development." Dev Biol **283**(2): 409-23.
- Aranda, M., H. Marques-Souza, et al. (2008). "The role of the segmentation gene hairy in *Tribolium*." Development genes and evolution **218**(9): 465-477.
- Berghammer, A. J., M. Klingler, et al. (1999). "A universal marker for transgenic insects." Nature **402**(6760): 370-1.
- Bergsten, S. E. and E. R. Gavis (1999). "Role for mRNA localization in translational activation but not spatial restriction of nanos RNA." Development **126**(4): 659-69.
- Binner, P. and K. Sander (1997). "Pair-rule patterning in the honeybee *Apis mellifera*: Expression of even-skipped combines traits known from beetles and fruitfly." Development Genes and Evolution **206**(7): 447-454.
- Bolognesi, R., L. Farzana, et al. (2008). "Multiple Wnt Genes Are Required for Segmentation in the Short-Germ Embryo of *Tribolium castaneum*." Current Biology **18**(20): 1624-1629.
- Bolognesi, R., T. D. Fischer, et al. (2009). "Loss of Tc-arrow and canonical Wnt signaling alters posterior morphology and pair-rule gene expression in the short-germ insect, *Tribolium castaneum*." Development genes and evolution **219**(7): 369-375.
- Brent, A. E., G. Yucel, et al. (2007). "Permissive and instructive anterior patterning rely on mRNA localization in the wasp embryo." Science **315**(5820): 1841-3.
- Brown, S. J., J. K. Parrish, et al. (1997). "Molecular characterization and embryonic expression of the even-skipped ortholog of *Tribolium castaneum*." Mechanisms of development **61**(1-2): 165-173.
- Brown, S. J., T. D. Shippy, et al. (2002). "*Tribolium* Hox genes repress antennal development in the gnathos and trunk." Mol Phylogenet Evol **24**(3): 384-7.
- Bucher, G., L. Farzana, et al. (2005). "Anterior localization of maternal mRNAs in a short germ insect lacking bicoid." Evolution & Development **7**(2): 142-149.

- Bucher, G. and M. Klingler (2004). "Divergent segmentation mechanism in the short germ insect *Tribolium* revealed by giant expression and function." *Development* **131**(8): 1729-1740.
- Bucher, G., J. Scholten, et al. (2002). "Parental RNAi in *Tribolium* (Coleoptera)." *Curr Biol* **12**(3): R85-6.
- Bull, A. L. (1982). "Stages of Living Embryos in the Jewel Wasp *Mormoniella*-(*Nasonia*)-*Vitripennis*-(Walker)(Hymenoptera, Pteromalidae)." *International Journal of Insect Morphology & Embryology* **11**(1): 1-23.
- Cande, J., Y. Goltsev, et al. (2009). "Conservation of enhancer location in divergent insects." *Proceedings of the National Academy of Sciences of the United States of America* **106**(34): 14414-14419.
- Casanova, J., M. Furriols, et al. (1995). "Similarities between trunk and spatzle, putative extracellular ligands specifying body pattern in *Drosophila*." *Genes Dev* **9**(20): 2539-44.
- Cerny, A. C., G. Bucher, et al. (2005). "Breakdown of abdominal patterning in the *Tribolium* Kruppel mutant jaws." *Development* **132**(24): 5353-5363.
- Cerny, A. C., D. Grossmann, et al. (2008). "The *Tribolium* ortholog of knirps and knirps-related is crucial for head segmentation but plays a minor role during abdominal patterning." *Developmental biology* **321**(1): 284-294.
- Chen, G., K. Handel, et al. (2000). "The maternal NF-kappa B/Dorsal gradient of *Tribolium castaneum*: dynamics of early dorsoventral patterning in a short-germ beetle." *Development* **127**(23): 5145-5156.
- Choe, C. P. and S. J. Brown (2007). "Evolutionary flexibility of pair-rule patterning revealed by functional analysis of secondary pair-rule genes, paired and sloppy-paired in the short-germ insect, *Tribolium castaneum*." *Developmental biology* **302**(1): 281-294.
- Choe, C. P. and S. J. Brown (2009). "Genetic regulation of engrailed and wingless in *Tribolium* segmentation and the evolution of pair-rule segmentation." *Developmental biology* **325**(2): 482-491.
- Choe, C. P., S. C. Miller, et al. (2006). "A pair-rule gene circuit defines segments sequentially in the short-germ insect *Tribolium castaneum*." **103**(17): 6560-6564.
- Cohen, S. M. and G. Jurgens (1990). "Mediation of *Drosophila* head development by gap-like segmentation genes." *Nature* **346**(6283): 482-5.

- Crozatier, M., D. Valle, et al. (1996). "Collier, a novel regulator of *Drosophila* head development, is expressed in a single mitotic domain." Curr Biol **6**(6): 707-18.
- da Fonseca, R. N., J. A. Lynch, et al. (2009). "Evolution of axis formation: mRNA localization, regulatory circuits and posterior specification in non-model arthropods." Current Opinion in Genetics & Development **19**(4): 404-411.
- da Fonseca, R. N., M. van der Zee, et al. (2010). "Evolution of extracellular Dpp modulators in insects: The roles of tolloid and twisted-gastrulation in dorsoventral patterning of the *Tribolium* embryo." Developmental Biology **345**(1): 80-93.
- da Fonseca, R. N., C. von Levetzow, et al. (2008). "Self-regulatory circuits in dorsoventral axis formation of the short-germ beetle *Tribolium castaneum*." Developmental Cell **14**(4): 605-615.
- Damen, W. G. (2007). "Evolutionary conservation and divergence of the segmentation process in arthropods." Dev Dyn **236**(6): 1379-91.
- Davis, G. K. and N. H. Patel (2002). "Short, long, and beyond: Molecular and embryological approaches to insect segmentation." Annual Review of Entomology **47**: 669-699.
- Dearden, P. K. (2006). "Germ cell development in the Honeybee (*Apis mellifera*); Vasa and Nanos expression." Bmc Developmental Biology **6**(6): -.
- Dearden, P. K., M. J. Wilson, et al. (2006). "Patterns of conservation and change in honey bee developmental genes." Genome Research **16**(11): 1376-1384.
- DiNardo, S., J. Heemskerk, et al. (1994). "The making of a maggot: patterning the *Drosophila* embryonic epidermis." Curr Opin Genet Dev **4**(4): 529-34.
- Driever, W. and C. Nusslein-Volhard (1988). "The bicoid protein determines position in the *Drosophila* embryo in a concentration-dependent manner." Cell **54**(1): 95-104.
- Driever, W., G. Thoma, et al. (1989). "Determination of spatial domains of zygotic gene expression in the *Drosophila* embryo by the affinity of binding sites for the bicoid morphogen." Nature **340**(6232): 363-7.
- Dubnau, J. and G. Struhl (1996). "RNA recognition and translational regulation by a homeodomain protein." Nature **379**(6567): 694-699.
- Economou, A. D. and M. J. Telford (2009). "Comparative gene expression in the heads of *Drosophila melanogaster* and *Tribolium castaneum* and the segmental affinity of the *Drosophila* hypopharyngeal lobes." Evol Dev **11**(1): 88-96.

- Ephrussi, A., L. K. Dickinson, et al. (1991). "*oskar* Organizes the Germ Plasm and Directs Localization of the Posterior Determinant *nanos*." Cell **66**: 37-50.
- Ephrussi, A. and R. Lehmann (1992). "Induction of germ cell formation by *oskar*." Nature **358**(6385): 387-92.
- Farzana, L. and S. J. Brown (2008). "Hedgehog signaling pathway function conserved in *Tribolium* segmentation." Dev Genes Evol **218**(3-4): 181-92.
- Fleig, R. and K. Sander (1986). "Embryogenesis of the Honeybee *Apis-Mellifera* L (Hymenoptera, Apidae) - an Sem Study." International Journal of Insect Morphology & Embryology **15**(5-6): 449-462.
- Francois, V., M. Solloway, et al. (1994). "Dorsal-ventral patterning of the *Drosophila* embryo depends on a putative negative growth factor encoded by the short gastrulation gene." Genes Dev **8**(21): 2602-16.
- Fujioka, M., J. B. Jaynes, et al. (1995). "Early even-skipped stripes act as morphogenetic gradients at the single cell level to establish engrailed expression." Development **121**(12): 4371-82.
- Furriols, M. and J. Casanova (2003). "In and out of Torso RTK signalling." Embo J **22**(9): 1947-52.
- Gabay, L., R. Seger, et al. (1997). "In situ activation pattern of *Drosophila* EGF receptor pathway during development." Science **277**(5329): 1103-6.
- Gonzalez-Gaitan, M., M. Rothe, et al. (1994). "Redundant functions of the genes *knirps* and *knirps*-related for the establishment of anterior *Drosophila* head structures." Proc Natl Acad Sci U S A **91**(18): 8567-71.
- Grossniklaus, U., R. K. Pearson, et al. (1992). "The *Drosophila* sloppy paired locus encodes two proteins involved in segmentation that show homology to mammalian transcription factors." Genes Dev **6**(6): 1030-51.
- Gutjahr, T., C. E. Vanario-Alonso, et al. (1994). "Multiple regulatory elements direct the complex expression pattern of the *Drosophila* segmentation gene *paired*." Mech Dev **48**(2): 119-28.
- Handel, K., A. Basal, et al. (2005). "*Tribolium castaneum* twist: gastrulation and mesoderm formation in a short-germ beetle." Development Genes and Evolution **215**(1): 13-31.

- Handel, K., C. G. Grunfelder, et al. (2000). "Tribolium embryogenesis: a SEM study of cell shapes and movements from blastoderm to serosal closure." Development Genes and Evolution **210**(4): 167-179.
- Hong, J. W., D. A. Hendrix, et al. (2008). "How the Dorsal gradient works: Insights from postgenome technologies." Proceedings of the National Academy of Sciences of the United States of America **105**(51): 20072-20076.
- Ingham, P. and P. Gergen (1988). "Interactions between the pair-rule genes runt, hairy, even-skipped and fushi tarazu and the establishment of periodic pattern in the Drosophila embryo." Development **104**(Supplement): 51-60.
- Jurgens, G. H., V. (1993). The terminal regions of the body pattern. The development of Drosophila melanogaster. M. A. Bate, A., Cold Spring Harbor Laboratory. **1**: 687-746.
- Keller, R. G., C. Desplan, et al. (2010). "Identification and characterization of Nasonia Pax genes." Insect Molecular Biology **19**: 109-120.
- Kiehart, D. P., C. G. Galbraith, et al. (2000). "Multiple forces contribute to cell sheet morphogenesis for dorsal closure in Drosophila." Journal of Cell Biology **149**(2): 471-490.
- Kirov, N., S. Childs, et al. (1994). "The Drosophila dorsal morphogen represses the tolloid gene by interacting with a silencer element." Mol Cell Biol **14**(1): 713-22.
- Kotkamp, K., M. Klingler, et al. (2010). "Apparent role of Tribolium orthodenticle in anteroposterior blastoderm patterning largely reflects novel functions in dorsoventral axis formation and cell survival." Development **137**(11): 1853-1862.
- Lehmann, R. and C. Nusslein-Volhard (1991). "The maternal gene nanos has a central role in posterior pattern formation of the Drosophila embryo." Development **112**(3): 679-91.
- Leptin, M. (1999). "Gastrulation in Drosophila: The logic and the cellular mechanisms." Embo Journal **18**(12): 3187-3192.
- Li, W. X. (2005). "Functions and mechanisms of receptor tyrosine kinase Torso signaling: lessons from Drosophila embryonic terminal development." Dev Dyn **232**(3): 656-72.
- Lynch, J. A., A. E. Brent, et al. (2006). "Localized maternal orthodenticle patterns anterior and posterior in the long germ wasp Nasonia." Nature **439**(7077): 728-32.
- Lynch, J. A. and C. Desplan (2006). "A method for parental RNA interference in the wasp Nasonia vitripennis." Nat Protoc **1**(1): 486-94.

- Lynch, J. A. and C. Desplan (2010). "Novel modes of localization and function of nanos in the wasp *Nasonia*." Development **137**(22): 3813-3821.
- Lynch, J. A., E. C. Olesnick, et al. (2006). "Regulation and function of *tailless* in the long germ wasp *Nasonia vitripennis*." Dev Genes Evol.
- Lynch, J. A., O. Ozuak, et al. (2011). "The Phylogenetic Origin of *oskar* Coincided with the Origin of Maternally Provisioned Germ Plasm and Pole Cells at the Base of the Holometabola." PLoS Genet **7**(4): e1002029.
- Lynch, J. A., A. D. Peel, et al. (2010). "EGF Signaling and the Origin of Axial Polarity among the Insects." Current Biology **20**(11): 1042-1047.
- Maderspacher, F., G. Bucher, et al. (1998). "Pair-rule and gap gene mutants in the flour beetle *Tribolium castaneum*." Development genes and evolution **208**(10): 558-568.
- Marques-Souza, H. (2007). Evolution of the gene regulatory network controlling trunk segmentation in insects, University of Köln. **Phd thesis**.
- Marques-Souza, H., M. Aranda, et al. (2008). "Delimiting the conserved features of *hunchback* function for the trunk organization of insects." Development **135**(5): 881-888.
- Martin, B. L. and D. Kimelman (2009). "Wnt signaling and the evolution of embryonic posterior development." Curr Biol **19**(5): R215-9.
- McGregor, A. P., M. Pechmann, et al. (2008). "Wnt8 is required for growth-zone establishment and development of opisthosomal segments in a spider." Curr Biol **18**(20): 1619-23.
- Meinhardt, H. and A. Gierer (2000). "Pattern formation by local self-activation and lateral inhibition." Bioessays **22**(8): 753-60.
- Miyawaki, K., T. Mito, et al. (2004). "Involvement of Wingless/Armadillo signaling in the posterior sequential segmentation in the cricket, *Gryllus bimaculatus* (Orthoptera), as revealed by RNAi analysis." Mech Dev **121**(2): 119-30.
- Mlodzik, M., G. Gibson, et al. (1990). "Effects of Ectopic Expression of *Caudal* during *Drosophila* Development." Development **109**(2): 271-277.
- Moussian, B. and S. Roth (2005). "Dorsoventral axis formation in the *Drosophila* embryo--shaping and transducing a morphogen gradient." Curr Biol **15**(21): R887-99.
- Nusse, R. (2005). "Wnt signaling in disease and in development." Cell Res **15**(1): 28-32.
- O'Connor, M. B., D. Umulis, et al. (2006). "Shaping BMP morphogen gradients in the *Drosophila* embryo and pupal wing." Development **133**(2): 183-193.

- Olesnick, E. C., A. E. Brent, et al. (2006). "A caudal mRNA gradient controls posterior development in the wasp *Nasonia*." *Development* **133**(20): 3973-3982.
- Oppenheimer, D. I., A. M. MacNicol, et al. (1999). "Functional conservation of the wingless-engrailed interaction as shown by a widely applicable baculovirus misexpression system." *Curr Biol* **9**(22): 1288-96.
- Panfilio, K. A. (2008). "Extraembryonic development in insects and the acrobatics of blastokinesis." *Developmental Biology* **313**(2): 471-491.
- Patel, N. H., B. G. Condron, et al. (1994). "Pair-rule expression patterns of even-skipped are found in both short- and long-germ beetles." *Nature* **367**(6462): 429-434.
- Patel, N. H., D. C. Hayward, et al. (2001). "Grasshopper hunchback expression reveals conserved and novel aspects of axis formation and segmentation." *Development* **128**(18): 3459-72.
- Peri, F., M. Technau, et al. (2002). "Mechanisms of Gurken-dependent pipe regulation and the robustness of dorsoventral patterning in *Drosophila*." *Development* **129**(12): 2965-75.
- Posnien, N., F. Bashasab, et al. (2009). "The insect upper lip (labrum) is a nonsegmental appendage-like structure." *Evol Dev* **11**(5): 480-8.
- Posnien, N. and G. Bucher (2010). "Formation of the insect head involves lateral contribution of the intercalary segment, which depends on Tc-labial function." *Dev Biol* **338**(1): 107-16.
- Posnien, N., J. B. Schinko, et al. (2010). "Genetics, development and composition of the insect head--a beetle's view." *Arthropod Struct Dev* **39**(6): 399-410.
- Pultz, M. A., J. N. Pitt, et al. (1999). "Extensive zygotic control of the anteroposterior axis in the wasp *Nasonia vitripennis*." *Development* **126**(4): 701-710.
- Pultz, M. A., L. Westendorf, et al. (2005). "A major role for zygotic hunchback in patterning the *Nasonia* embryo." *Development* **132**(16): 3705-3715.
- Pultz, M. A., K. K. Zimmerman, et al. (2000). "A genetic screen for zygotic embryonic lethal mutations affecting cuticular morphology in the wasp *Nasonia vitripennis*." *Genetics* **154**(3): 1213-1229.
- Rafiqi, A. M., S. Lemke, et al. (2008). "Evolutionary origin of the amnioserosa in cyclorrhaphan flies correlates with spatial and temporal expression changes of zen." *Proceedings of the National Academy of Sciences of the United States of America* **105**(1): 234-239.

- Ray, R. P., K. Arora, et al. (1991). "The control of cell fate along the dorsal-ventral axis of the *Drosophila* embryo." Development **113**(1): 35-54.
- Reeves, G. T. and A. Stathopoulos (2009). "Graded dorsal and differential gene regulation in the *Drosophila* embryo." Cold Spring Harb Perspect Biol **1**(4): a000836.
- Richards, S., R. A. Gibbs, et al. (2008). "The genome of the model beetle and pest *Tribolium castaneum*." Nature **452**(7190): 949-955.
- RiveraPomar, R. and H. Jackle (1996). "From gradients to stripes in *Drosophila* embryogenesis: Filling in the gaps." Trends in Genetics **12**(11): 478-483.
- RiveraPomar, R., D. Niessing, et al. (1996). "RNA binding and translational suppression by bicoid." Nature **379**(6567): 746-749.
- Roth, S. (2003). "The origin of dorsoventral polarity in *Drosophila*." Philos Trans R Soc Lond B Biol Sci **358**(1436): 1317-29; discussion 1329.
- Roth, S. and T. Schupbach (1994). "The relationship between ovarian and embryonic dorsoventral patterning in *Drosophila*." Development **120**(8): 2245-57.
- Rushlow, C. A., K. Han, et al. (1989). "The graded distribution of the dorsal morphogen is initiated by selective nuclear transport in *Drosophila*." Cell **59**(6): 1165-77.
- Sanchez, L., C. Chaouiya, et al. (2008). "Segmenting the fly embryo: logical analysis of the role of the segment polarity cross-regulatory module." Int J Dev Biol **52**(8): 1059-75.
- Savard, J., H. Marques-Souza, et al. (2006). "A segmentation gene in *Tribolium* produces a polycistronic mRNA that codes for multiple conserved peptides." Cell **126**(3): 559-569.
- Schaeffer, V., D. Killian, et al. (2000). "High bicoid levels render the terminal system dispensable for *Drosophila* head development." Development **127**(18): 3993-9.
- Schaeper, N. D., M. Pechmann, et al. "Evolutionary plasticity of collier function in head development of diverse arthropods." Dev Biol **344**(1): 363-76.
- Schinko, J. B., N. Kreuzer, et al. (2008). "Divergent functions of orthodenticle, empty spiracles and buttonhead in early head patterning of the beetle *Tribolium castaneum* (Coleoptera)." Developmental biology **317**(2): 600-613.
- Schinko, J. B., M. Weber, et al. (2010). "Functionality of the GAL4/UAS system in *Tribolium* requires the use of endogenous core promoters." Bmc Developmental Biology **10**: -.

- Schmidt-Ott, U. and G. M. Technau (1992). "Expression of en and wg in the embryonic head and brain of Drosophila indicates a refolded band of seven segment remnants." Development **116**(1): 111-25.
- Scholtz, G. and G. D. Edgecombe (2006). "The evolution of arthropod heads: reconciling morphological, developmental and palaeontological evidence." Dev Genes Evol **216**(7-8): 395-415.
- Schoppmeier, M., S. Fischer, et al. (2009). "An Ancient Anterior Patterning System Promotes Caudal Repression and Head Formation in Ecdysozoa." Current Biology **19**(21): 1811-1815.
- Schoppmeier, M. and R. Schröder (2005). "Maternal Torso Signaling Controls Body Axis Elongation in a Short Germ Insect." **15**(23): 2131-2136.
- Schröder, R. (2003). "The genes orthodenticle and hunchback substitute for bicoid in the beetle Tribolium." Nature **422**: 621-625.
- Schröder, R. (2006). "vasa mRNA accumulates at the posterior pole during blastoderm formation in the flour beetle Tribolium castaneum." Development Genes and Evolution **216**(5): 277-283.
- Schröder, R., C. Eckert, et al. (2000). "Conserved and divergent aspects of terminal patterning in the beetle Tribolium castaneum." Proceedings of the National Academy of Sciences of the United States of America **97**(12): 6591-6596.
- Shinmyo, Y., T. Mito, et al. (2005). "caudal is required for gnathal and thoracic patterning and for posterior elongation in the intermediate-germband cricket Gryllus bimaculatus." Mech Dev **122**(2): 231-9.
- Shippy, T. D., S. J. Brown, et al. (2000). "Maxillopedia is the Tribolium ortholog of proboscipedia." Evol Dev **2**(3): 145-51.
- Small, S., R. Kraut, et al. (1991). "Transcriptional regulation of a pair-rule stripe in Drosophila." Genes Dev **5**(5): 827-39.
- Smibert, C. A., J. Wilson, et al. (1996). "smaug protein represses translation of unlocalized nanos mRNA in the Drosophila embryo." Genes Dev **10**(20): 2600-9.
- Sommer, R. J. and D. Tautz (1993). "Involvement of an orthologue of the Drosophila pair-rule gene hairy in segment formation of the short germ-band embryo of Tribolium (Coleoptera)." Nature **361**(6411): 448-450.

- Sprenger, F., M. M. Trosclair, et al. (1993). "Biochemical analysis of torso and D-raf during *Drosophila* embryogenesis: implications for terminal signal transduction." Mol Cell Biol **13**(2): 1163-72.
- Sprenger, F. N.-V., C. (1993). The terminal system of axis determination in the *drosophila* embryo. The development of *Drosophila melanogaster*. M. A. Bate, A., Cold Spring Harbor Laboratory. **1**: 365-386.
- Stathopoulos, A. and M. Levine (2002). "Dorsal gradient networks in the *Drosophila* embryo." Dev Biol **246**(1): 57-67.
- Stathopoulos, A., M. Van Drenth, et al. (2002). "Whole-genome analysis of dorsal-ventral patterning in the *Drosophila* embryo." Cell **111**(5): 687-701.
- Stauber, M., H. Jackle, et al. (1999). "The anterior determinant bicoid of *Drosophila* is a derived Hox class 3 gene." Proceedings of the National Academy of Sciences of the United States of America **96**(7): 3786-3789.
- Stevens, L. M., D. Beuchle, et al. (2003). "The *Drosophila* embryonic patterning determinant torsolike is a component of the eggshell." Curr Biol **13**(12): 1058-63.
- Stevens, L. M., H. G. Frohnhofer, et al. (1990). "Localized requirement for torso-like expression in follicle cells for development of terminal Anlagen of the *Drosophila* embryo." Nature **346**(6285): 660-3.
- Steward, R., S. B. Zusman, et al. (1988). "The dorsal protein is distributed in a gradient in early *Drosophila* embryos." Cell **55**(3): 487-95.
- Stuart, J. J., S. J. Brown, et al. (1991). "A deficiency of the homeotic complex of the beetle *Tribolium*." Nature **350**(6313): 72-4.
- Tautz, D., M. Friedrich, et al. (1994). "Insect embryogenesis - what is ancestral and what is derived? ." Development Supplement: 193-199.
- Trauner, J., J. Schinko, et al. (2009). "Large-scale insertional mutagenesis of a coleopteran stored grain pest, the red flour beetle *Tribolium castaneum*, identifies embryonic lethal mutations and enhancer traps." Bmc Biology **7**: -.
- Treisman, J., P. Gonczy, et al. (1989). "A single amino acid can determine the DNA binding specificity of homeodomain proteins." Cell **59**: 553-562.
- van der Zee, M., N. Berns, et al. (2005). "Distinct functions of the *Tribolium* *zerknüllt* genes in serosa specification and dorsal closure." Current Biology **15**(7): 624-636.

- van der Zee, M., O. Stockhammer, et al. (2006). "Sog/Chordin is required for ventral-to-dorsal Dpp/BMP transport and head formation in a short germ insect." Proceedings of the National Academy of Sciences of the United States of America **103**(44): 16307-16312.
- Von Ohlen, T. and C. Q. Doe (2000). "Convergence of dorsal, Dpp, and Egfr signaling pathways subdivides the Drosophila neuroectoderm into three dorsal-ventral columns." Developmental Biology **224**(2): 362-372.
- Weigel, D., G. Jurgens, et al. (1990). "Two gap genes mediate maternal terminal pattern information in Drosophila." Science **248**(4954): 495-8.
- Weinstock, G. M., G. E. Robinson, et al. (2006). "Insights into social insects from the genome of the honeybee *Apis mellifera*." Nature **443**(7114): 931-949.
- Werren, J. H., S. Richards, et al. (2010). "Functional and Evolutionary Insights from the Genomes of Three Parasitoid *Nasonia* Species." Science **327**(5963): 343-348.
- Wheeler, S. R., M. L. Carrico, et al. (2005). "The *Tribolium* columnar genes reveal conservation and plasticity in neural precursor patterning along the embryonic dorsal-ventral axis." Developmental Biology **279**(2): 491-500.
- Wilson, M. J. and P. K. Dearden (2009). "Tailless patterning functions are conserved in the honeybee even in the absence of Torso signaling." Developmental Biology **335**(1): 276-287.
- Wilson, M. J., M. Havler, et al. "Giant, Kruppel, and caudal act as gap genes with extensive roles in patterning the honeybee embryo." Dev Biol **339**(1): 200-11.
- Wimmer, E. A., S. M. Cohen, et al. (1997). "buttonhead does not contribute to a combinatorial code proposed for Drosophila head development." Development **124**(8): 1509-17.
- Wolff, C., R. Sommer, et al. (1995). "Conserved and divergent expression aspects of the Drosophila segmentation gene hunchback in the short germ band embryo of the flour beetle *Tribolium*." Development **121**(12): 4227-4236.
- Yip, M. L. R., M. L. Lamka, et al. (1997). "Control of germ-band retraction in Drosophila by the zinc-finger protein HINDSIGHT." Development **124**(11): 2129-2141.
- Zhang, Z. Y., L. M. Stevens, et al. (2009). "Sulfation of Eggshell Components by Pipe Defines Dorsal-Ventral Polarity in the Drosophila Embryo." Current Biology **19**(14): 1200-1205.

Chapter 2 - A segmentation clock operating in blastoderm and germband stages of insect development

Ezzat El-Sherif¹, Michalis Averof² Susan J. Brown³

Summary

In *Drosophila*, all segments form in the blastoderm where morphogen gradients spanning the entire anterior-posterior axis of the embryo provide positional information. However, in the beetle *Tribolium castaneum* and most other insects, a number of anterior segments form in the blastoderm, and the remaining segments form sequentially from a posterior growth zone during germband elongation. Recently, the cyclic nature of pair-rule gene expression was demonstrated in the growth zone of *Tribolium*, indicating that a vertebrate-like segmentation clock is employed in the germband stage of its development. This suggests that two mechanisms might function in the same organism: a *Drosophila*-like mechanism in the blastoderm, and a vertebrate-like mechanism in the germband. Here we show that segmentation at *both* blastoderm and germband stages of *Tribolium* is based on a segmentation clock. Specifically, we show that the *Tribolium* primary pair-rule gene, *Tc-even-skipped* (*Tc-eve*), is expressed in waves propagating from the posterior pole and progressively slowing until they freeze into stripes; such dynamics are a hallmark of clock-based segmentation. Phase shifts between *Tc-eve* transcripts and protein confirm that these waves are due to expression dynamics. Moreover, by tracking cells in live embryos and by analyzing mitotic profiles, we found that neither cell movement nor oriented cell division could explain the observed wave dynamics of *Tc-eve*. These results pose intriguing evolutionary questions, since *Drosophila* and *Tribolium* segment their blastoderms using the same genes but different mechanisms.

¹ Genetics Program, Kansas State University, Manhattan, KS 66506, USA.

² Institute of Molecular Biology and Biotechnology (IMBB-FORTH), GR-70013, Heraklion, Crete, Greece.

³ Division of Biology, Kansas State University, Manhattan, KS 66506, USA.

Introduction

Early in embryogenesis, the anterior-posterior (AP) axis of an arthropod embryo is established as a series of body segments. In *Drosophila*, global, long-range morphogen gradients initiated by maternal factors provide positional information for a downstream cascade of genes that ultimately partitions the AP axis into segments (Rivera-Pomar and Jackle, 1996). This mechanism is possible in a blastoderm where morphogens are free to diffuse in a syncytial environment to form gradients that span the entire region to be segmented. However, in most other insects, posterior segments are specified sequentially in a cellularized environment out of a posterior pool of cells, referred to as the 'growth zone' (Davis and Patel, 2002). For this mode of segmentation, morphogen gradients spanning the entire AP axis have not been discovered.

Vertebrate somitogenesis also occurs in a cellular environment where segments form sequentially during AP axis elongation. Somitogenesis relies on the 'clock and wavefront' mechanism, where the expression of multiple genes (including genes of the Notch, Wnt and FGF signaling pathways (Dequeant et al., 2006; Krol et al., 2011)) oscillate in the presomatic mesoderm (PSM) posterior to an arrest front (defined by a threshold within the overlapping domain of posterior Wnt and FGF gradients (Aulehla et al., 2003; Dubrulle et al., 2001) and an opposing retinoic acid gradient (Diez del Corral et al., 2003)). Anterior to the arrest front, oscillation ceases, producing stripes of gene expression. While the genetic and biochemical details are not yet understood, oscillations seem to be arrested gradually (Giudicelli et al., 2007), resulting in kinematic waves of expression that slow down and shrink as they propagate along the PSM (Palmeirim et al., 1997).

A clock and wavefront model has been proposed to act in arthropods as well (Peel et al., 2005), since what appear to be waves of gene expression propagating within the growth zone have been reported in several arthropods (Chipman and Akam, 2008; Chipman et al., 2004; Pueyo et al., 2008; Stollewerk et al., 2003). Recent work demonstrates that *Tc-odd-skipped* (*Tc-odd*) expression in the growth zone of the *Tribolium* germband oscillates in a manner that cannot be explained by cell movements (Sarrazin et al., 2012).

Most insects form anterior segments in the blastoderm and posterior segments from a posterior growth zone (Davis and Patel, 2002). It is conceivable that these insects utilize two different modes of segmentation: a *Drosophila*-like mechanism in the blastoderm and clock-based mechanism in the germband. In this report, we show that the beetle *Tribolium castaneum*

utilizes a clock-based segmentation mechanism in both blastoderm and germband stages of its development. Specifically, we show that the *Tribolium* primary pair-rule gene *Tc-even-skipped* (*Tc-eve*) is expressed in waves propagating in both blastoderm and germband stages. These dynamics are evident from the observed phase shift between *Tc-eve* transcripts and proteins. By tracking cells in live embryos and by analyzing mitotic profiles, we confirm that the waves of *Tc-eve* expression in the blastoderm cannot be explained by cell movement or by oriented cell division.

Waves of *Tc-eve* gene expression are observed in both blastoderm and germband stages of *Tribolium* development

The three *Tc-eve* stripes that form during blastoderm stages were previously thought to form by subdividing a broad posterior expression domain (Figure 2.1, class B1), through clearing of expression to form the interstripe regions (Figure 2.1, classes B6 and B9) (Brown et al., 1997; Patel et al., 1994). By carefully examining a large number of fixed embryos at the blastoderm stage, we found that *Tc-eve* expression is considerably more dynamic and several intermediate staining patterns are discernible (Figure 2.1, classes B0-B9). Each primary *Tc-eve* stripe first appears as a cap of expression at the posterior pole of the embryo (Figure 2.1, classes B1, B4 and B8), which extends anteriorly, clears from the posterior pole, continuously shrinks in width, and eventually freezes into a stable stripe of expression. Later, each primary *Tc-eve* stripe splits into two secondary (segmental) stripes (Figure 2.1 B9-G6).

The fourth primary *Tc-eve* stripe starts to form in the germband, with similar dynamics to that of blastodermal stripes. *Tc-eve* expression emanates from the posterior end of the growth zone (Figure 2.1 G2), expands to fill the growth zone (Figure 2.1 G3), then shrinks and stabilizes into a stripe at the anterior border of the growth zone (Figure 2.1 G4). The remaining stripes that form during germband elongation show similar dynamics (Supp. Figure 2.1 and Supp. Table 2.1).

To verify that the differences in the blastoderm *Tc-eve* expression patterns represent a genuine temporal sequence of expression, and are not due to embryo-to-embryo variation, we examined *Tc-eve* expression in twelve consecutive 1-hour developmental windows, spanning the blastoderm stage (12 to 24 hours post egg lay at 23-24° C; see Methods). For every time window, we determined the percentage of embryos displaying a given *Tc-eve* expression pattern (classes

B0 to B9 for blastoderm, class G for all germband stages; see Table 1.1). The overall pattern of class distributions supports the notion that these patterns represent the temporal sequence of *Tc-eve* expression. For example, class B3 embryos appear for the first time in the 14 to 15 hour window, indicating that they are more advanced in age compared to embryos in B1 and B2. Since we now have verified that B0 to B9 represent genuine temporal sequence of expressions, we will henceforth use them as developmental stages.

Figure 2.1 Waves of *Tc-eve* expression propagate from posterior to anterior in both blastoderm and germband stages of *Tribolium* development.

Progression of *Tc-eve* expression from early blastoderm to early germband stages is shown. Classes B0-B9 (blastoderm stages) and G1-G4 (germband stages) represent distinct *Tc-eve* expression patterns, arranged in a putative temporal sequence (see Table 2.1). Propagation of the first three waves of *Tc-eve* expression is highlighted in red (first stripe), blue (second stripe) and green (third stripe). *Tc-eve* oscillation in the posterior end of the embryo is marked by circles; high expression levels are marked by filled circles, low levels by open circles. DAPI staining of blastoderm stages is shown on the right. Classes coinciding with extensive mitoses are enclosed in yellow rectangles. Anterior to the left.

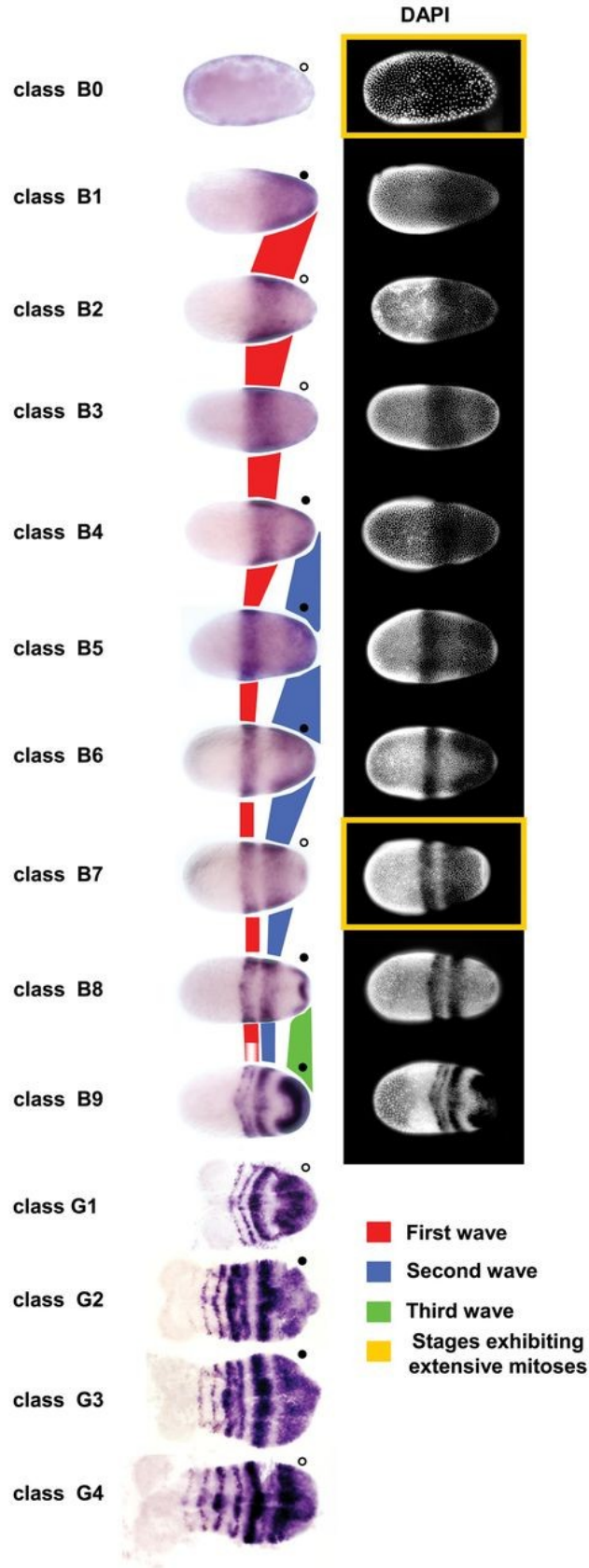













Table 2.1 Mapping the temporal order of *Tc-eve* patterns.

The proportion of each class of *Tc-eve* pattern (blastoderm stages B0-B9; all germband stages combined in G) was recorded in egg collections spanning the blastoderm and early germband stages [12-24 hours after egg laying (AEL), at 23-24°C] in 1-hour developmental windows. The last row in the table shows the average percentage of each class over all egg collections, which estimates the proportion of each class in total (spanning the entire 12-24 hour period).

egg collection (hours AEL)	class	B0	B1	B2	B3	B4	B5	B6	B7	B8	B9	G
												
12→13 (n = 28)		82.1%	17.9%									
13→14 (n = 52)		32.7%	65.4%	1.9%								
14→15 (n = 49)		12.2%	79.6%	6.1%	2.1%							
15→16 (n = 64)		3.1%	68.8%	15.6%	7.8%	4.7%						
16→17 (n = 38)		2.6%	28.9%	10.5%	18.4%	15.8%	21.2%	2.6%				
17→18 (n = 48)		4.2%	8.3%	6.3%	10.4%	14.6%	20.8%	18.8%	16.6%			
18→19 (n = 25)			8%	4%	4%	8%	8%	52%	16%			
19→20 (n = 22)					9.1%	13.7%	4.5%	9.1%	50%	4.5%	9.1%	
20→21 (n = 58)						3.4%	3.4%	3.4%	25.9%	29.3%	32.8%	1.8%
21→22 (n = 41)									4.9%	24.4%	48.8%	21.9%
22→23 (n = 48)										2.1%	31.3%	66.6%
23→24 (n = 48)											6.3%	93.7%
Average		11.4%	23.1%	3.7%	4.3%	5%	4.8%	7.2%	9.5%	5%	10.7%	15.3%

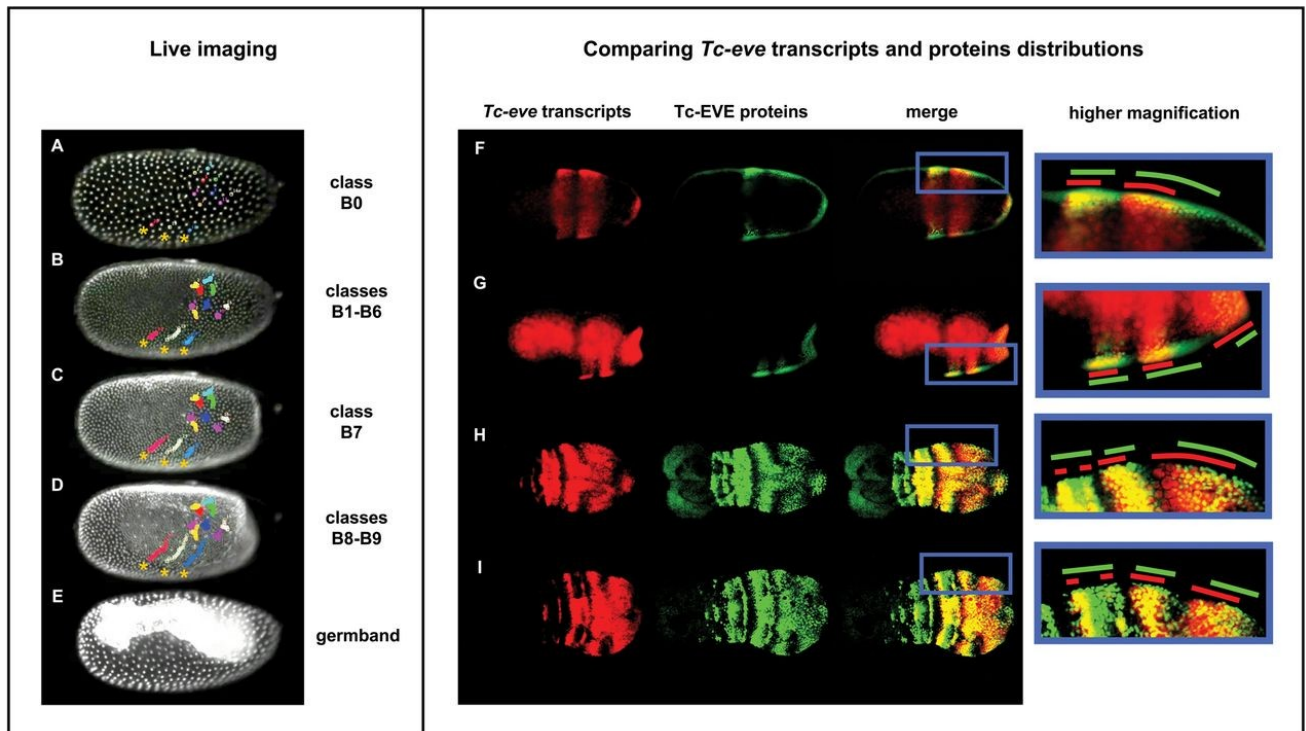
These observations suggest that *Tc-eve* dynamics in both the blastoderm and the germband can be described as waves of gene expression that emanate from the posterior end and propagate anteriorly while shrinking in width. These dynamics have the characteristic appearance of kinematic waves generated by an oscillator under the control of a posterior-to-anterior frequency gradient (Movie 2.1) (Palmeirim et al., 1997). The oscillation of *Tc-eve* expression can be followed in cells at the posterior end of the embryos in Figure 2.1 (filled circles represent high expression levels, open circles represent low expression levels).

***Tc-eve* waves are due to transcription dynamics, rather than cell movement or oriented cell division**

To address the possibility that the observed dynamics of *Tc-eve* expression are due to cell movement, we used a transgenic line expressing nuclear-localized GFP driven by a *Tribolium* ubiquitous promoter (EFA-nGFP line) (Sarrazin et al., 2012) to track cell movements in live embryos starting from early blastoderm stage (B0) and continuing through the germband (Movie 2.2 and Figure 2.2 A-E). Blastoderm *Tc-eve* patterns (B0-B9) were registered with time-lapse movies based on overall morphology and nuclear density in the blastoderm (see Methods). In stages B0 to B7, nuclear movement in most of the blastoderm is very limited and mostly random. We observe some slow movements of the most lateral nuclei in a posterior and ventral direction (marked by asterisks in Figure 2.2 A-C), which represent the earliest sign of germband condensation, and inward movements of cells at the posterior pole, to produce the characteristic posterior flattening of the late blastoderm. Late in stage B7, a burst of mitoses in the embryonic field differentiates it from the serosa. During stages B8 and B9, the germband anlage rapidly condenses towards the ventral side of the embryo; this involves rapid movements of nuclei from the lateral sides of the blastoderm in a posterior and ventral direction (see three tracks marked by asterisks in Figure 2.2 D). These movements do not explain the dynamics of *Tc-eve* expression, which involve much faster changes and shifts of expression from the posterior pole towards the middle of the embryo.

Figure 2.2 *Tc-eve* waves are due to transcription dynamics, rather than cell movements.

(A-E) Stills from live imaging of an EFA-nGFP transgenic *Tribolium* embryo (supplementary material Movie 2.2), from early blastoderm (A) to germband (E) stages; the corresponding *Tc-eve* patterns from Figure 2.1 are indicated on the right. Colored circles track the movement of nuclei, showing that cell movement cannot explain *Tc-eve* dynamics. Three dorsolateral cells are marked with asterisks in A-D. (F-I) Concurrent *Tc-eve* in situ hybridization (red; first column) and Tc-EVE antibody staining (green; second column) were merged (third column) to reveal the phase shift between mRNA and protein distributions. The fourth column shows higher magnifications of the region of interest; red and green lines mark the extent of *Tc-eve* transcript and Tc-EVE protein distributions, respectively. The fact that Tc-EVE stripes lag behind those of *Tc-eve* indicates that *Tc-eve* stripes propagate as waves from posterior to anterior. The fact that the phase shift decreases as the stripes mature suggests that the waves are slowing down before they eventually freeze and split into secondary stripes. Similar dynamics are seen at different stages. Anterior to the left; ventral is up in A-E.



Oriented cell divisions could in principle also contribute to the observed dynamics of gene expression. We therefore examined whether oriented mitoses occur during stages B0-B9. After synchronous mitoses phase in early blastoderm (class B0), no mitoses were detected in B1 to B5 stage embryos, and only limited random mitoses were detected in stage B6 ($n=10$ for each class). Stage B7 blastoderms were found to undergo extensive cell division in all cells except those of the serosa. These mitoses are randomly oriented (Supp. Figure 2.2). During stages B8 and B9, mitotic activity decreased and only a very limited number of random mitotic plates were observed. In the germband stage, Sarrazin et al. (2012) showed that the growth zone extends by convergent extension and experiences low mitotic activity until the formation of the fifth pair-rule stripe (Sarrazin et al., 2012). Hence, neither cell movement nor oriented cell division contributes significantly to *Tc-eve* dynamics in blastoderm or germband stages.

To directly confirm that *Tc-eve* waves are due to expression dynamics, we compared the relative distribution of *Tc-eve* transcripts and Tc-EVE protein within individual embryos (Figure 2.2 F-J). If *Tc-eve* is expressed as waves, we expect the short delay between transcription and translation to be reflected in a small shift between the mRNA and protein distributions. When a wave of expression freezes into a stripe, transcripts and proteins should precisely co-localize. Indeed, we observed that the Tc-EVE protein distribution lags behind that of *Tc-eve* transcripts as each wave propagates from the posterior pole, both in the blastoderm (Figure 2.2 F, G) and in the germband growth zone (Figure 2.2 H,I). The two patterns precisely co-localize in the stable/mature primary stripes, which then split into secondary stripes. Interestingly, each primary stripe exhibits smaller phase shift between mRNA and protein as it moves anteriorly (Figure 2.2 F-I) reflecting a gradual slowing of each stripe as it matures. This outcome is consistent with a model where the frequency of *Tc-eve* oscillation changes in a posterior to anterior gradient (Movie 2.3).

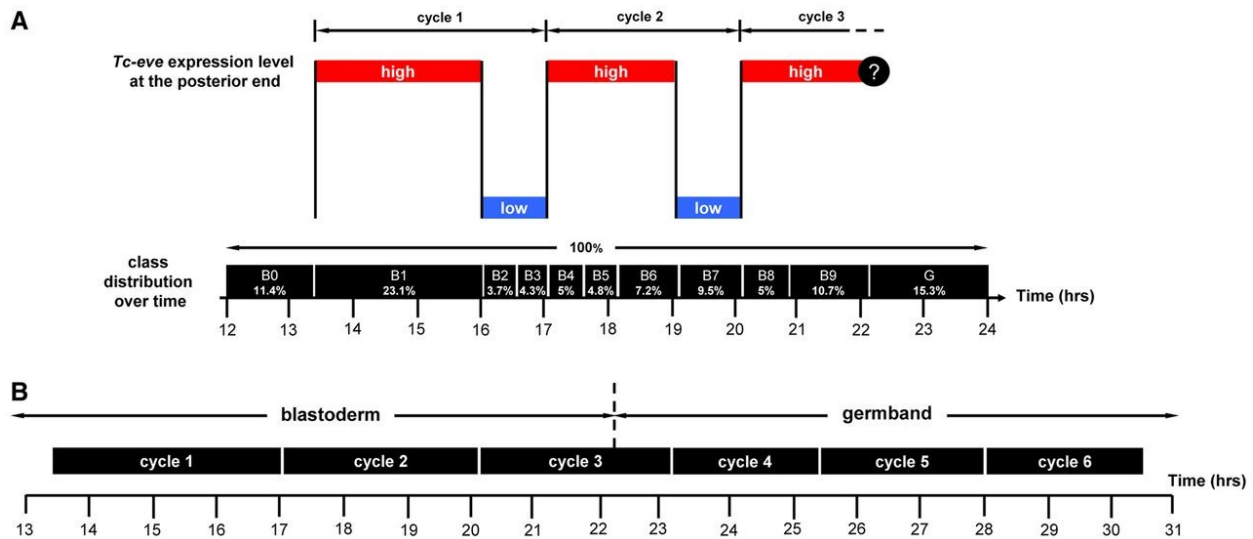
Determining the frequency of *Tc-eve* oscillations

Fixed embryos provide only spatial information about *Tc-eve* expression (Figure 2.1), but by analyzing the distribution of expression patterns over several developmental windows (as in Table 2.1) we can gain some temporal information about *Tc-eve* dynamics (e.g. its periodicity, or lack thereof). The average percentage of embryos found in each class (shown in the last row of Table 2.1) can be used to estimate the duration of each class (vertical black bars in Figure 2.3 A).

A waveform of *Tc-eve* oscillations at the posterior end of the blastoderm was drawn by tracking *Tc-eve* expression levels (closed and open circles in Figure 2.1) during each class (Figure 2.3 A). From this analysis, the frequency of *Tc-eve* oscillation at the posterior end of the blastoderm was determined to be around one cycle per three hours at 23-24° C, for the first two cycles of *Tc-eve*.

Figure 2.3 Periodicity of Tc-eve oscillation in the blastoderm and germband.

(A) The duration of each class of *Tc-eve* expression (estimated from Table 2.1, bottom row) is represented by the width of the black boxes. This is equivalent to combining all egg collections into one large collection, spanning 12-24 hours after egg laying, then using the overall percentage of embryos in each class as an estimate of its duration (percentages rather than absolute numbers are used in calculations to correct for differences in the number of eggs in each collection). *Tc-eve* expression at the posterior end of the blastoderm is shown above the black boxes (red bars, high *Tc-eve*; blue bars, low *Tc-eve*; question mark indicates uncertainty due to primitive pit formation). (B) The estimated duration of *Tc-eve* cycles for blastoderm (taken from A) and germband (determined from Supp. Table 2.1, for stripes 4, 5 and 6) are represented by the width of the black boxes.



To confirm the periodicity of the first two cycles and to determine whether the third cycle has the same period, we calculated the proportions of embryos undergoing first, second, and third cycles of *Tc-eve* expression in an egg collection spanning the period from 10 to 26

hours after egg lay. We found similar proportions of embryos in each cycle (31.4% in cycle 1, 30.8% in cycle 2, and 37.8% in cycle 3; $n=143$) indicating that the three cycles are of almost equal duration. A similar analysis of germband stages, using 6 consecutive 3-hour developmental windows, indicated the period of *Tc-eve* cycles in the germband is similar (except for the eighth cycle; see Table S1), but on average slightly shorter than that found in the blastoderm (Figure 2.3B). Future experiments with reporter constructs and live imaging will be needed to determine if this subtle difference is significant. *Tc-odd* oscillates out of phase with *Tc-eve*, and its fourth cycle was estimated to be around 95 minutes at 30° C (Sarrazin et al., 2012). This is approximately half the periodicity determined for *Tc-eve* (3 hours), consistent with a doubling of developmental rates between 24°C and 30°C (Park and Marian Burton, 1948).

Probable molecular basis and implications for segmentation mechanisms

A molecular candidate for the presumed clock is the negative feedback circuit composed of the three *Tribolium* primary pair-rule genes: *Tc-eve*, *Tc-runt*, and *Tc-odd* (Choe et al., 2006). Two of these genes, *Tc-eve* and *Tc-odd* have been found to oscillate in *Tribolium* (this report and (Sarrazin et al., 2012)). Possible candidates for the wavefront include *Tc-caudal*, a gene essential for segmentation (Copf et al., 2004) that is expressed in a posterior gradient during blastoderm stage and is then expressed in the posterior growth zone during germband stage (Schulz et al., 1998). Another candidate is canonical Wnt pathway activity: two Wnt ligands (*Tc-Wnt1* and *Tc-Wnt8/D*) are expressed at the posterior tip of the germband (Bolognesi et al., 2008a), which could generate a posterior-to-anterior gradient of Wnt activity. Wnt ligands are also expressed posteriorly in the blastoderm, but they are functionally dispensable during this stage (Bolognesi et al., 2008b; Bolognesi et al., 2009). However, it was found recently that a negative regulator of the canonical Wnt pathway, *axin*, is anteriorly localized in the blastoderm, possibly resulting in a ligand-independent posterior-to-anterior Wnt activity gradient (Fu et al., 2012).

The original formulation of the clock and wavefront model postulated an oscillator controlled by a continuously *moving* gradient (wavefront), within which the oscillation persists and outside of which the oscillation freezes (Cooke and Zeeman, 1976). Interestingly, even a *static* smooth gradient is capable of generating striped expression (see Movie 2.1) (Beck and Varadi, 1972). This could explain the formation of the first three *Tc-eve* stripes in the blastoderm

in the absence of posterior elongation, although the possibility of a continuously retracting wavefront in the blastoderm phase cannot be excluded.

Materials and Methods

In situ hybridization and immunocytochemistry

In situ hybridization was performed using DIG-labeled RNA probes and anti-DIG::AP antibody (Roche). Signal was developed using NBT/BCIP (BM Purple, Roche), or Fast Red/HNPP (Roche). Immunocytochemistry was performed using anti-EVE (mouse monoclonal antibody 2B8, hybridoma bank, University of Iowa) and anti-EN (mouse monoclonal antibody 4D9, Santa Cruz Technology) as primary, and anti-mouse::POD as secondary antibody (ABC kit, Vector). DAB was used as a substrate to produce golden brown signal, and AlexaFluor 488 tyramide (Invitrogen) to give green fluorescent signal.

Wildtype strains and transgenic lines

All expression analysis was performed using GA-1 strain embryos. Live imaging was done using the EFA-nGFP line (Sarrazin et al., 2012).

Live imaging and cell tracking

EFA-nGFP embryos were dechorionated by immersing in 1% bleach for 30 seconds. Embryos were then placed on a microscope glass slide and covered with halocarbon oil 700 (Sigma); no coverslip was used. The time-lapse movie was taken by capturing 5 focal planes every 5 minutes, over approximately 11 hours at 26-28°C, on a Leica M205 FA stereoscope at 200x magnification. Movie 2.2 shows a single focal plane at a speed of 6 frames (30 minutes real time) per second. GFP-tagged nuclei were tracked using the ImageJ plugin MTrackJ (Meijering et al., 2012).

Egg collections for developmental time windows

One hour developmental windows were generated by incubating one hour egg collections at 23-24°C for the desired length of time (Table 2.1). For 3-hour developmental windows (Supp. Table 2.1), eggs were collected after three hours instead of one hour.

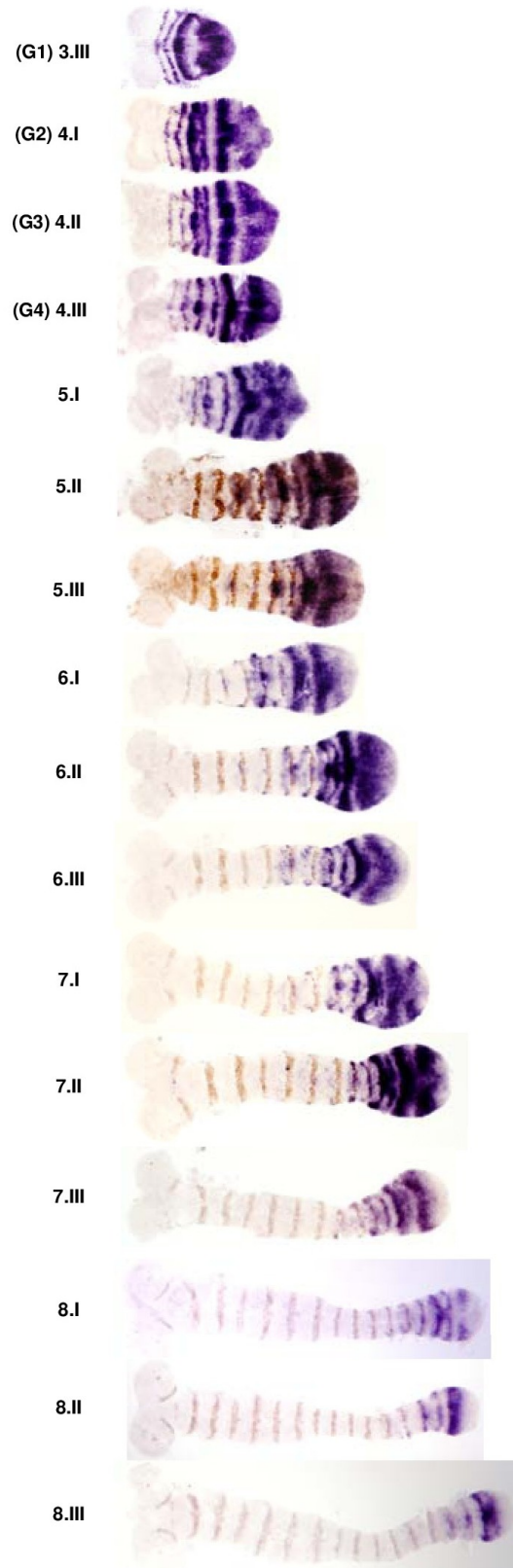
Correlation of time-lapse movie and blastoderm stainings

Based on embryo morphology and nuclear density, blastoderm classes (B0-B9) were correlated with the time-lapse images. The B0 stage is characterized by low nuclear density (up to mitotic cycle 13) and a rounded posterior end, B1-B6 stage embryos have higher nuclear density and the posterior end is still rounded (after mitotic cycle 13), B7 stage is characterized by flattening of the posterior pole, and B8-B9 embryos are identified by primitive pit formation.

Supplementary materials

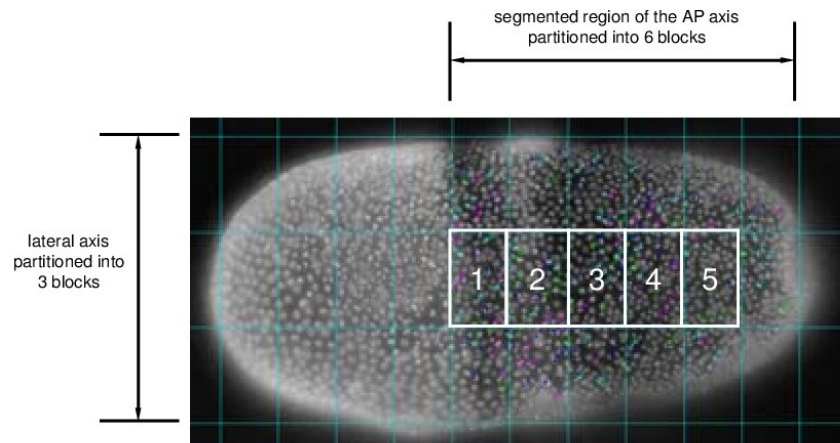
Supp. Figure 2.1 *Tc-eve* expression dynamics in the germband.

Germband embryos in progressively older stages of development were stained to visualize *Tc-eve* transcripts (purple) and Tc-ENGRAILED (Tc-EN) protein (golden brown). Following the classification adopted for *Tc-odd* by Sarrazin et al. (2012), we divided each cycle of *Tc-eve* into three phases: n.I, n.II, and n.III, where n is the primary *Tc-eve* stripe that is being generated in the growth zone. In phase I, *Tc-eve* is expressed as a dot at the tip of each of the two ectodermal plates abutting the mesoderm. In phase II, *Tc-eve* expression expands to fill the growth zone. In phase III, *Tc-eve* clears from the posterior part of the growth zone forming a new stripe. Note that as each primary *Tc-eve* stripe matures, it splits into two transient secondary/segmental stripes that are eventually replaced by Tc-EN expression. The formation of the 8th primary stripe is delayed, as phase 8.I starts well after the 7th primary stripe has matured and split into secondary stripes. For the first four embryos, the classification used in Figure 2.1 is also indicated (G1 to G4). Anterior to left.

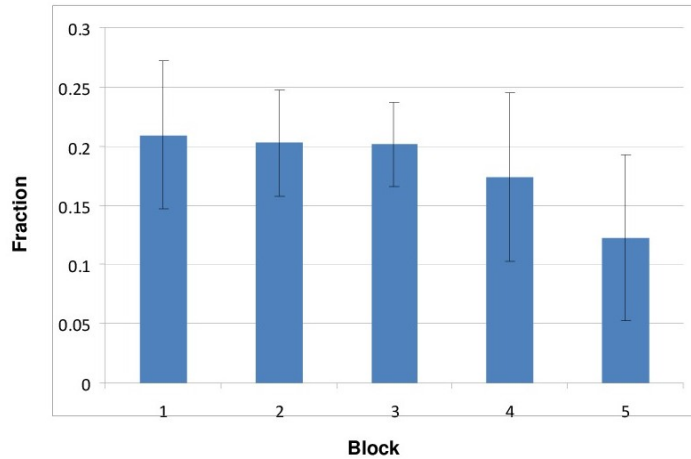


Supp. Figure 2.2 No significant localized or oriented cell division in the segmented part of class B7 blastoderms.

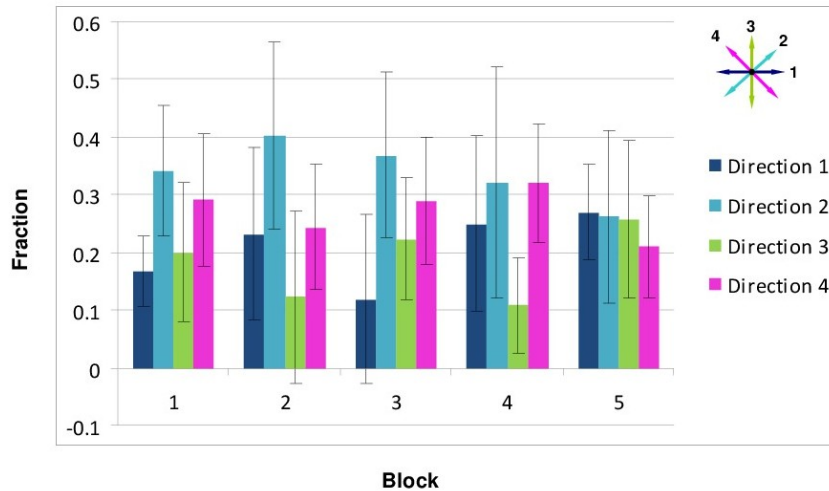
Six B7 blastoderms undergoing mitoses in the region of the prospective germband were examined for localized or oriented cell division. The ventral side of each embryo was divided into 3x6 blocks of equal size, encompassing the domain of *Tc-eve* expression. We focused our analysis on the five blocks shown in (a); anterior to the left. For each block, the number (b) and orientation (c) of mitotic figures was determined. (b) Similar numbers of mitoses (in all directions) were observed in each block, relative to the total number of mitoses in all five blocks, indicating that there is no significant localized cell division. The proportion of mitoses occurring in each orientation within each block is shown in (c), which indicates no significant bias in the direction of cell divisions.



(a)





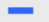
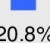




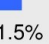
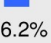




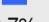

(b)



(c)

Supp. Table 2.1 Primary *Tc-eve* stripes are generated approximately every 3 hours in the germband.

The emergence of primary *Tc-eve* stripes from the growth zone was determined in consecutive 3-hour time windows, 22 to 40 hours post egg lay at 23-24° C. The emergence of primary stripes 3-8 peaked in consecutive time windows, indicating that *Tc-eve* primary stripes emerge approximately with a 3-hour periodicity. The 7th cycle seems to last longer than previous cycles. However, most of the 7th cycle embryos found in 34→37 egg collection were in phase 7.III (86%, $n=14$), probably reflecting the delay in phase 8.I, which takes much longer to appear.

egg cycle collection	3	4	5	6	7	8
22 → 25 (n=82)	 35.4%	 54.9%	 9.7%			
25 → 28 (n=82)		 20.8%	 59.8%	 20.7%		
28 → 31 (n=35)			 17.1%	 51.4%	 31.5%	
31 → 34 (n=37)				 16.2%	 78.4%	 5.4%
34 → 37 (n=36)					 38.9%	 61.1%
37 → 40 (n=23)					 8.7%	 91.3%
Average	5.95%	12.6%	14.43%	14.68%	26.3%	26.4%

Movie 2.1 Computer simulation of *Tc-eve* dynamics in the blastoderm.

Tc-eve expression (shown in blue) in the blastoderm is modeled by an array of oscillators along the horizontal axis (representing the AP axis; posterior to the right). Each oscillator runs independently with a frequency determined by a spatial gradient (shown in red). The frequency gradient starts with zero value at 20% from the anterior and increases linearly to reach a maximum value of 100% (1 cycle per unit time) at the posterior end. The simulation runs for 2.5 cycles, corresponding to the cycles of *Tc-eve* expression that occur in the blastoderm. Spatial resolution used in this simulation (10^4 points along AP axis) gives similar qualitative results as actual resolution (around 70 nuclei along AP axis) but better visualization. The simulation was performed using Matlab.

Movie 2.2 Time-lapse recording of nuclear GFP in *Tribolium* blastoderm and early germband.

The movie captures >11 hours of development at 26-28°C, at 5 minutes per frame. Two waves of mitotic divisions in early blastoderm (at 00:15 and 2:00 hours) and a burst of mitosis in the condensing germ rudiment (~6:35 hours) appear as a transient loss of GFP nuclear localization. We estimate that stages prior to *Tc-eve* expression (B0) correspond to 0:00 to 2:30, and *Tc-eve* stripes 1 and 2 (B1-B7) are generated between 2:30 and 6:30; class B9 is estimated to be at 8:15. Colored circles show the tracked nuclei (see Materials and methods).

Movie 2.3 Computer simulation of phase shifts between *Tc-eve* transcript and Tc-EVE protein distributions in the blastoderm.

Upper panel represents *Tc-eve* mRNA expression in the blastoderm, similar to Movie 2.1 (mRNA expression in red; the frequency gradient, thick black line). The middle panel represents Tc-EVE protein distribution (shown in green), and was produced by introducing a delay of 4×10^{-4} unit time relative to *Tc-eve* mRNA expression. The merge of *Tc-eve* expression and Tc-EVE distribution is shown in the lower panel; yellow represents the overlap between them. Note the progressive decrease in the phase shift between *Tc-eve* mRNA and Tc-EVE protein. The phase shift in more mature stripes is smaller than that in younger stripes. Spatial resolution used in this simulation (10^4 points along AP axis) gives similar qualitative results as actual resolution (around 70 nuclei along AP axis) but better visualization. Anterior to the left. The simulation was performed using Matlab.

Acknowledgements

We are thankful to Andrew Peel for helpful comments on the manuscript, Michelle Gordon and Barb VanSlyke for technical support, and the Bodossaki Foundation for donating the stereoscope used for time-lapse recordings. This work was supported by NIH grant no. 5R01HD29594, and K-INBRE grant no. P20RR016475.

References

Aulehla, A., Wehrle, C., Brand-Saberi, B., Kemler, R., Gossler, A., Kanzler, B. and Herrmann, B. G. (2003). Wnt3a plays a major role in the segmentation clock controlling somitogenesis. *Dev Cell* 4, 395-406.

- Beck, M. T. and Varadi, Z. B. (1972). One, Two and Three-dimensional Spatially Periodic Chemical Reactions. *Nature* 235, 15-16.
- Bolognesi, R., Beermann, A., Farzana, L., Wittkopp, N., Lutz, R., Balavoine, G., Brown, S. J. and Schroder, R. (2008a). Tribolium Wnts: evidence for a larger repertoire in insects with overlapping expression patterns that suggest multiple redundant functions in embryogenesis. *Dev Genes Evol* 218, 193-202.
- Bolognesi, R., Farzana, L., Fischer, T. D. and Brown, S. J. (2008b). Multiple Wnt Genes Are Required for Segmentation in the Short-Germ Embryo of *Tribolium castaneum*. *Current Biology* 18, 1624-1629.
- Bolognesi, R., Fischer, T. D. and Brown, S. J. (2009). Loss of Tc-arrow and canonical Wnt signaling alters posterior morphology and pair-rule gene expression in the short-germ insect, *Tribolium castaneum*. *Dev Genes Evol* 219, 369-75.
- Brown, S. J., Parrish, J. K., Beeman, R. W. and Denell, R. E. (1997). Molecular characterization and embryonic expression of the even-skipped ortholog of *Tribolium castaneum*. *Mech Dev* 61, 165-73.
- Chipman, A. D. and Akam, M. (2008). The segmentation cascade in the centipede *Strigamia maritima*: involvement of the Notch pathway and pair-rule gene homologues. *Dev Biol* 319, 160-9.
- Chipman, A. D., Arthur, W. and Akam, M. (2004). A double segment periodicity underlies segment generation in centipede development. *Curr Biol* 14, 1250-5.
- Choe, C. P., Miller, S. C. and Brown, S. J. (2006). A pair-rule gene circuit defines segments sequentially in the short-germ insect *Tribolium castaneum*. 103, 6560-6564.
- Cooke, J. and Zeeman, E. C. (1976). A clock and wavefront model for control of the number of repeated structures during animal morphogenesis. *J Theor Biol* 58, 455-76.
- Copf, T., Schroder, R. and Averof, M. (2004). Ancestral role of caudal genes in axis elongation and segmentation. *Proc Natl Acad Sci U S A* 101, 17711-5.
- Davis, G. K. and Patel, N. H. (2002). Short, long, and beyond: molecular and embryological approaches to insect segmentation. *Annu Rev Entomol* 47, 669-99.
- Dequeant, M. L., Glynn, E., Gaudenz, K., Wahl, M., Chen, J., Mushegian, A. and Pourquie, O. (2006). A complex oscillating network of signaling genes underlies the mouse segmentation clock. *Science* 314, 1595-8.

- Diez del Corral, R., Olivera-Martinez, I., Goriely, A., Gale, E., Maden, M. and Storey, K. (2003). Opposing FGF and retinoid pathways control ventral neural pattern, neuronal differentiation, and segmentation during body axis extension. *Neuron* 40, 65-79.
- Dubrulle, J., McGrew, M. J. and Pourquie, O. (2001). FGF signaling controls somite boundary position and regulates segmentation clock control of spatiotemporal Hox gene activation. *Cell* 106, 219-32.
- Fu, J., Posnien, N., Bolognesi, R., Fischer, T. D., Rayl, P., Oberhofer, G., Kitzmann, P., Brown, S. J. and Bucher, G. (2012). Asymmetrically expressed axin required for anterior development in *Tribolium*. *Proc Natl Acad Sci U S A* 109, 7782-6.
- Giudicelli, F., Ozbudak, E. M., Wright, G. J. and Lewis, J. (2007). Setting the tempo in development: an investigation of the zebrafish somite clock mechanism. *PLoS Biol* 5, e150.
- Krol, A. J., Roellig, D., Dequeant, M. L., Tassy, O., Glynn, E., Hattem, G., Mushegian, A., Oates, A. C. and Pourquie, O. (2011). Evolutionary plasticity of segmentation clock networks. *Development* 138, 2783-92.
- Meijering, E., Dzyubachyk, O. and Smal, I. (2012). Methods for cell and particle tracking. *Methods Enzymol* 504, 183-200.
- Palmeirim, I., Henrique, D., Ish-Horowicz, D. and Pourquie, O. (1997). Avian hairy gene expression identifies a molecular clock linked to vertebrate segmentation and somitogenesis. *Cell* 91, 639-48.
- Park, T. and Marian Burton, F. (1948). The Fecundity and Development of the Flour Beetles, *Tribolium Confusum* and *Tribolium Castaneum*, at Three Constant Temperatures. *Ecology* 29, 368-374.
- Patel, N. H., Condrón, B. G. and Zinn, K. (1994). Pair-rule expression patterns of even-skipped are found in both short- and long-germ beetles. *Nature* 367, 429-434.
- Peel, A. D., Chipman, A. D. and Akam, M. (2005). Arthropod segmentation: beyond the *Drosophila* paradigm. *Nat Rev Genet* 6, 905-16.
- Pueyo, J. I., Lanfear, R. and Couso, J. P. (2008). Ancestral Notch-mediated segmentation revealed in the cockroach *Periplaneta americana*. *Proc Natl Acad Sci U S A* 105, 16614-9.
- Rivera-Pomar, R. and Jackle, H. (1996). From gradients to stripes in *Drosophila* embryogenesis: Filling in the gaps. *Trends in Genetics* 12, 478-483.

Sarrazin, A. F., Peel, A. D. and Averof, M. (2012). A segmentation clock with two-segment periodicity in insects. *Science* 336, 338-41.

Schulz, C., Schroder, R., Hausdorf, B., Wolff, C. and Tautz, D. (1998). A caudal homologue in the short germ band beetle *Tribolium* shows similarities to both, the *Drosophila* and the vertebrate caudal expression patterns. *Dev Genes Evol* 208, 283-9.

Stollewerk, A., Schoppmeier, M. and Damen, W. G. (2003). Involvement of Notch and Delta genes in spider segmentation. *Nature* 423, 863-5.

Chapter 3 - Caudal regulates the spatiotemporal dynamics of pair-rule waves in *Tribolium*

Ezzat El-Sherif¹, Xin Zhu², Jinping Fu², Susan J. Brown²

Summary

In the short-germ beetle *Tribolium castaneum*, waves of pair-rule gene expression propagate from the posterior end of the embryo towards the anterior and eventually freeze into stable stripes, partitioning the anterior-posterior axis into segments. These waves, like their counterparts in vertebrates, are assumed to arise due to the modulation of a molecular clock by a posterior-to-anterior frequency gradient. Here we provide evidence that the posterior gradient of *Tc-caudal* expression regulates the oscillation frequency of pair-rule gene expression in *Tribolium*. We show this by correlating the gradient of *Tc-caudal* expression to the spatiotemporal dynamics of *Tc-even-skipped* expression in wild type as well as in different RNAi knockdowns of *Tc-caudal* regulators. Our results highlight the role of a frequency gradient in pattern formation.

Introduction

The anterior-posterior (AP) axis of arthropods, annelids, and vertebrates is partitioned into segments. The French flag model, in which threshold concentrations of morphogen gradients are interpreted by downstream genes to partition a developing tissue (Rogers and Schier, 2011; Wolpert, 1969), has been the main theoretical framework to explain segmentation in *Drosophila*. Specifically, gradients of maternal factors span the AP axis of *Drosophila* providing positional information to downstream gap genes, which in turn diffuse in the syncytial blastoderm to form more localized morphogen gradients. Both maternal and gap gene gradients further provide positional information to the pair-rule genes whose striped expression is the first indication of segmentation in the embryo (Lawrence, 1992).

¹ Genetics Program, Kansas State University, Manhattan, KS 66506, USA.

² Division of Biology, Kansas State University, Manhattan, KS 66506, USA.

In *Drosophila*, all segments form more or less simultaneously in a syncytial blastoderm of fixed AP axis length. In contrast, vertebrate segmentation (somitogenesis) takes place sequentially in an elongating cellularized embryo. Therefore, a different model, the ‘clock and wavefront’, was adopted to explain segmentation in vertebrates (Cooke and Zeeman, 1976; Oates et al., 2012). Multiple genes (*hairy/enhancer-of-split* and genes of Notch, Wnt and FGF signaling pathways) exhibit oscillatory expression in the presomitic mesoderm (PSM) of the vertebrate embryo and are thought to be constituents of a molecular clock (Dequeant et al., 2006; Palmeirim et al., 1997). In cells located anterior to a wavefront oscillations are arrested into stable stripes. The wavefront is defined by a threshold within the overlapping domains of posterior Wnt and fibroblast growth factor (FGF) gradients (Aulehla et al., 2003; Dubrulle et al., 2001) and an opposing retinoic acid gradient (Diez del Corral et al., 2003). Oscillations seem to be arrested gradually (i.e. are modulated by a frequency gradient) as evidenced by kinematic waves that sweep the PSM from posterior to anterior (Palmeirim et al., 1997).

In most short-germ arthropods, anterior segments form in a blastoderm, as in *Drosophila*, while posterior segments form subsequently during the germband stage out of a population of cells at the posterior end of the embryo (termed the ‘growth zone’) (Davis and Patel, 2002), reminiscent of somitogenesis in vertebrates. Although it is conceivable that short-germ arthropods utilize a ‘French flag’-based segmentation mechanism in the blastoderm and a ‘clock and wavefront’ mechanism in the germband, it has recently been shown that a segmentation clock operates in both the germ-band (Sarrazin et al., 2012) and blastoderm (El-Sherif et al., 2012) of the short-germ insect *Tribolium castaneum*. Waves of gene expression of the pair-rule gene, *Tc-even-skipped* (*Tc-eve*), were found to propagate from posterior to anterior in both blastoderm and germband (El-Sherif et al., 2012); such dynamics are a hallmark of clock-based segmentation.

The identification of factors providing positional information for segmentation in the blastoderm of short-germ arthropods has been controversial (Brown et al., 2001; Kotkamp et al., 2010; Lynch et al., 2006; Peel et al., 2005; Schroder, 2003). Demonstration of the clock-based nature of short-germ segmentation fuels this debate as attention now turns to the search for factors functioning as a wavefront. It has been speculated that the homeodomain transcription factor Caudal (Cad) plays a prominent role in AP patterning in arthropods since its expression overlaps with the newly forming stripes in most arthropods (Chipman, 2008). Cad is required for

segmentation in the *Drosophila* abdomen (Macdonald and Struhl, 1986), and for posterior patterning in other species (Edgar et al., 2001; Epstein et al., 1997). It was found to play an even more prominent role in the segmentation of non-dipteran insects. It is required for trunk segmentation in *Nasonia vitripennis* (Olesnický et al., 2006) and both trunk and gnathal segmentation in *Tribolium* (Copf et al., 2004) and *Gryllus bimaculatus* (Shinmyo et al., 2005). However, the exact role of Cad in segmentation is still not known. Here we test the idea that the posterior gradient of *Tribolium cad* (*Tc-cad*) expression regulates the oscillation frequency of pair-rule gene expression, resulting in expression waves in the *Tribolium* blastoderm. The expression of *Tc-eve* was abolished in strong *Tc-cad* RNAi knock-down embryos, but in weak *Tc-cad* knock-down embryos, the expression domain of *Tc-eve* was posteriorly shifted and its oscillation frequency reduced. Perturbing the *Tc-cad* gradient in different ways by knocking-down several of its regulators further showed that the extension, intensity, and slope of *Tc-cad* gradient correlated with the extension, frequency, and width of *Tc-eve* waves, respectively. Computer modeling suggested that these observations are consistent with the hypothesis that *Tc-cad* functions as a frequency gradient that regulates the spatiotemporal dynamics of pair-rule gene oscillation in *Tribolium*. These observations, combined with the continued expression of *Tc-cad* in a posterior gradient suggest that *Tc-cad* also acts as a wavefront in the elongating germband. Our study highlights the concept of a frequency gradient as a pattern formation mechanism. Using computer modeling we show that a graded frequency profile might even be essential within the clock-and-wavefront model as a buffer against noise.

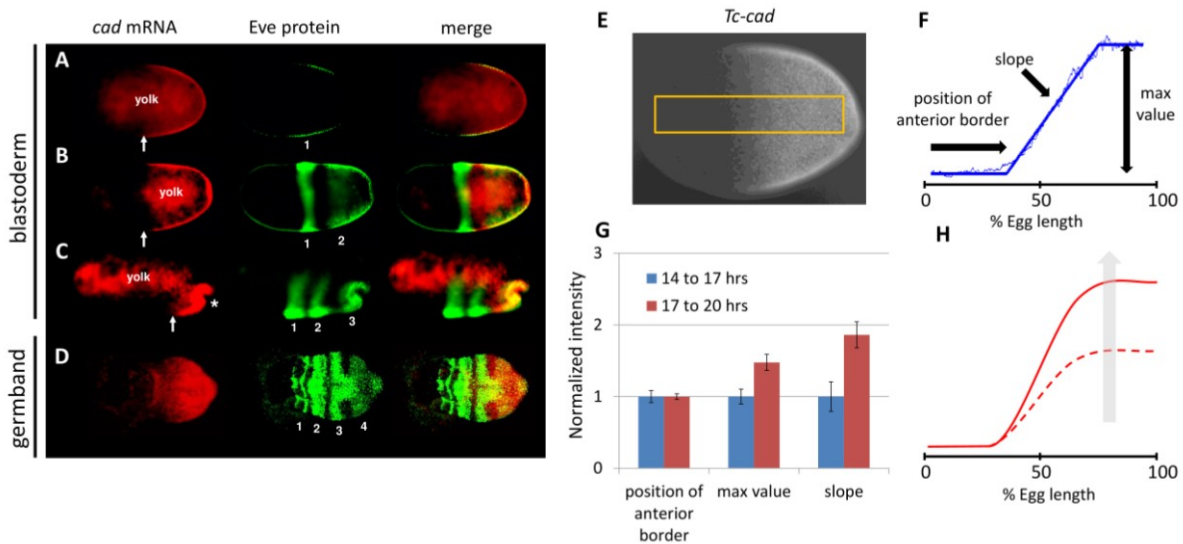
Results

Characterizing Tc-cad expression in Tribolium

The wave dynamics of *Tc-eve* in *Tribolium* can be explained by assuming a posterior-to-anterior gradient that positively regulates the frequency of *Tc-eve* oscillations (El-Sherif et al., 2012). *Tc-cad* is an obvious candidate to encode such a frequency gradient because its mRNA expression forms a posterior-to-anterior gradient that overlaps the arising *Tc-eve* expression waves at the posterior throughout *Tribolium* segmentation (Figure 3.1 A-D).

Figure 3.1 *Tc-cad* expression in *Tribolium*.

(A-D) Concurrent *Tc-cad* *in situ* hybridization (red; first column) and Tc-EVE antibody staining (green; second column) were merged (third column) to show that *Tc-cad* expression overlaps with the emerging first two stripes of Tc-Eve in the blastoderm (A, B), and retreats to the posterior while the third stripe emerges (C). *Tc-cad* expression is confined in the growth zone during the germband stage to overlap with emerging stripes (fourth stripe in D). (E, F) Measuring *Tc-cad* expression across AP axis of the blastoderm (E, Methods) and fitting raw measurements (thin blue line in F) to a linear-with-plateau curve (thick blue line in F) and calculating its three descriptors (F, Methods). (G, H) As revealed by the change in the three descriptors of *Tc-cad* gradient over time (G), *Tc-cad* expression gradient builds up during 14-17 hours AEL but does not shift. *Tc-cad* dynamics are summarized in H; dashed curve: early, solid curve: late expression. Anterior to left. Error bars represent 95% confidence intervals.



Since studying segmentation in the germband phase of *Tribolium* is hindered by the truncation phenotype found in most segmentation gene knock-downs, we largely restricted our analysis to the blastoderm stage. The expression of *Tc-cad* in the blastoderm (Figure 3.1 E) can be approximated with reasonable accuracy, by a posterior-to-anterior linear gradient that plateaus at the posterior end (Figure 3.1 F). This curve can be characterized by three descriptors: maximum posterior (plateau) value, position of anterior border, and slope (Figure 3.1 F). To study the temporal dynamics of *Tc-cad* gradient during the blastoderm stage, we simultaneously fixed and stained two 3-hour egg collections: 14 to 17 and 17 to 20 hours after egg lay (AEL) (see

Methods), spanning the time periods when the first and second stripes of *Tc-eve* were forming in wild type (WT), respectively (analysis of later times is precluded by primitive pit formation, star in Figure 3.1 C). For each embryo in these egg collections, *Tc-cad* gradient was measured and then fitted to a linear-with-plateau curve (Methods and Figure 3.1 E, F). The three descriptors of the curve were calculated for each embryo, and averaged for each egg collection (Figure 3.1 G). From Figure 3.1 G, we noticed that during the formation of the first and second *Tc-eve* stripes, the anterior border of *Tc-cad* expression gradient did not experience a significant shift (which is also evident in Figure 3.1 A, D). However, both the maximum posterior value and the slope of the *Tc-cad* gradient increased over time. This means that *Tc-cad* gradient built up during the formation of the first and second *Tc-eve* stripes, but did not undergo a substantial shift along the AP axis (Figure 3.1 H). The buildup phase of *Tc-cad* was restricted to the time period from 14 to 16, after which the *Tc-cad* gradient was more or less static (Supp. Figure 3.1). This argues against a substantial role of *Tc-cad* temporal dynamics in the wave expression of *Tc-eve*. By the time the third stripe formed, *Tc-cad* gradient retreated toward posterior (**Figure 3.1 C**).

The spatial distribution of *Tc-cad* renders it a probable candidate for a wavefront in a clock-and-wavefront model. Although in the traditional model a wavefront should be posteriorly retracting (like *Tc-cad* expression during the germband stage), a *static* but *smooth* gradient (like *Tc-cad* expression during the formation of the first two stripes of *Tc-eve* in the blastoderm stage) that modulates the frequency of *T-eve* oscillations is capable in principle of forming a striped expression pattern (Movies 3.1 A, upper panel, and (El-Sherif et al., 2012)).

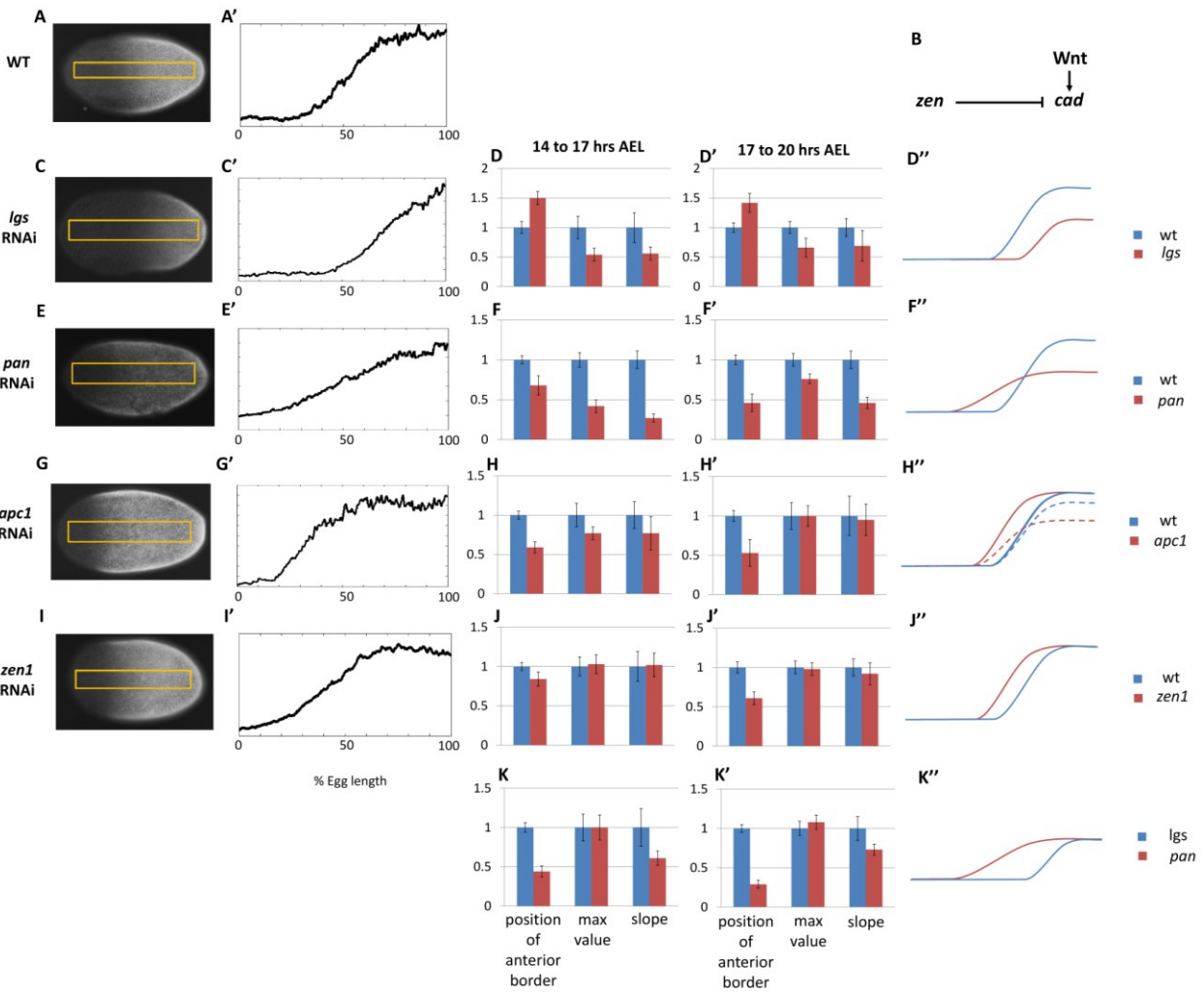
Regulation of the Tc-cad gradient

In both vertebrates and arthropods, canonical Wnt is a positive regulator of *cdx/cad* (Fu et al., 2012; McGregor et al., 2008; Pilon et al., 2007). Once bound by Wnt ligand, the receptor Frizzled recruits the β -catenin destruction complex (comprising Axin, APC, and other factors), rendering β -catenin free to enter the nucleus and bind Pangolin (TCF) with the help of Legless (Lgs), Pygopus (Pygo) and other coactivators (Logan and Nusse, 2004) to activate Wnt targets. In *Tribolium*, *wnt1* and *wnt8* are expressed at the posterior pole of the blastoderm, and at the posterior end of the growth-zone in the germband stage (Bolognesi et al., 2008), which is expected to produce posterior gradient of Wnt activity, the formation of which might be assisted

by the anterior localization of Wnt repressors in the blastoderm stage (Bucher et al., 2005; Fu et al., 2012).

Figure 3.2 Characterization of *Tc-cad* gradient in WT and RNAi knockdowns of *Tc-cad* regulators.

(A, A') *cad* gradient in WT. (B) A model for *cad* regulation in the *Tribolium* blastoderm. (C-D'') *cad* gradient expression in a *lgs* RNAi embryo (C, C'), and the average of its three descriptors normalized to WT values (Methods) in 14-17 AEL (D) and 17-20 AEL (D'). As inferred from (D, D'), the *cad* gradient in a *lgs* RNAi embryo compared to that in WT is summarized in (D''); not to scale). The same was performed for *pan* (E-F''), *apc1* (G-H''), dashed curve for 14-17 AEL and solid curve for 17-20 AEL), and *zen1* (I-J'') RNAi embryos. (K-K'') the average of the three descriptors of the *cad* expression gradient in *pan* RNAi normalized to *lgs* RNAi values (Methods). Anterior to the left. Error bars represent 95% confidence intervals.



We characterized the effect of manipulating Wnt activity on *Tc-cad* expression in the *Tribolium* blastoderm. Knocking down *Tc-lgs*, (a positive Wnt regulator) shifted the *Tc-cad* expression gradient posteriorly. In addition to repositioning the anterior border of the *Tc-cad* gradient, the posterior maximum value and gradient slope were reduced in *Tc-lgs* RNAi embryos compared to WT (see Figure 3.2 C-D'').

Knocking down *Tc-apc1*, (a negative Wnt regulator) repositioned the *Tc-cad* gradient anteriorly (Figure 3.2 G-H''). Interestingly, the maximum posterior value of the *Tc-cad* expression gradient at 14-17 hours AEL was lower in *Tc-apc1* RNAi embryos than in WT embryos (Figure 3.2 H), but eventually reached WT levels by 17-20 hours AEL (Figure 3.2 H').

Thus, it appears that the *Tc-cad* expression gradient takes longer to mature in *Tc-apc1* RNAi than in WT embryos, which might be indicative of early negative Wnt regulation of *Tc-cad*.

Knocking down another Wnt regulator, *Tc-pan*, also perturbed the *Tc-cad* expression gradient. Pan, a component of the activator complex, also acts as a repressor in the absence of nuclear β -catenin (Cavallo et al., 1998). Hence, we expected Wnt activity to be reduced posteriorly but increased anteriorly in *Tc-pan* RNAi embryos compared to WT, resulting in a shallower Wnt gradient across the blastoderm, and consequently a shallower *Tc-cad* gradient. As expected, the border of the *Tc-cad* gradient in *Tc-pan* RNAi embryos shifted anteriorly, the gradient reached a lower maximum posterior value, and the slope was lower compared to WT (Figure 3.2 E-F’’).

In *Drosophila*, two Hox3 type genes are involved in early patterning: *bicoid* (*bcd*), which is expressed anteriorly and plays a major role in AP patterning, and *zerknüllt* (*zen*), which is expressed dorsally and specifies the amnioserosa (Stauber et al., 1999). *Tribolium* lacks *bcd* (Brown et al., 2001) but one of its *zen* homolog, *Tc-zen1*, is expressed both anteriorly and dorsally (Falciani et al., 1996). Anterior expression precedes dorsal expression and is suspected to play a role in AP patterning (van der Zee et al., 2005). As shown in Figure 3.2 I-J’’, the *Tc-cad* gradient in *Tc-zen1* RNAi embryos shifts anteriorly, but has the same slope and maximum posterior expression level as WT, indicating that *Tc-zen1* represses *Tc-cad* anteriorly (see Figure 3.2 B for a summary of *Tc-cad* regulation).

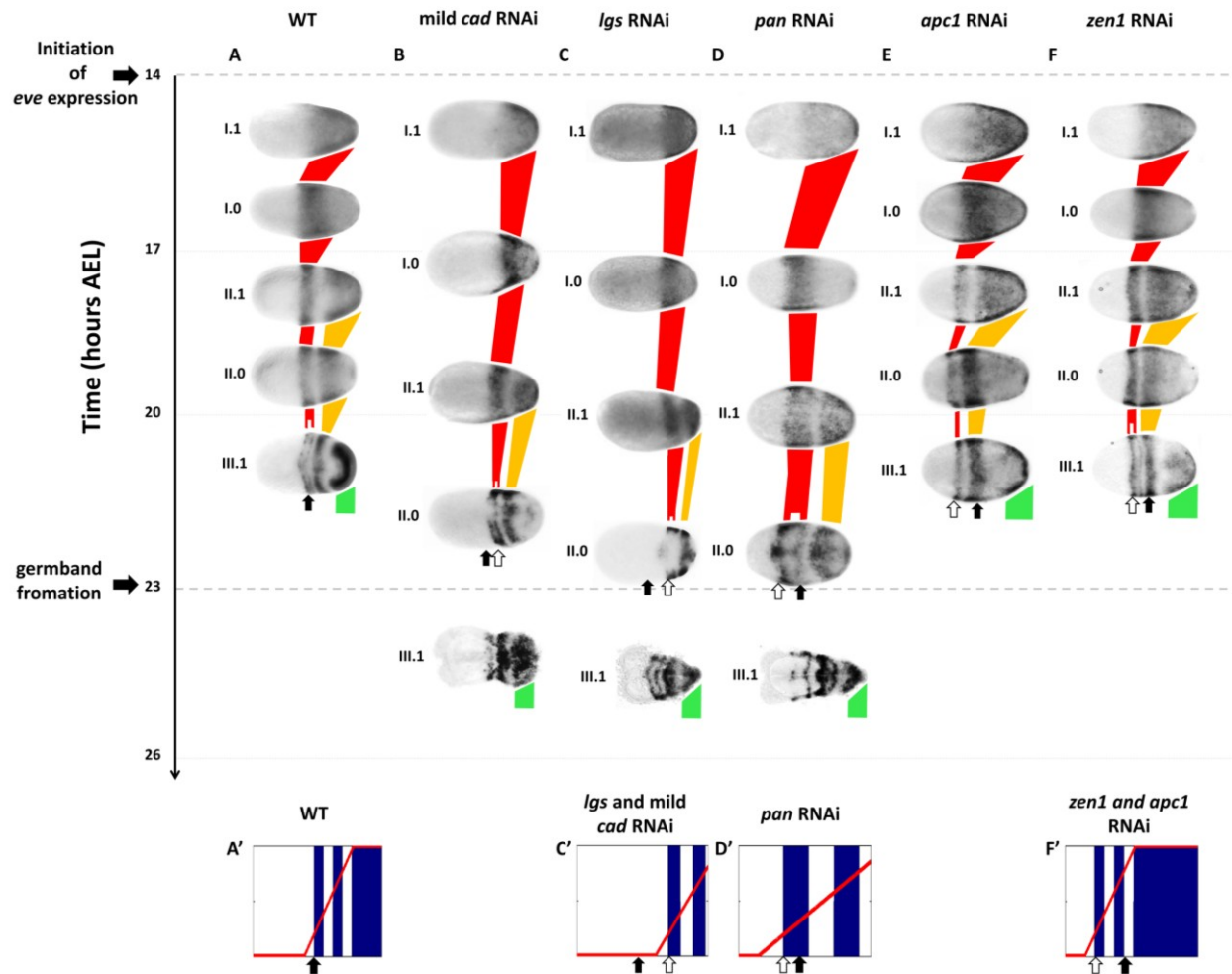
Tc-cad* gradient regulates *Tc-eve* waves in *Tribolium

In *Tribolium*, *Tc-eve* is expressed in waves that shrink while propagating from posterior to anterior (Figure 3.3 A) (El-Sherif et al., 2012). Previous studies implicate *cad* in the regulation of *eve* in arthropods (Copf et al., 2004; Shinmyo et al., 2005). To examine a possible role of *Tc-cad* in regulating *Tc-eve*, we characterized the dynamics of *Tc-eve* expression in WT and embryos depleted of *Tc-cad*. Strong knockdown of *Tc-cad* completely abolished *Tc-eve* expression (Supp. Figure 3.2). We produced milder effects by injecting lower concentrations of *Tc-cad* dsRNA. In these embryos waves of *Tc-eve* expression propagated from posterior to anterior (Figure 3.3 B); however, their final positions in the blastoderm were shifted posteriorly compared to WT (compare Figure 3.3 B with Figure 3.3 A).

The maximum frequency of *Tc-eve* oscillations in a *Tribolium* embryo can be measured by tracing *Tc-eve* expression over time at the posterior end. In each of a number of successive 3-hour egg collections covering the formation of anterior *Tc-eve* stripes (14-17, 17-20, 20-23, and 23-26 hours AEL; for *Tc-apc1* and *Tc-zen1* RNAi, 23-26 hours AEL egg collections could not be used since aberrant germband formation hindered the examination of *Tc-eve* expression in these RNAi knockdown embryos), the number of embryos belonging to each cycle was counted. Cycle I embryos were those going from high to low *Tc-eve* expression level at the posterior end in order to from the first *Tc-eve* stripe, while cycle II embryos were those going from high to low *Tc-eve* expression level at the posterior end in order to from the second *Tc-eve* stripe, and so on. For the WT control, a new *Tc-eve* cycle peaked every 3-hour egg collection (Figure 3.4 A, blue bars), consistent with the ~3 hours periodicity we previously reported for *Tc-eve* oscillations at 23-24°C (El-Sherif et al., 2012). For mild *Tc-cad* RNAi, while cycle I was initiated at 14 to 17 hrs AEL similar to WT, cycle I persisted through 17 to 20 hrs AEL (Figure 3.4 A, red bar). Figure 3.4 A can be used to estimate the duration of *Tc-eve* cycles I and II (Figure 3.4 A', Methods). As shown in Figure 3.4 A', both cycles I and II in mild *Tc-cad* RNAi lasted longer than their WT counterparts.

Figure 3.3 *Tc-eve* expression in WT, mild *Tc-cad* RNAi, and *Tc-cad* regulators RNAi.

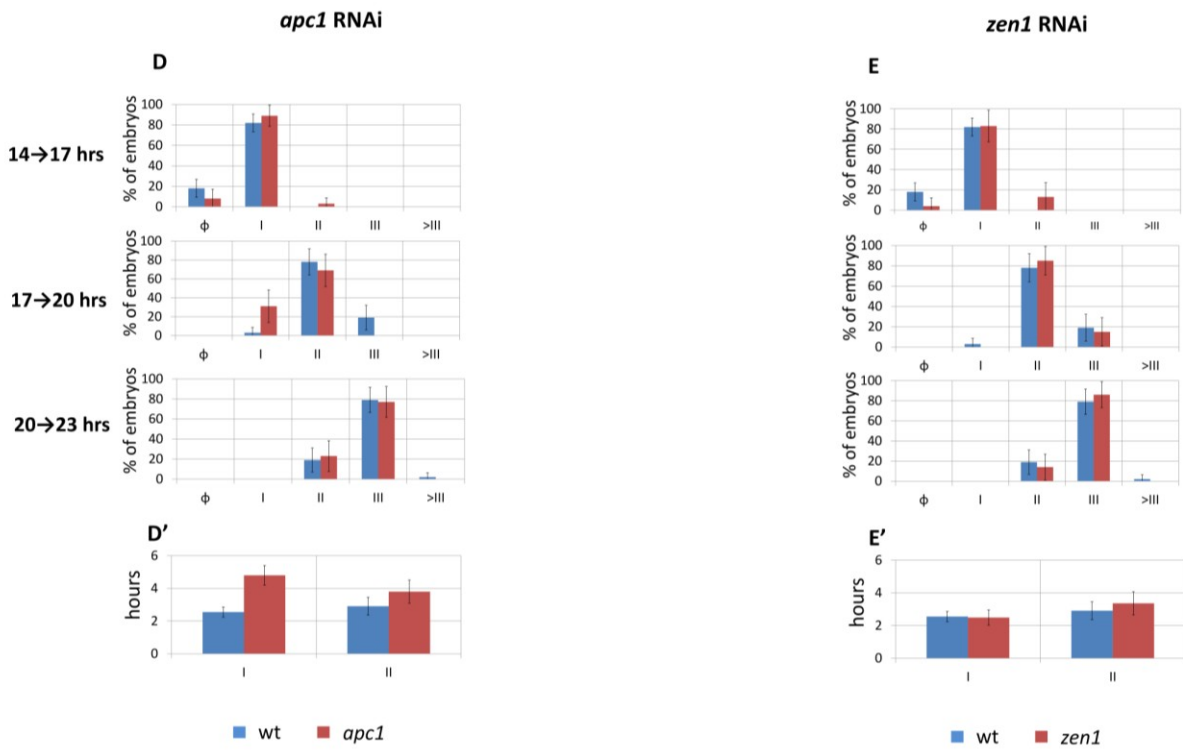
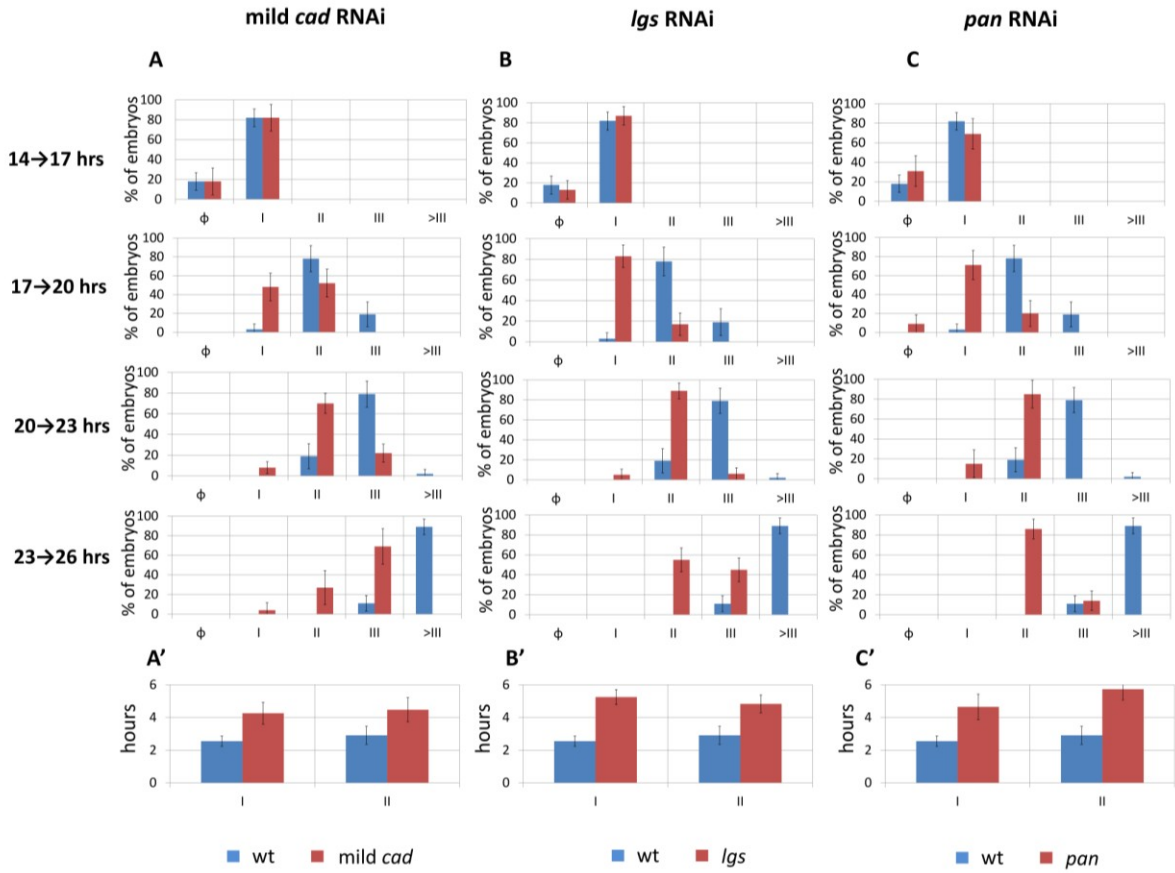
Tc-eve expression waves in WT (A), mild *Tc-cad* RNAi (B), *Tc-lgs* RNAi (C), *Tc-pan* RNAi (D), *Tc-apc1* RNAi (E), and *Tc-zen1* RNAi (F) embryos (First cycle/wave/stripe in red, second in yellow, and third in green). *Tc-eve* expression patterns were classified according to the cycle of *eve* oscillation in the posterior end of the embryo (roman numerals) and the phase of the cycle (1 for high phase, and 0 for low; e.g. I.1: high phase of the first cycle). Embryos were mapped on the time axis according to data from Figure 3.4. Arrows indicate the position of the anterior border of *Tc-eve* expression at 20-23 hours AEL in WT (black arrow) and in different knockdowns (white arrows). Shown also are snapshots of computer simulations (see Movies 3.1) of a *Tc-eve* oscillator the frequency of which is modulated by the *Tc-cad* gradient in WT (A'), mild *Tc-cad* and *Tc-lgs* RNAi (C'), *Tc-pan* RNAi (D'), *Tc-apc1* and *Tc-zen* RNAi (F') embryos; blue: *Tc-eve* expression, red curve: *cad* expression gradient. Anterior to the left.



In *Tc-lgs* RNAi, the anterior border of *Tc-cad* is shifted posteriorly and the transcription level at the posterior end of the blastoderm is reduced (Figure 3.2 C-D’). In accordance with the posterior shift of *Tc-cad* gradient, a posterior shift of *Tc-eve* waves were observed in *Tc-lgs* RNAi embryos (compare Figure 3.3 C with Figure 3.3 A). Corresponding with the reduction in posterior *Tc-cad* level, the frequency of *Tc-eve* oscillations is reduced (Figure 3.4 B, B’). Both the posterior shift and the reduced frequency of *Tc-eve* oscillations at the posterior end of the blastoderm upon the reduction of *Tc-cad* gradient (either in mild *Tc-cad* RNAi or *Tc-lgs* RNAi) can be predicted by a model in which *Tc-cad* gradient modulates the frequency of *Tc-eve* oscillations (Movies 3.1 A, compare Figure 3.3 C’ to Figure 3.3 A’).

Figure 3.4 Temporal dynamics of *Tc-eve* expression at the posterior end of the embryo in knockdown of *Tc-cad* and its regulators in comparison with that of WT.

(A, B, C, D, E) percentage distributions of *Tc-eve* expression classes (classification was based on *Tc-eve* oscillation cycle in the posterior, see Figure 3.3) in different timed egg collections in multiple RNAi knockdowns (red bars) in comparison with WT (blue bars): (A) mild *Tc-cad* (B) *Tc-lgs* (C) *Tc-pan* (D) *Tc-apc1*, and (E) *Tc-zen1* RNAi embryos. Class distributions were used to estimate the duration of different *Tc-eve* oscillation cycles (A', B', C', D', and E'; see Methods). Error bars represent 95% confidence intervals.



In contrast to the posterior shift in *Tc-lgs* RNAi embryos, *Tc-cad* gradient shifted anteriorly in *Tc-pan* RNAi embryos (Figure 3.2 E-F''). Correspondingly, *Tc-eve* waves experienced a similar shift towards anterior in *Tc-pan* RNAi compared to WT (compare Figure 3.3 D to Figure 3.3 A). However, similar to *Tc-lgs* RNAi, *Tc-cad* experienced a reduction at the posterior end in *Tc-pan* RNAi embryos (Figure 3.2 E-F''). Correspondingly, the frequency of *Tc-eve* oscillations was also reduced there (Figure 3.4 C, C'). In addition to the anterior shift and the frequency reduction of *Tc-eve* waves, the widths of *Tc-eve* stripes in *Tc-pan* RNAi embryos were strikingly wider than those of WT (compare Figure 3.3 D to Figure 3.3 A). This can be explained by the stretching effect of *Tc-pan* knock-down on the *Tc-cad* gradient, as evident from the lower slope of *Tc-cad* gradient in *Tc-pan* RNAi embryos compared to WT (Figure 3.2 F-F''). However, although the slope of *Tc-cad* gradient was reduced in both *Tc-lgs* and *Tc-pan* RNAi embryos, it resulted in a detectable change in stripe widths only in *Tc-pan*, perhaps because the slope reduction in *Tc-pan* was severer. To directly confirm this, we simultaneously fixed and stained *Tc-lgs* and *Tc-pan* RNAi embryos and compared the *Tc-cad* gradient in these two cases (Figure 3.2 K-K''). While the level of *Tc-cad* expression at the posterior end in both *Tc-lgs* and *Tc-pan* was similar, the slope in case of *Tc-pan* RNAi is lower. The anterior shift, reduced frequency of *Tc-eve* oscillations at the posterior end of the blastoderm, and the wider *Tc-eve* stripe widths upon reducing and stretching the *Tc-cad* gradient in *Tc-pan* RNAi can be predicted by a model in which *Tc-cad* gradient modulates the frequency of *Tc-eve* oscillations (Movies 3.1 B, Figure 3.3 D').

In *Tc-apc1* RNAi embryos, *Tc-eve* waves shifted towards anterior (compare Figure 3.3 E to Figure 3.3 A) in accordance with the anterior shift in *Tc-cad* gradient (Figure 3.2 G-H''). We detected an increase in the period of cycle I in *Tc-apc1* RNAi embryos compared to WT (Figure 3.4 D'), in accordance with the lower maximum posterior value of *Tc-cad* in *T-apc1* RNAi during 14-17 AEL (Figure 3.2 H). However, the period of cycle II in *Tc-apc1* RNAi was close to its value in WT, in accordance with eventual increase of the maximum posterior value of *Tc-cad* in *T-apc1* RNAi during 17-20 AEL (Figure 3.2 H').

In *Tc-zen1* RNAi, *Tc-eve* waves shifted towards anterior (compare Figure 3.3 F to Figure 3.3 A) in accordance with the anterior shift of *Tc-cad* (Figure 3.2 I-J''). The temporal dynamics of *Tc-cad* posterior level in *Tc-zen1* RNAi was similar to that of WT (Figure 3.2 J-J'');

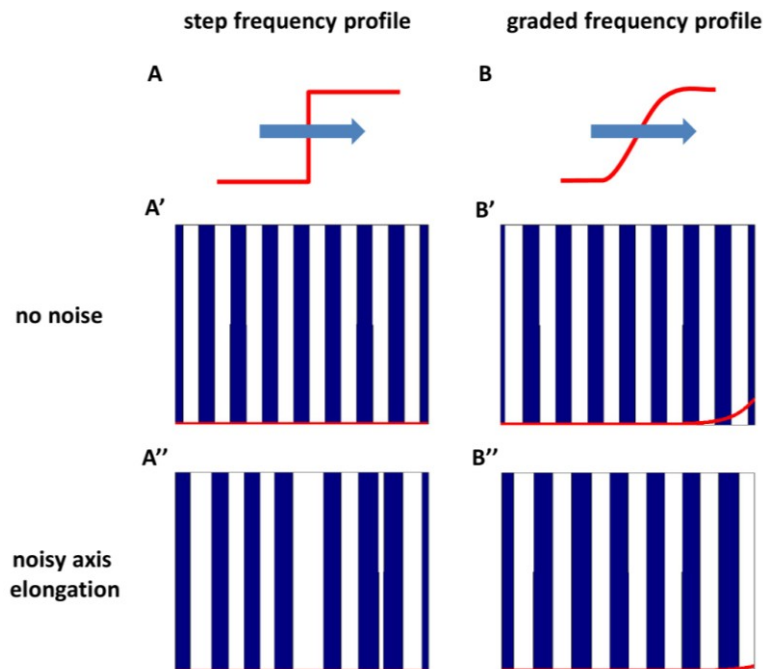
correspondingly, the timing of *Tc-eve* waves in *Tc-zen1* RNAi and WT are very similar (Figure 3.4 E, E'). The anterior shift of *Tc-eve* waves upon anterior extension of *Tc-cad* gradient (in *Tc-zen1* and *Tc-apc1* RNAi) can be predicted by a model in which *Tc-cad* gradient modulates the frequency of *Tc-eve* oscillations (Movies 3.1 C, Figure 3.3 F').

Graded frequency profile as a buffer against noise

Axis elongation is an essential component of the clock-and-wavefront model. We have previously shown that segmentation in the blastoderm of *Tribolium* seems to be clock-based. Despite the lack of axis elongation at the blastoderm stage, we did not exclude the possibility of the existence of a retreating frequency gradient (wavefront). In the current study, we have given evidence that *Tc-cad* acts as a frequency gradient that modulates pair-rule oscillations in the blastoderm. Although a static step frequency gradient (i.e. suddenly dropping from non-zero to zero frequency) does not possess patterning capacity, a static but gradually decreasing frequency gradient is capable of generating a striped pattern. Indeed, the first two stripes of *Tc-eve* form during a time period when the *Tc-cad* gradient is largely static. After the formation of the first two stripes, *Tc-cad* then abruptly retreats to the very posterior end of the embryo in the prospective growth zone. Later during axis elongation in the germband stage, *Tc-cad* expression retreats posteriorly with every newly forming *Tc-eve* stripe (Figure 3.1 D). Here the patterning capacity of the gradually decreasing frequency gradient tolerated a pause then a sudden jump in axis elongation. This indicates that a gradually decreasing frequency gradient might act as a buffer against erratic axis elongation. To investigate this possibility, we created a two computer models for the clock-and-wavefront mechanism: one with a step frequency profile (Figure 3.5 A) and the other with a gradually decreasing frequency gradient (Figure 3.5 B). Both generated almost identical striped pattern in the absence of noise (Figure 3.5 A', B'). However, after adding noise to axis elongation, the clock-and-wavefront with step frequency gradient generated irregularly sized stripes (Figure 3.5 A''), while with gradually decreasing frequency gradient, regular stripes were generated (Figure 3.5 B''). Note that an erratically moving wavefront could result from either jumpy axis elongation or due to noise in the gene expression of the wavefront (*Tc-cad* in case of *Tribolium*, and *wnt* and *fgf* in case of vertebrates). This means that the patterning capacity of a gradually decreasing frequency gradient could act as a buffer against noise in axis elongation or wavefront gene expression.

Figure 3.5 Frequency profile and robustness of the clock-and-wavefront model.

A computer simulation of the clock-and-wavefront model with a step frequency profile (A, red curve; arrow indicates the direction of frequency profile movement) generated uniformly sized stripes if no noise was added (A') while it generated irregularly sized stripes in case of noisy frequency profile movement (A''). Utilizing a graded frequency profile (B) results in uniformly sized stripes if no noise was added (B') or (to a large degree) in the case of noisy frequency profile movement (B''). See Movies 3.2.



Conclusion

In this work we showed that an anterior-to-posterior gradient of *Tc-cad* expression in *Tribolium* regulates the wave expression of the pair-rule gene *Tc-eve*. By examining the spatiotemporal dynamics of *Tc-eve* expression in WT and different knockdowns of *Tc-cad* regulators, three correlations were evident: (1) the spatial extent of *Tc-cad* correlates with that of *Tc-eve* waves, (2) the level of *Tc-cad* expression at the posterior end of the blastoderm correlates with the frequency of *Tc-eve* oscillations, and (3) the slope of *Tc-cad* gradient correlates with the width of *Tc-eve* stripes. These three correlations are consistent with the hypothesis that the *Tc-cad* gradient modulates the speed of pair-rule clock resulting in waves of gene expression, which

can simulated by computer modeling. A clock regulated by a frequency gradient is one way of transforming a temporal process into a spatial one; another would be the clock-and-wavefront model. One advantage of patterning with a frequency gradient is that axis elongation is not necessary, which might explain how the *Tribolium* blastoderm is segmented. Another advantage, as we showed using computer modeling, is that even within the framework of the clock-and-wavefront, utilizing a graded frequency profile renders the segmentation process more robust against noise in axis elongation and wavefront gene expression.

Materials and Methods

In situ hybridization, immunocytochemistry, and RNAi

In situ hybridization was performed using DIG-labeled RNA probes and anti-DIG::AP antibody (Roche). Signal was developed using NBT/BCIP (BM Purple, Roche), or Fast Red/HNPP (Roche). Immunocytochemistry was performed using anti-EVE (mouse monoclonal antibody 2B8, hybridoma bank, University of Iowa) as primary, and anti-mouse::POD as secondary antibody (ABC kit, Vector). AlexaFluor 488 tyramide (Invitrogen) was used to give green fluorescent signal. All expression analyses were performed using embryos from uninjected GA-1 strain (WT) or adult GA-1 females injected with double-stranded RNA (ds RNA) of the gene of interest. dsRNA was synthesized using the T7 megascript kit (Ambion) and mixed with injection buffer (5 mM KCl, 0.1 mM KPO₄, pH 6.8) before injection.

Egg collections for developmental time windows

One hour developmental windows were generated by incubating one hour egg collections at 23-24°C for the desired length of time. For 3-hour developmental windows, eggs were collected after three hours instead of one hour. The beetles were reared in whole-wheat flour supplemented with 5% dried yeast.

Comparing Tc-cad gradients in two egg collections

To compare the *Tc-cad* gradient in two different egg collections (either from two different time windows, from WT versus knockdown, or from two different knockdowns) we simultaneously fixed and performed chromogenic *in situ* staining for the two egg collections to

show *Tc-cad* expression. We specified a box (yellow in Figure 3.1 E and Figure 3.2 A, C, E, G, I) of enough width to span most of the AP axis (away from out of focus edges) and of enough height for the box to be confined within the embryo across the whole AP axis. We then calculated the average intensity of each one-pixel-width column of the box, to get a one dimensional array holding *Tc-cad* intensity values across the AP axis (using ImageJ). We then fitted (least squares, using Matlab) *Tc-cad* intensity values to linear-with-plateau curves (defined by the three curve descriptors in Figure 3.1 F), and calculated the average values of the 3 curve descriptors for each egg collection. We finally normalized the average value of one egg collection to the other.

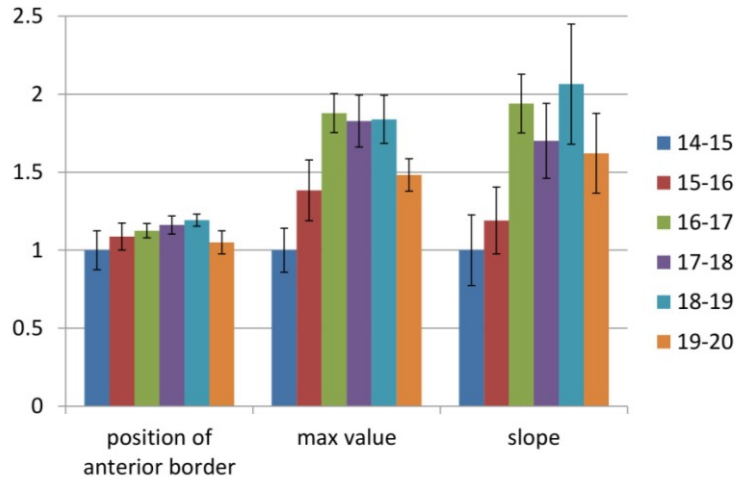
Calculating class durations from class distribution graphs

Class durations (Figure 3.4 A', B', C', D', E') were calculated from the corresponding class distribution graphs (Figure 3.4 A, B, C, D, E) by averaging the percentage of the occurrence of each class across all examined timed egg collections. This is equivalent to combining all egg collections into one large collection, spanning 14-26 hours AEL (in Figure 3.4 A, B, C) or 14-23 hours AEL (in Figure 3.4 D, E), then using the overall percentage of embryos in each class as an estimate of its duration. Percentages rather than absolute numbers are used in calculations to correct for differences in the number of eggs in each collection.

Supplementary materials

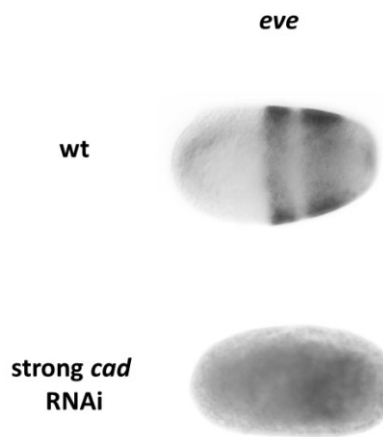
Supp. Figure 3.1 Detailed temporal dynamics of *T-cad* expression gradient in the blastoderm.

Shown is the change in the three descriptors of *Tc-cad* expression gradient with time during 14-20 AEL. *Tc-cad* expression gradient builds up during 14-16 hours AEL (but without appreciable AP shift). During 16-19 hours AEL, the gradient is more or less static, but starts to drop after 19 hours AEL. Error bars represent 95% confidence intervals.



Supp. Figure 3.2 *Tc-eve* is abolished in severe *Tc-cad* knockdown.

Shown are two embryos with comparable stage (flat posterior stage). *Tc-eve* is expressed in two stripes in WT while its expression is abolished in strong *Tc-cad* RNAi. Anterior to left.



Movies 3.1 Modeling *Tc-eve* waves in WT and knockdowns.

Tc-eve expression (blue) in the blastoderm was modeled by an array of oscillators along the horizontal axis (representing the AP axis; posterior to the right). Each oscillator runs independently with a frequency determined by a spatial gradient (red). Simulations were run using a frequency gradient (red) corresponding to *Tc-cad* in WT and contrasted to simulations run using a frequency gradient corresponding to *Tc-cad* in *Tc-lgs* RNAi (A; posteriorly shifted

with reduced posterior value and small decrease in slope, as compared to WT), in *Tc-pan* RNAi (B; anteriorly shifted with reduced posterior value and large decrease in slope, as compared to WT), and in *Tc-apc1* or *Tc-zen1* RNAi (C; anteriorly shifted with the same posterior value and slope as WT). The buildup dynamics of *Tc-cad* expression gradient were ignored for simplicity. Spatial resolution used in this simulation (2000 points along AP axis) gives similar qualitative results as actual resolution (around 70 nuclei along AP axis) but better visualization. Simulations were performed using Matlab.

Movies 3.2 Utilizing a graded frequency profile renders the clock-and-wavefront more robust to noise in axis elongation.

Shown are computer simulations of an array of oscillators along the horizontal axis (representing the AP axis; posterior to the right). Each oscillator (which output is shown in blue) runs independently with a frequency determined by a spatial gradient (frequency profile; shown in red) that moves from anterior to posterior (representing axis elongation). The frequency profile is either step or graded and its velocity is either uniform or noisy (a baseline velocity plus white noise). Simulations done with step frequency profile resulted in uniformly sized stripes in case of uniform axis elongation (A) while resulted in irregularly sized in case of noisy axis elongation (B). Simulations done with graded frequency profile resulted in uniformly sized stripes in case of both uniform axis elongation (C) and (to a large degree) noisy axis elongation (D). Simulations were performed using Matlab.

References

- Aulehla, A., Wehrle, C., Brand-Saberi, B., Kemler, R., Gossler, A., Kanzler, B., and Herrmann, B.G. (2003). Wnt3a plays a major role in the segmentation clock controlling somitogenesis. *Dev. Cell.* 4, 395-406.
- Bolognesi, R., Beermann, A., Farzana, L., Wittkopp, N., Lutz, R., Balavoine, G., Brown, S.J., and Schroder, R. (2008). Tribolium Wnts: evidence for a larger repertoire in insects with overlapping expression patterns that suggest multiple redundant functions in embryogenesis. *Dev. Genes Evol.* 218, 193-202.
- Brown, S., Fellers, J., Shippy, T., Denell, R., Stauber, M., and Schmidt-Ott, U. (2001). A strategy for mapping bicoid on the phylogenetic tree. *Curr. Biol.* 11, R43-4.

- Bucher, G., Farzana, L., Brown, S.J., and Klingler, M. (2005). Anterior localization of maternal mRNAs in a short germ insect lacking bicoid. *Evol. Dev.* 7, 142-149.
- Cavallo, R.A., Cox, R.T., Moline, M.M., Roose, J., Polevoy, G.A., Clevers, H., Peifer, M., and Bejsovec, A. (1998). *Drosophila* Tcf and Groucho interact to repress Wingless signalling activity. *Nature* 395, 604-608.
- Chipman, A.D. (2008). Thoughts and speculations on the ancestral arthropod segmentation pathway. In *Evolving Pathways: Key Themes in Evolutionary Developmental Biology*, Minelli, Alessandro, and Fusco, Giuseppe eds., Cambridge University Press) pp. 343-358.
- Cooke, J., and Zeeman, E.C. (1976). A clock and wavefront model for control of the number of repeated structures during animal morphogenesis. *J. Theor. Biol.* 58, 455-476.
- Copf, T., Schroder, R., and Averof, M. (2004). Ancestral role of caudal genes in axis elongation and segmentation. *Proc. Natl. Acad. Sci. U. S. A.* 101, 17711-17715.
- Davis, G.K., and Patel, N.H. (2002). Short, long, and beyond: molecular and embryological approaches to insect segmentation. *Annu. Rev. Entomol.* 47, 669-699.
- Dequeant, M.L., Glynn, E., Gaudenz, K., Wahl, M., Chen, J., Mushegian, A., and Pourquie, O. (2006). A complex oscillating network of signaling genes underlies the mouse segmentation clock. *Science* 314, 1595-1598.
- Diez del Corral, R., Olivera-Martinez, I., Goriely, A., Gale, E., Maden, M., and Storey, K. (2003). Opposing FGF and retinoid pathways control ventral neural pattern, neuronal differentiation, and segmentation during body axis extension. *Neuron* 40, 65-79.
- Dubrulle, J., McGrew, M.J., and Pourquie, O. (2001). FGF signaling controls somite boundary position and regulates segmentation clock control of spatiotemporal Hox gene activation. *Cell* 106, 219-232.
- Edgar, L.G., Carr, S., Wang, H., and Wood, W.B. (2001). Zygotic expression of the caudal homolog pal-1 is required for posterior patterning in *Caenorhabditis elegans* embryogenesis. *Dev. Biol.* 229, 71-88.
- El-Sherif, E., Averof, M., and Brown, S.J. (2012). A segmentation clock operating in blastoderm and germband stages of *Tribolium* development. *Development* 139, 4341-4346.

- Epstein, M., Pillemer, G., Yelin, R., Yisraeli, J.K., and Fainsod, A. (1997). Patterning of the embryo along the anterior-posterior axis: the role of the caudal genes. *Development* *124*, 3805-3814.
- Falciani, F., Hausdorf, B., Schroder, R., Akam, M., Tautz, D., Denell, R., and Brown, S. (1996). Class 3 Hox genes in insects and the origin of zen. *Proc. Natl. Acad. Sci. U. S. A.* *93*, 8479-8484.
- Fu, J., Posnien, N., Bolognesi, R., Fischer, T.D., Rayl, P., Oberhofer, G., Kitzmann, P., Brown, S.J., and Bucher, G. (2012). Asymmetrically expressed axin required for anterior development in *Tribolium*. *Proc. Natl. Acad. Sci. U. S. A.* *109*, 7782-7786.
- Kotkamp, K., Klingler, M., and Schoppmeier, M. (2010). Apparent role of *Tribolium* orthodenticle in anteroposterior blastoderm patterning largely reflects novel functions in dorsoventral axis formation and cell survival. *Development* *137*, 1853-1862.
- Lawrence, P.A. (1992). *The Making of a Fly: the Genetics of Animal Design* (Oxford, UK: Blackwell Scientific).
- Logan, C.Y., and Nusse, R. (2004). The Wnt signaling pathway in development and disease. *Annu. Rev. Cell Dev. Biol.* *20*, 781-810.
- Lynch, J.A., Brent, A.E., Leaf, D.S., Pultz, M.A., and Desplan, C. (2006). Localized maternal orthodenticle patterns anterior and posterior in the long germ wasp *Nasonia*. *Nature* *439*, 728-732.
- Macdonald, P.M., and Struhl, G. (1986). A molecular gradient in early *Drosophila* embryos and its role in specifying the body pattern. *Nature* *324*, 537-545.
- McGregor, A.P., Pechmann, M., Schwager, E.E., Feitosa, N.M., Kruck, S., Aranda, M., and Damen, W.G. (2008). Wnt8 is required for growth-zone establishment and development of opisthosomal segments in a spider. *Curr. Biol.* *18*, 1619-1623.
- Oates, A.C., Morelli, L.G., and Ares, S. (2012). Patterning embryos with oscillations: structure, function and dynamics of the vertebrate segmentation clock. *Development* *139*, 625-639.
- Olesnický, E.C., Brent, A.E., Tonnes, L., Walker, M., Pultz, M.A., Leaf, D., and Desplan, C. (2006). A caudal mRNA gradient controls posterior development in the wasp *Nasonia*. *Development* *133*, 3973-3982.

- Palmeirim, I., Henrique, D., Ish-Horowicz, D., and Pourquie, O. (1997). Avian hairy gene expression identifies a molecular clock linked to vertebrate segmentation and somitogenesis. *Cell* *91*, 639-648.
- Peel, A.D., Chipman, A.D., and Akam, M. (2005). Arthropod Segmentation: beyond the *Drosophila* paradigm. *Nat. Rev. Genet.* *6*, 905-916.
- Pilon, N., Oh, K., Sylvestre, J.R., Savory, J.G., and Lohnes, D. (2007). Wnt signaling is a key mediator of Cdx1 expression in vivo. *Development* *134*, 2315-2323.
- Rogers, K.W., and Schier, A.F. (2011). Morphogen gradients: from generation to interpretation. *Annu. Rev. Cell Dev. Biol.* *27*, 377-407.
- Sarrazin, A.F., Peel, A.D., and Averof, M. (2012). A segmentation clock with two-segment periodicity in insects. *Science* *336*, 338-341.
- Schroder, R. (2003). The genes orthodenticle and hunchback substitute for bicoid in the beetle *Tribolium*. *Nature* *422*, 621-625.
- Shinmyo, Y., Mito, T., Matsushita, T., Sarashina, I., Miyawaki, K., Ohuchi, H., and Noji, S. (2005). caudal is required for gnathal and thoracic patterning and for posterior elongation in the intermediate-germband cricket *Gryllus bimaculatus*. *Mech. Dev.* *122*, 231-239.
- Stauber, M., Jackle, H., and Schmidt-Ott, U. (1999). The anterior determinant bicoid of *Drosophila* is a derived Hox class 3 gene. *Proc. Natl. Acad. Sci. U. S. A.* *96*, 3786-3789.
- van der Zee, M., Berns, N., and Roth, S. (2005). Distinct functions of the *Tribolium* zerknüllt genes in serosa specification and dorsal closure. *Curr. Biol.* *15*, 624-636.
- Wolpert, L. (1969). Positional information and the spatial pattern of cellular differentiation. *J. Theor. Biol.* *25*, 1-47.

Chapter 4 - Conclusions

Clock-based segmentation in *Tribolium*

In Chapter 2, I showed that the anterior to posterior progression of *Tc-eve* stripe formation reflects an underlying segmentation clock functioning in the *Tribolium* blastoderm and germband. Sequential segmentation (Liu and Kaufman, 2005; Nakao, 2010) and posterior-to-anterior shifts of pair-rule gene expression (Garcia-Solache et al., 2010) in the blastoderm of other insects have also been reported. Careful examination of stripe formation dynamics will determine whether these insects utilize clock-based or *Drosophila*-like segmentation mechanisms. Interestingly, even the expression of posterior pair-rule genes in *Drosophila* undergo posterior to anterior shifts (Keranen et al., 2006). Although limited and not reflecting an overt oscillatory process, as in *Tribolium*, these shifts may be a vestige of an ancestral clock-based mechanism.

The role of Caudal in segmentation

In *Drosophila*, maternal *cad* mRNA (*Dm-cad*) is ubiquitously expressed in the early blastoderm (Mlodzik and Gehring, 1987). A posterior-to-anterior protein gradient of Dm-Cad forms due to translational repression of the reciprocal gradient of Dm-Bicoid (Dubnau and Struhl, 1996). Dm-Cad acts as an activator of posterior gap (Schulz and Tautz, 1995) and pair-rule genes (Hader et al., 1998) and was found to bind to their enhancer elements (Dearolf et al., 1989; Rivera-Pomar et al., 1995). However, the mild segmentation defects in embryos in which the shape of Dm-Cad gradient has been altered argues against its function as a morphogen gradient (Macdonald and Struhl, 1986; Mlodzik et al., 1990). In the wasp *Nasonia vitripennis*, *Nv-cad* plays a more prominent role in activating gap and pair-rule genes, and a limited positioning role (Olesnicky et al., 2006). In the cricket *Gryllus bimaculatus*, *Gb-cad* was found to activate the pair-rule gene *Gb-eve*, and activate and position gap gene domains. This indicates that *cad* might act as a morphogen gradient in more basal insects. In Chapter 3, I described similar results in *Tribolium*. I showed that in strong *Tc-cad* RNAi, expression of *Tc-eve* was abolished (Supp. Figure 3.2); while in weak *Tc-cad* RNAi, a posterior shift in its expression was observed (Figure 3.3 B). However, a morphogen gradient acting through concentration thresholds is less likely to act in positioning the highly dynamic pair-rule expression domains in

Tribolium. Instead, I argue that *Tc-cad* regulates the frequency of a pair-rule clock resulting in wave dynamics. Frequency regulation can be achieved through simple activation (see below) which is consistent with our results and with observations in other arthropods.

Three *cad* homologs are found in mouse: *Cdx1*, *Cdx2*, and *Cdx4*. They are expressed in nested domains in the posterior of the embryo. The *Cdx1-Cdx2* double mutant exhibits fused somites (Savory et al., 2011), suggesting a role in somitogenesis. However, the *Cdx1-Cdx2* double mutant also shows downregulation of some caudalizing factors involved in somitogenesis (like *wnt3a*) that are themselves *Cdx* regulators (Grainger et al., 2012; Savory et al., 2009). *Cdx* genes also directly regulate Hox genes in a dose dependent manner (Deschamps and van Nes, 2005; Gaunt et al., 2004), and even regulate their activation times (Schyr et al., 2012).

In summary, *cad(-related)* genes are involved in patterning the posterior of many species. While it is not clear whether they play a permissive or instructive role, there is evidence that they might act as a morphogen gradient for gap genes in basal insects (like in *Gryllus*) and for Hox genes in vertebrates. In this study, I showed that *Tc-cad* regulates the spatiotemporal dynamics of *Tribolium* pair-rule genes in a dose dependent manner, stressing the instructive role of *cad* in the development of basal insects.

The patterning capacity of frequency gradients and the robustness of the clock-and-wavefront model

In the original formulation of the clock-and-wavefront model, the anterior-to-posterior movement of a step frequency profile (i.e. suddenly dropping from non-zero to zero frequency) over an oscillating field of cells sequentially generates a striped pattern in an anterior-to-posterior order (Cooke and Zeeman, 1976). Later, this mechanism was modified by assuming a graded frequency profile to accommodate the observation that oscillations organize into kinematic waves in the chick PSM (Palmeirim et al., 1997). Several efforts have been made to identify molecular gradient(s) that regulate the frequency of the vertebrate segmentation clock. A posterior-to-anterior Wnt activity gradient was found to define the PSM oscillation domain in the mouse (Aulehla et al., 2003; Aulehla et al., 2008). Furthermore, down-regulation of Wnt activity reduced the clock frequency in both mouse and chick (Gibb et al., 2009). However, an elevated and flattened constitutive stabilization of β -catenin in the mouse PSM led to a mere extension of the oscillation domain, arguing against a role for the shape of Wnt activity gradient in

segmentation (Aulehla et al., 2008). A posterior-to-anterior FGF gradient in the PSM was found to define where oscillations are arrested (Dubrulle et al., 2001; Naiche et al., 2011; Sawada et al., 2001); however, manipulating the level of FGF signaling does not alter the clock period (Dubrulle et al., 2001; Gibb et al., 2009). A gradient of Her13.2 in zebrafish was suggested to modulate clock frequency through heterodimerization with other zebrafish clock constituents: Her1 and Her7 (Cinquin, 2007; Kawamura et al., 2005). However, this idea was recently challenged (Schroter et al., 2012).

It is not known whether the gradual arrest of oscillations and the resulting kinematic waves in vertebrates have any functional role or are a mere peculiarity, since, based on computer simulations of the clock-and-wavefront model, stripe widths depend only on the wavefront velocity and the maximum clock period, but not on the shape of the frequency profile (Oates et al., 2012). Although used for cosmetic means within the clock-and-wavefront model, a graded frequency profile (even a static one) by itself has a patterning capacity (Murray, 2002). Kinematic waves were observed in an oscillating Zhabotinskii chemical reaction, where a reactant controlling the frequency of oscillation is distributed in a gradient (Beck and Varadi, 1972; Thoenes, 1973). Since a static step frequency profile is unable to generate any stripes, the patterning capacity of a graded frequency profile might explain how blastodermal *Tc-eve* stripes in *Tribolium* form in the absence of axis elongation. Although the possibility of a yet unidentified frequency gradient that sweeps across the blastoderm still exists, I showed in Chapter 3 that a strong candidate for the frequency gradient in *Tribolium*, *Tc-cad*, does not appreciably shift during the formation of the first two *Tc-eve* stripes (Figure 3.1 G, H).

In addition to its necessity in the absence of axis elongation, employing a graded frequency profile renders the clock-and-wavefront robust against erratic axis elongation and/or noise in wavefront gene expression, as shown by computer simulations (Figure 3.5 and Movies 3.2). This improvement in robustness might be due to the distributed nature by which oscillations are arrested in the case of graded frequency profile, in contrast to the total reliance on a single threshold in the case of a step frequency profile.

The molecular basis of clock modulation by a frequency gradient

In chapter 3 and 4, I argued that the dynamics of *Tc-eve* expression are that of a clock whose frequency is regulated by a gradient, resulting in waves of gene expression. The molecular

basis of the corresponding wave dynamics in vertebrate somitogenesis has not been resolved to date. However, some models based on *in silico* experimentations were suggested. Graded reaction rates of a molecular clock (Tiedemann et al., 2007; Uriu et al., 2009) or a graded competitive dimerization (Campanelli and Gedeon, 2010; Cinquin, 2007) results in the desired dynamics. Other gene regulatory network (GRN) realizations of the clock-and-wavefront model successfully generated striped expression (Francois et al., 2007), but were unable to reproduce the wave dynamics of clock gene expression.

One of the most well characterized GRNs in development is that of the *Drosophila* gap network (Jaeger, 2011). Detailed characterization of the spatiotemporal dynamics of gap gene expression was used to build a computer model of the gap GRN that was able to predict elusive posterior-to-anterior shifts of gap gene domain borders (Jaeger et al., 2004). These domain shifts are mainly due to the asymmetric cross-repressions between adjacent gap domains, with posterior dominance (Jaeger et al., 2004; Manu et al., 2009). A GRN was devised to explain a similar phenomenon of gene expression propagation in the vertebrate neural tube, which interestingly is also comprised of cross-repressions with posterior dominance (Balaskas et al., 2012; Panovska-Griffiths et al., 2012).

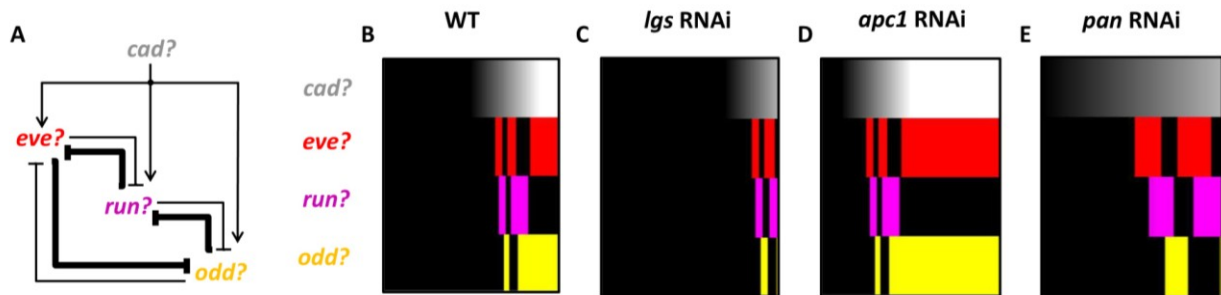
Here I propose a GRN composed of three genes with asymmetric cross-repressions (Figure 4.1 A) composed of two repressilators: one of strong repressive links in one direction, and another with cross repressive links in the opposite direction (Figure 4.1A, Equation 4.1). If the three genes are regulated by a posterior-to-anterior activator, this network is surprisingly able to generate cyclic waves that propagate from posterior to anterior (Movies 4.1, Figure 4.1 B) with little tuning of parameters (Equation 4.1). *Tribolium* primary pair-rule genes (*Tc-even-skipped*, *Tc-runt*, *Tc-odd-skipped*) might be wired into a similar configuration and activated by the graded expression of *Tc-cad* to produce pair-rule waves (Figure 4.1 A). Down-regulating the graded activator reduced the number of stripes formed and resulted in a posterior shift (Figure 4.1 C, reminiscent of *Tc-lgs* RNAi phenotype in *Tribolium*, Chapter 3). Expanding the graded activator resulted into an anterior shift (Figure 4.1 D, reminiscent of the *Tc-apc1* RNAi phenotype). Down-regulating and stretching the graded activator reduced the number of stripes formed and resulted in an anterior shift in addition to wider waves (reminiscent of *Tc-pan* RNAi phenotype).

However, this GRN is unable to reproduce all the reported pair-rule knock-down phenotypes (Choe et al., 2006; data not shown). This might be attributed to the late developmental time at which these phenotypes were documented. A careful analysis of pair-rule gene expression at relevant times in WT as well as knock-downs is needed to correctly test pair-rule GRN models.

The question now is how the proposed GRN produce the observed wave dynamics and how this is relevant to the concept of clock modulation by a frequency gradient. In this model, at the highest concentration of the morphogen activator (representing *Tc-cad*) cells cycle through different expressions pair-rule genes. Reduced cycling frequency more anteriorly at lower values of *Tc-cad* might be due to its effect on transcription rates of pair-rule genes. However, a dynamical system approach like that applied to the *Drosophila* gap network (Manu et al., 2009) is needed for clock-based patterning mechanisms.

Figure 4.1 Probable molecular basis for frequency regulation.

The proposed GRN (A) generates waves of gene expression (B) that propagate from posterior (right) to anterior (left). (C-E) GRN outputs upon manipulating the graded activator (corresponding to *Tc-cad*, in grayscale). (C) reducing the graded activator (corresponding to *Tc-lgs* RNAi). (D) expanding the graded activator (corresponding to *Tc-apc1* RNAi). (E) down-regulating and stretching the graded activator (corresponding to *Tc-pan* RNAi). Anterior to the left.



Supplementary materials

Equation 4.1 Differential equation representation of the proposed pair-rule GRN.

The Hill function coefficient n represents weak repressions (set to 1 in my simulation), m represents strong repression (set to 6 in my simulations), α represents mRNA decay rates (set to 1 for the three genes).

$$\begin{aligned}\frac{deve}{dt} &= cad \frac{1}{1 + odd^n + run^m} - \alpha eve \\ \frac{drun}{dt} &= cad \frac{1}{1 + eve^n + odd^m} - \alpha run \\ \frac{dodd}{dt} &= cad \frac{1}{1 + run^n + eve^m} - \alpha odd\end{aligned}$$

Movies 4.1 Simulation of the proposed pair-rule GRN in WT and knockdowns.

Simulation of the differential equation representation (Equation 4.1) of pair-rule GRN in WT (A), *Tc-lgs* RNAi (B), *Tc-apc1* RNAi (C), and *Tc-pan* RNAi (D). *Tc-cad* expression in grayscale, *Tc-eve* in red, *Tc-run* in violet, and *odd* in yellow. Simulations were performed using Matlab.

References

- Aulehla, A., Wehrle, C., Brand-Saberi, B., Kemler, R., Gossler, A., Kanzler, B., and Herrmann, B.G. (2003). Wnt3a plays a major role in the segmentation clock controlling somitogenesis. *Dev. Cell.* 4, 395-406.
- Aulehla, A., Wiegraebe, W., Baubet, V., Wahl, M.B., Deng, C., Taketo, M., Lewandoski, M., and Pourquie, O. (2008). A beta-catenin gradient links the clock and wavefront systems in mouse embryo segmentation. *Nat. Cell Biol.* 10, 186-193.
- Balaskas, N., Ribeiro, A., Panovska, J., Dessaud, E., Sasai, N., Page, K.M., Briscoe, J., and Ribes, V. (2012). Gene regulatory logic for reading the Sonic Hedgehog signaling gradient in the vertebrate neural tube. *Cell* 148, 273-284.
- Beck, M.T., and Varadi, Z.B. (1972). One, Two and Three-dimensional Spatially Periodic Chemical Reactions. *Nature Physical Science* 235, 15-16.

- Campanelli, M., and Gedeon, T. (2010). Somitogenesis Clock-Wave Initiation Requires Differential Decay and Multiple Binding Sites for Clock Protein. *PLoS Comput Biol* 6, e1000728.
- Choe, C.P., Miller, S.C., and Brown, S.J. (2006). A pair-rule gene circuit defines segments sequentially in the short-germ insect *Tribolium castaneum*. *103*, 6560-6564.
- Cinquin, O. (2007). Repressor dimerization in the zebrafish somitogenesis clock. *PLoS Comput. Biol.* 3, e32.
- Cooke, J., and Zeeman, E.C. (1976). A clock and wavefront model for control of the number of repeated structures during animal morphogenesis. *J. Theor. Biol.* 58, 455-476.
- Dearolf, C.R., Topol, J., and Parker, C.S. (1989). The caudal gene product is a direct activator of fushi tarazu transcription during *Drosophila* embryogenesis. *Nature* 341, 340-343.
- Deschamps, J., and van Nes, J. (2005). Developmental regulation of the Hox genes during axial morphogenesis in the mouse. *Development* 132, 2931-2942.
- Dubnau, J., and Struhl, G. (1996). RNA recognition and translational regulation by a homeodomain protein. *Nature* 379, 694-699.
- Dubrulle, J., McGrew, M.J., and Pourquie, O. (2001). FGF signaling controls somite boundary position and regulates segmentation clock control of spatiotemporal Hox gene activation. *Cell* 106, 219-232.
- Francois, P., Hakim, V., and Siggia, E.D. (2007). Deriving structure from evolution: metazoan segmentation. *Mol. Syst. Biol.* 3, 154.
- Garcia-Solache, M., Jaeger, J., and Akam, M. (2010). A systematic analysis of the gap gene system in the moth midge *Clogmia albipunctata*. *Dev. Biol.* 344, 306-318.
- Gaunt, S.J., Cockley, A., and Drage, D. (2004). Additional enhancer copies, with intact cdx binding sites, anteriorize *Hoxa-7/lacZ* expression in mouse embryos: evidence in keeping with an instructional cdx gradient. *Int. J. Dev. Biol.* 48, 613-622.
- Gibb, S., Zagorska, A., Melton, K., Tenin, G., Vacca, I., Trainor, P., Maroto, M., and Dale, J.K. (2009). Interfering with Wnt signalling alters the periodicity of the segmentation clock. *Dev. Biol.* 330, 21-31.
- Grainger, S., Lam, J., Savory, J.G., Mears, A.J., Rijli, F.M., and Lohnes, D. (2012). Cdx regulates *Dll1* in multiple lineages. *Dev. Biol.* 361, 1-11.

- Hader, T., La Rosee, A., Zibold, U., Busch, M., Taubert, H., Jackle, H., and Rivera-Pomar, R. (1998). Activation of posterior pair-rule stripe expression in response to maternal caudal and zygotic knirps activities. *Mech. Dev.* *71*, 177-186.
- Irvine, K.D., and Wieschaus, E. (1994). Cell intercalation during *Drosophila* germband extension and its regulation by pair-rule segmentation genes. *Development* *120*, 827-841.
- Jaeger, J. (2011). The gap gene network. *Cell Mol. Life Sci.* *68*, 243-274.
- Jaeger, J., Surkova, S., Blagov, M., Janssens, H., Kosman, D., Kozlov, K.N., Manu, Myasnikova, E., Vanario-Alonso, C., Samsonova, M., Sharp, D.H., and Reinitz, J. (2004). Dynamic control of positional information in the early *Drosophila* embryo. *Nature* *430*, 368-371.
- Kawamura, A., Koshida, S., Hijikata, H., Sakaguchi, T., Kondoh, H., and Takada, S. (2005). Zebrafish hairy/enhancer of split protein links FGF signaling to cyclic gene expression in the periodic segmentation of somites. *Genes Dev.* *19*, 1156-1161.
- Keranen, S.V., Fowlkes, C.C., Luengo Hendriks, C.L., Sudar, D., Knowles, D.W., Malik, J., and Biggin, M.D. (2006). Three-dimensional morphology and gene expression in the *Drosophila* blastoderm at cellular resolution II: dynamics. *Genome Biol.* *7*, R124.
- Liu, P.Z., and Kaufman, T.C. (2005). even-skipped is not a pair-rule gene but has segmental and gap-like functions in *Oncopeltus fasciatus*, an intermediate germband insect. *Development* *132*, 2081-2092.
- Macdonald, P.M., and Struhl, G. (1986). A molecular gradient in early *Drosophila* embryos and its role in specifying the body pattern. *Nature* *324*, 537-545.
- Manu, Surkova, S., Spirov, A.V., Gursky, V.V., Janssens, H., Kim, A.R., Radulescu, O., Vanario-Alonso, C.E., Sharp, D.H., Samsonova, M., and Reinitz, J. (2009). Canalization of gene expression and domain shifts in the *Drosophila* blastoderm by dynamical attractors. *PLoS Comput. Biol.* *5*, e1000303.
- Mlodzik, M., and Gehring, W.J. (1987). Expression of the caudal gene in the germ line of *Drosophila*: formation of an RNA and protein gradient during early embryogenesis. *Cell* *48*, 465-478.
- Mlodzik, M., Gibson, G., and Gehring, W.J. (1990). Effects of ectopic expression of caudal during *Drosophila* development. *Development* *109*, 271-277.
- Murray, J.D. (2002). *Mathematical Biology: An introduction* Springer).

- Naiche, L.A., Holder, N., and Lewandoski, M. (2011). FGF4 and FGF8 comprise the wavefront activity that controls somitogenesis. *Proc. Natl. Acad. Sci. U. S. A.* *108*, 4018-4023.
- Nakao, H. (2010). Characterization of Bombyx embryo segmentation process: expression profiles of engrailed, even-skipped, caudal, and wnt1/wingless homologues. *J. Exp. Zool. B. Mol. Dev. Evol.* *314*, 224-231.
- Oates, A.C., Morelli, L.G., and Ares, S. (2012). Patterning embryos with oscillations: structure, function and dynamics of the vertebrate segmentation clock. *Development* *139*, 625-639.
- Olesnický, E.C., Brent, A.E., Tonnes, L., Walker, M., Pultz, M.A., Leaf, D., and Desplan, C. (2006). A caudal mRNA gradient controls posterior development in the wasp *Nasonia*. *Development* *133*, 3973-3982.
- Palmeirim, I., Henrique, D., Ish-Horowicz, D., and Pourquie, O. (1997). Avian hairy gene expression identifies a molecular clock linked to vertebrate segmentation and somitogenesis. *Cell* *91*, 639-648.
- Panovska-Griffiths, J., Page, K.M., and Briscoe, J. (2012). A gene regulatory motif that generates oscillatory or multiway switch outputs. *J. R. Soc. Interface* *10*, 20120826.
- Rivera-Pomar, R., Lu, X., Perrimon, N., Taubert, H., and Jackle, H. (1995). Activation of posterior gap gene expression in the *Drosophila* blastoderm. *Nature* *376*, 253-256.
- Savory, J.G., Bouchard, N., Pierre, V., Rijli, F.M., De Repentigny, Y., Kothary, R., and Lohnes, D. (2009). Cdx2 regulation of posterior development through non-Hox targets. *Development* *136*, 4099-4110.
- Savory, J.G., Mansfield, M., Rijli, F.M., and Lohnes, D. (2011). Cdx mediates neural tube closure through transcriptional regulation of the planar cell polarity gene Ptk7. *Development* *138*, 1361-1370.
- Sawada, A., Shinya, M., Jiang, Y.J., Kawakami, A., Kuroiwa, A., and Takeda, H. (2001). Fgf/MAPK signalling is a crucial positional cue in somite boundary formation. *Development* *128*, 4873-4880.
- Schroter, C., Ares, S., Morelli, L.G., Isakova, A., Hens, K., Soroldoni, D., Gajewski, M., Julicher, F., Maerkl, S.J., Deplancke, B., and Oates, A.C. (2012). Topology and dynamics of the zebrafish segmentation clock core circuit. *PLoS Biol.* *10*, e1001364.
- Schulz, C., and Tautz, D. (1995). Zygotic caudal regulation by hunchback and its role in abdominal segment formation of the *Drosophila* embryo. *Development* *121*, 1023-1028.

- Schyr, R.B., Shabtai, Y., Shashikant, C.S., and Fainsod, A. (2012). Cdx1 is essential for the initiation of HoxC8 expression during early embryogenesis. *FASEB J.* 26, 2674-2684.
- Thoenes, D. (1973). Spatial oscillations in the Zhabotinskii reaction. *Nature Physical Science* 243, 18-20.
- Tiedemann, H.B., Schneltzer, E., Zeiser, S., Rubio-Aliaga, I., Wurst, W., Beckers, J., Przemeck, G.K., and Hrabe de Angelis, M. (2007). Cell-based simulation of dynamic expression patterns in the presomitic mesoderm. *J. Theor. Biol.* 248, 120-129.
- Uriu, K., Morishita, Y., and Iwasa, Y. (2009). Traveling wave formation in vertebrate segmentation. *J. Theor. Biol.* 257, 385-396.